Stony Brook University

Low-Level Vibrations Maintain the Intervertebral Disc during Unloading

A Dissertation Presented

by

Nilsson Holguin

to

The Graduate School

in Partial fulfillment of the

Requirements

for the Degree of

Doctor of Philosophy

in

Biomedical Engineering

Stony Brook University

December 2010

Stony Brook University

The Graduate School

Nilsson Holguin

We, the dissertation committee for the above candidate for the

Doctor of Philosophy degree,
hereby recommend acceptance of this dissertation.

Stefan Judex, Ph.D., Advisor
Associate Professor
Department of Biomedical Engineering

Michael Hadjiargyrou, Ph.D., Committee Chair
Associate Professor
Department of Biomedical Engineering

Clinton Rubin, Ph.D.
Distinguished Professor and Chair
Department of Biomedical Engineering

Dawn Elliott, Ph.D., External Member
Associate Professor
Department of Orthopaedic Surgery
University of Pennsylvania

This dissertation is accepted by the Graduate School

Lawrence Martin
Dean of the Graduate School

Abstract of the Dissertation

Low-Level Vibrations Maintain the Intervertebral Disc during Unloading

by

Nilsson Holguin

Doctor of Philosophy

in

Biomedical Engineering

Stony Brook University

2010

Changes in intervertebral disc (IVD) biochemistry, morphology and mechanics have been characterized only incompletely in the rat hindlimb unloading (HU) model. Although exposure to chronic vibrations can be damaging, low-magnitude vibrations can attenuate the geometric changes of the IVD due to altered spinal loading. Here, we tested the hypothesis that low-magnitude, high-frequency vibrations will mitigate the hypotrophy, biochemical degradation and deconditioning of the IVD during HU. When applied as whole-body vibrations through all four paws, Sprague-Dawley rats were subjected to HU and exposed to daily periods (15min/d) of either ambulatory activities (HU+AMB) or whole body vibrations superimposed upon ambulation (HU+WBV; WBV at 45Hz, 0.3g). After 4wks and, compared to age-matched control rats (AC), the lumbar IVD of HU+AMB had a 22% smaller glycosaminoglycans/collagen ratio, 12% smaller posterior IVD height, and 13% smaller cross-sectional area. Compared to HU+AMB rats, the addition of low-level vibratory loading did not significantly alter IVD biochemistry,

posterior height, area, or volume, but directionally altered IVD geometry. When subjected to upright vibrations through the hindpaws, rats were HU for 4wks. A subset of HU rats stood in an upright posture on a vertically oscillating plate (0.2g) at 45- or 90-Hz (HU+45 or HU+90). After 4wks, regardless of sham (HU+SC) loading (HU±SC) and, compared to AC, IVD of HU±SC had 10% less height, 39% smaller nucleus pulposus area, less glycosaminoglycans in the nucleus pulposus (21%), anterior annulus fibrosus (16%) and posterior annulus fibrosus (19%), 76% less tension-compression neutral zone (NZ) modulus, 26% greater compressive modulus, 25% greater initial elastic damping modulus, 26% less torsional NZ stiffness, no difference in collagen content and a weaker relationship between tension-compression NZ modulus and posterior height change. Exogenously introduced oscillations maintained the morphology, glycosaminoglycan content and axial elastic properties of IVD. Compared to HU±SC, the IVD of HU+90 had 8% larger average height, 35% greater nucleus pulposus area, more glycosaminoglycans in the nucleus pulposus (24%), anterior annulus fibrosus (17%) and posterior annulus fibrosus (19%), 339% greater tension-compression NZ modulus, 18% smaller compressive modulus, and maintained the relationship between tension-compression NZ modulus and posterior height change, but no difference in torsional NZ stiffness or initial elastic damping modulus. In summary, very brief, small mechanical signals partially protected the IVD during hindlimb unloading.

TABLE OF CONTENTS

LIST OF TABLES

LIST OF FIGURES

Figure 7. *Posture of an animal during (a) hindlimb unloading during which the angle between the torso and the ground was about 30^{o} (85). (b) For 15min/d rats were released from HU and placed into an upright position in an acrylic tube (height: 30.5 cm, inner diameter: 10.2 cm) in which they received a low-level, vertical vibratory signal (45Hz or 90Hz) or sham loading (0Hz). The white arrow points to where the motion at L5 was measured in two rats.*

Figure 8. *Height map of an IVD. ANT corresponded to the average IVD height of the anterior half of the IVD while POS corresponded to the average IVD height of the posterior half of the IVD.*

Figure 9. *Displacements of the vibrating plate (0.2g) at 45Hz (grey dashed) and 90Hz (grey) and of the rat L5 region at 0Hz (solid), 45Hz (dotted) and 90Hz (bold) vibrations. Compared to the vibrating plate, the measured frequency at L5 was maintained in the upright rat but the amplitude was dampened by ~35% at both frequencies.*

Figure 10. A*verage (AVG), anterior (ANT) and posterior (POS) height of the IVD of AC (n=11), HU±SC (n=22), HU+45 (n=11) and HU+90 (n=11); mean+SD. IVD of HU±SC had less AVG, ANT and POS IVD height than of AC. Vibrations at 90Hz maintained AVG and ANT IVD height, while vibrations at 45Hz maintained ANT but not POS IVD height. † compared to AC, ‡ compared to HU; p <0.05*

Figure 11. *Volume across lumbar discs of AC (n=11), HU±SC (n=22), HU+45 (n=11) and HU+90(n=11); mean+SD. Compared to AC, hindlimb unloaded IVD, with or without upright*

posture, had less volume between L2 and L5. Vibrations at 45Hz did not maintain the IVD volume at L3-L4 compared to AC. † compared to AC; p <0.05

Figure 12. *Sulfated-glycosaminoglycan (sGAG) content of the whole IVD (TOTAL), nucleus pulposus (NP), anterior annulus fibrosus (AAF) and posterior annulus fibrosus (PAF) of BC (TOTAL n=11; Region n=5), AC (TOTAL n=11; Region n=5), HU±SC (TOTAL n=22; Region n=10), HU+45 (TOTAL n=11; Region n=5) and HU+90 (TOTAL n=11; Region n=5); mean+SD. IVD of HU±SC had less sGAG content than of AC at every region. TOTAL and AAF of HU+45 IVD was less than of AC. Compared to HU±SC, vibrations at 90Hz maintained sGAG content at every region, and was greater than of HU+45 at AAF. Overall, the total content of HU+90 IVD was greater than of HU±SC and HU+45. † compared to AC, ‡ compared to HU,* **§** *compared to HU+45; p <0.05*

Figure 13. *sGAG content of the PAF of individual lumbar discs from AC (n=5), HU±SC (n=10), HU+45 (n=5) and HU+90 (n=5) animals; mean+SD. At L4-L5, sGAG content of PAF IVD of HU±SC was less than of AC but 90Hz vibrations maintained it. Contrarily, at L3-L4, PAF of HU+45 IVD had less sGAG content than of AC, HU±SC and HU+90 IVD. Lastly, the interaction of disc level and vibration application was greater in the cephalic PAF of HU+90 IVD than of HU+45 or HU±SC. † compared to AC, ‡ compared to HU,* **§** *compared to HU+45; p <0.05*

Figure 14. *Change of IVD Height from baseline of AC (n=7), HU±SC (n=14) and HU+90 (n=7); mean+SD. The hashed line was the mean HU value and the solid line was the mean HU+SC*

value. The introduction of 90Hz mechanical signals to upright posture maintained the change in IVD height. † compared to AC, ‡ compared to HU±SC; p <0.05

Figure 15. *Nucleus pulposus area of AC (n=7), HU±SC (n=14) and HU+90 (n=7) IVD; mean+SD. The hashed line was the mean HU value and the solid line was the mean HU+SC value. Compared to AC, IVD of hindlimb unloaded, with or without upright loading, animals had less nucleus pulposus area and 90 Hz vibrations maintained the nucleus pulposus area. † compared to AC, ‡ compared to HU+SC; p <0.05*

Figure 16. *Compressive, tensile and neutral zone modulus of L4-L5 segment from AC (n=7), HU±SC (n=14) and HU+90 (n=7) animals; mean+SD. The hashed line was the mean HU value and the solid line was the mean HU+SC value. Compared to AC, HU±SC segments had weaker neutral zone moduli and HU+SC segment had greater compressive moduli. HU+90 segments had greater neutral zone moduli and less compressive moduli than HU±SC segments. † compared to AC, ‡ compared to HU±SC; p <0.05*

Figure 17. *Group regressions between neutral zone modulus and change in posterior disc height of AC (n=7), HU±SC (n=14) and HU+90 (n=7) animals. The hashed line is the regression for both HU and HU+SC values. High-frequency vibrations prevented a loss in the relationship from hindlimb unloading with or without sham loading. * regression, † compared to AC, ‡ compared to HU±SC; p <0.05*

Figure 18. *Using mean values from the polynomial fit, the creep behavior of the AC (n=7), HU±SC (n=14) and HU+90 (n=7) animals were similar.*

Figure 19. *Excellent regression between neutral zone torsional stiffness and average paraspinal muscle area across the mean of BC (n=7), AC (n=7), HU (n=7), HU+SC (n=7) and HU+90 (n=7).*

Figure 20. *Change in paraspinal muscle area at L4 and L5 of AC (n=7), HU±SC (n=14) and HU+90 (n=7) animals; mean+SD. The hashed line was the mean HU value and the solid line was the mean HU+SC value. Unloading with and without upright loading increased the psoas area at L4 and L5. At L4, paraspinal area of HU±SC rats was less than of AC rats. At L5, paraspinal area of HU+90 rats was less than of HU±SC and AC rats. * compared to baseline of same animal*, † *compared to AC,* ‡ *compared to HU±SC; p <0.05*

Figure 21. *Regression between change in muscle volume from L4 to L5 and change in L4-L5 length of AC (n=7), HU±SC (n=14) and HU+90 (n=7) animals; mean+SD. Each datum was a rat. Excellent regressions existed for AC rats with growth of lumbar length in every rat. The relationship was moderate for rats that were hindlimb unloaded with or without interruption by brief, upright posture with a few rats experiencing loss of lumbar length. The inclusion of 90Hz vibrations to upright posture maintained the relationship and growth of lumbar length in every rat. * p<.05*

ACKNOWLEDGMENTS

The dissertation is here and I have several wonderful people to thank for their diverse supportive roles. First, I must thank Stefan Judex, my advisor. The man in the trenches with me who read every misspelled word, every incomplete sentence, every unintelligible paragraph and made it sound like magic; it is a gift. Clinton Rubin, the guy in the big chair, whose insight is fun to behold and wonderful to absorb made me proud to say I was a graduate student in the department of Biomedical Engineering (BME) at Stony Brook University. Now, to leave out students would be a crime. During the final, early morning hours before delivering my Masters Thesis presentation, Adiba Ali sacrificed sleep to help me and even though I thank her profusely, I am indebted to her. Fred Serra-Hsu, the most mature graduate student in the department, is and will continue to be a close friend and helps despite rather sleeping. Garrulous Gavin Olender was the first person I met on the floor and for obvious reasons guided the BME tour. I must say that talking with him played a part in my decision to study at Stony. Paul “Mickey Mouse” Pena and Wasnard “Wazzy” Victor are models of persistence. Now more recently, Dr. Steven “McQueen” Tommasini, Andi “That’s-cute” Trinward, Dr. Ete “Say-what’s-on-my-mind” Chan, Gunes “I’ll-take-it’s-free” Uzer, Gabe “What-are-you-talking-about?” Pagnotti, Johanna “I’m-just-saying” Sisalima, Minyi “New Orleans” Hu, and Shiyun “Come-on!” Xu truly made working in the lab fun. To my lovely Odie, who humbles me, helps me in more ways than she really knows, and listens to me even when I lack sense and to my family at Stony Brook, Queens and Colombia, I love you all. This is for you.

I

INTRODUCTION

Spinal Epidemiology of Astronauts

Astronauts returning from spaceflight show disrupted intervertebral disc (IVD) structure, loss of spinal curvature, lower back pain (LBP) and herniated nucleus pulposus (NP) at a greater incidence than the general population and the army aviators population (120, 214, 233). The etiologies of the above mentioned issues remain unclear. However, the changes caused by reduced weight-bearing may also include but are not limited to leg pain (214), joint damage (10), muscle loss (143) and bone loss (140). These issues may be compounded as wound healing is impaired with microgravity and immobilization (59, 162, 191).

More than 50% of astronauts complain of LBP during space missions as well upon returning to earth, and in 28% of crewmembers, the pain is described as moderate to intense (233). A further characterization of the pain propounds a maximum effect in the first week of microgravity exposure, focused in the lumbar region and incidence independent of previous flight history or age (233). On earth, LBP is an epidemic in the U.S., with more than 80% of the adult population experiencing a severe episode during their lifetime (91) and 18% of the population will experience LBP at any time (188). In an industrial setting, 28% of the working population will experience LBP, where 8% of the whole population will be rendered disabled by LBP in any one year (212). In addition, similar to the exposure to microgravity, reduced weight bearing during bed rest and immobilization produces LBP (102, 211). In 2000, the US's total impact costs of LBP were estimated at $115 billion (50).

Indeed, altered IVD height alone can exacerbate LBP through processes such as increased tension on dorsal nerve roots attached to intrathecal ligaments (129) or stimulation

of nociceptive sinuvertebral nerves(200), which innervate up to one-third of the annulus fibrosus and the anterior dura mater (52), strain of neighboring facet joint capsules (107), disc degeneration (167) or herniation of the disc (167). Epidemiological data of the incidence of herniation of the NP in the 216 astronauts from April 1959 to September 1996 report 19 herniated NPs, 47% of which occurred in the lumbar region (120). A more up to date study (April 1959-December 2006) showed an increased risk of herniation immediately after spaceflight with ~39% of the herniation occurring within 1 year post-landing (119). Therefore, the attenuation of detrimental changes to the spines of unloaded musculatures is of significant importance to prolonged space mission members, the immobilized or persons subjected to bed rest since remedies for LBP both on earth as in space are mostly palliative.

Normal Intervertebral Disc

The IVD is the fibrocartilaginous, articulating connective tissue between the vertebral bodies. It serves three functions: (1) holds vertebrae together like a ligament; (2) absorbs axial shock; and (3) facilitates the 3-D motion of the vertebral bodies. Healthy, adult IVD are predominantly avascular and aneural. The IVD is composed of three major regions: a stiff, outer, collagenous annulus fibrosus (AF) and a soft, central NP. The AF is composed of concentric rings or lamellas of collagen fiber bundles that bind the IVD anteriorly and posteriorly to the longitudinal ligaments and superiorly and inferiorly to the hyaline cartilage endplates and vertebrae. The NP functions as a hydraulic cushion distributing loads generated from weightbearing and endogenous muscle loading to the stress-resistant annulus fibrosus (6). The extracellular matrix of the IVD is primarily comprised of water, proteoglycans, collagen and cells.

Discal hydration is critical for solute transport and biomechanical resistance and thus the plasma contains a large concentration cations (e.g., sodium and potassium) and a low concentration of anions (e.g., chloride and sulfate) (207). The IVD is a largely avascular tissue and thus relies on static and cyclic dynamic forces to induce the influx and efflux of fluids (193) for the transport of nutrients and wastes from the spinal cord. While diffusion is considered the main component driving small solute transport, e.g., oxygen and glucose, load-induced fluid flow may be the contributing factor in the transport of large molecules in the IVD (176, 227). Biomechanically, the ability of the disc to resist the compressive stresses that consistently berate the disc depends on the integrity of its matrix. The compressive stress on the cartilage that will prevent it from swelling is called the swelling pressure. The swelling pressure is equivalent to the sum of the osmotic pressure and the elastic stress of the proteoglycan-collagen network matrix, but the osmotic pressure is the dominant resistive force against the swelling pressure (110). The GAGs on the proteoglycans provide the hydration to maintain the osmotic pressure in cartilage (227). Therefore, a change in swelling or compressive pressure is linked to changes in proteoglycan content (86, 106, 156, 187). However, the degree of cellular stimulation to hydrostatic pressure is dependent on the location of the cell, with NP cells being more responsive than AF cells (142).

Proteoglycans, e.g., aggrecan, biglycan, decorin, and fibromodulin, have a protein center composed of at least one glycosaminoglycan (GAG) chain (114, 131). GAGs are hydrophilic and promote the absorption of fluid into the IVD allowing much of the compressive loads common to the spine. The most common GAGs in the IVD are keratin sulfates and chondroitin-sulfates, of which the concentration of the latter GAGs serve as the predominant water-attractive force

in the IVD (117, 226). The quantity of GAGs increases towards the center of the disc (9). Their distribution is heterogeneous, constituting 50% of the dry weight of a young NP while a small fraction of the AF (63). In addition to its water retentive nature, proteoglycans serve to bind the collagen frame-work.

Collagen, e.g., type I, II, III, VI, IX, X, XI, XII, and XIV, is another major component in the extracellular matrix. The collagen frame-work provides tensile strength, stability between vertebrae, resists bulging and provides supportive loading capabilities. Similar to the site-specific distribution of GAGs, collagen is unevenly distributed in the disc but in the reverse pattern where 67% of the collagen dry weight is in the AF and 25% is in the NP (42). Although there are many types of collagen present in the IVD, 80% of the collagen is composed of types I and II (63). The outer IVD is predominately collagen type I with a diminishing concentration near the NP (165). By contrast, type II collagen is responsible for a dominant amount of the collagen found in the NP. In particular, lumbar IVD have about 15-25 lamellas in the AF (159) and are oriented at 20-40^{o} to the transverse plane adding to the disc's anisotropic behavior (215). The tensile strength of the collagen fibrils depends on the intra- and inter-molecular cross-links (64).

Biosynthesis of GAGs involves many IVD cell organelles and cytoskeletal structures. After ribosomal synthesis, the GAG peptide is translated in the cystol (229). The early polypeptide is then translocated to the lumen of the endoplasmic reticulum where GAG chains are initially added to the core protein. Further translation and modifications occur as the GAG is transported through the Golgi apparatus. Post-translational changes occurring in the Golgi include extension of the GAG chains and sulfation by enzymes bound to the lumen. Lastly, the

GAG is secreted from the cell to interact with other matrix constituents to form the extracellular matrix. Similar to GAGs, collagen is synthesized in the cell, secreted and can be further modified in the extracellular matrix (179). Mechanical loading can regulate the production of GAGs or collagen along any step in the pathway (69, 131).

The cell population of the IVD is diverse and varies according location and age. Fibroblast-like cells encompass much of the cells of the outer AF, while the inner AF is inhabited by more chondrocytic cells (74). In humans, the immature NP contains notochordal cells which are the remainders of the embryonic notochord (222). During aging and at the first signs of degeneration, the notochordal cells of the NP begin to disappear and are replaced by chondrocytic cells (171). Notochordal cells also differ to mature disc cells in their morphology, with notochordal cells being larger and containing vacuoles of various sizes and numbers (82, 100, 101). Notochordal cells may stimulate the production of the extracellular matrix directly (164) and indirectly via chondrocytic cells (8). Increased mechanical loading can instigate the disappearance of notochordal cells (81), potentially initiating disc degeneration.

Intervertebral Disc Degeneration (DD)

The IVD is one of the first tissues to experience degenerative changes from age (58). Boos et al. (29) provide a descriptive account of the deleterious alterations age has on the IVD. By the end of the first decade of life the IVD shows age-related alterations. By as early as age two, NP cells decay, minute clefts form, cell density changes, and the matrix of the cartilage end-plates degenerates. Eventually, the vascularity of the bony vertebral end plate diminishes dramatically and the vascular supply that was once present in the AF of the IVD at birth disappears (194). By the end of the second decade the demarcation between the NP and AF becomes unclear. The

hydration and PG content of the disc continues to decline with age (68). Furthermore, the thinning and cracking of the cartilage end plates precedes the decreased hydration (117) and fissures of the NP. The outer rims of the AF are affected later on in life.

Altered conditions may accelerate the degeneration of the disc. Disc degeneration is characterized by reductions in GAG and water content (4, 35) leading to reduced height and while disc height loss is typically viewed as a symptom of aging, there is a paucity of quantitative data confirming whether the culprit is aging or degeneration (35). The degeneration of the disc is a gradual process and it is exemplified in many ways; morphology, biochemistry, and biomechanics (42, 111, 189). Nevertheless, similar changes from aging occur to the IVD during degeneration in earth-bound individuals and thus, degeneration affects the disc's two major regions in different ways. The NP's cellular composition, in terms of PG, GAG and water content, is altered the most (4, 35). Histologically, the NP appears increasingly opaque as the collagen fibrils grow in diameter and number (112). Morphologically, the ratio of the NP area over the total IVD area and the disc's height tends to decrease (150, 184). Biomechanically, the NP becomes less hydrated and begins to resemble a solid (35, 111, 112). In turn, the AF's integrity also incurs changes in the form of radial fissures (167) and posterior disc protrusions (27, 60) as a result of the decreased size of the NP leading to increased stress distributions (6).

The height and convexity of the IVD experiences reductive changes with age and degeneration (47, 150, 184, 209). Two accepted methods of measuring disc height are the Farfan Index and the Dabbs method (53, 66). The Farfan Index was created to compensate for the magnification issue of radiographs (28) and is measured as the anterior disc height plus

posterior disc height divided by anterior-posterior diameter (66, 67). The FI disc height is linked with histological disc grading but also linked with MRI disc degenerative grading, both of which show losses of disc height with degeneration (47, 189). Lastly, convexity may also indicate degenerative changes in the IVD by in vivo MRI (22, 189) and is calculated as the ratio of the central disc height and of the mean of the anterior and posterior disc height (22). Thus, these measures of disc shape may be used to note the initiation of disc degradation.

Spine Changes from Real and Simulated Weightlessness

Space flight endangers the spinal health of the crew and is associated with the aforementioned back pain but also includes abnormally expanded IVD and loss of spinal curvature (214, 219, 233). Earth-based, bed rest protocols studying the effects of short term and long term lumbar unloading replicate the expansion of the IVD and loss of spinal curvature, but also show an increased spinal compressibility (39, 145, 154), an indicator of reduced stiffness and IVD degeneration (90). Furthermore, reambulation from extended bed rest does not immediately return the size of the IVD to normal (145). Along these lines, mechanical unloading can influence the biochemical composition and genetic expressions in the IVD to alter the molecular composition of the extracellular matrix and, ultimately, the integrity of the IVD.

Using an animal model of weightlessness, i.e., hindlimb unloading (HU), studies demonstrate reduced proteoglycan content as compared to normal ambulatory animals (106, 187, 206). In addition, HU produces fluid shifts, reduces the hydrostatic pressure of the IVD and leads to apoptosis of chondrocytes (15, 87, 88). Contrarily, HU and short duration spaceflight increase the size and number of notochordal cells (71, 241), presumably due to the reduced compressive stress on the IVD which may resemble the loads encountered during early

development. This cellular population inversion may explain the lack of severe degeneration in spaceflight and hindlimb unloaded animals since notochordal cell disappearance precedes disc degeneration. In terms of recovery from unloading, animals that are reloaded for 3 wks after hindlimb unloading continue to exhibit proteoglycan content losses in the AF while the changes in the NP are normalized (241). HU and microgravity reduce the mRNA levels of anabolic proteins (203) and anti-catabolic proteins, while increasing the mRNA levels of catabolic proteins (241).

Concomitant to the disc changes, in a 4–6 month space mission, astronauts lose about 1-1.6% bone per month in the spine (140, 144, 177). Research suggests that bone loss incurred during space flight persists for multiple years after return to normal gravity (40). Another major constituent but endogenous loading factor of the spine is muscle which undergoes atrophy from loss of functional weight-bearing (21, 146). Similarly, hindlimb unloading leads to bone loss, decreased muscle fiber cross-sectional area of types I and II, and recovery is slow (115, 234, 244).

Current IVD Countermeasures to Weightlessness

Currently, no prophylaxes or treatments for IVD pathology exacerbated by extended periods of non-weightbearing are available. Walking exercises with and without loaded backpacks showed that the application of even large mechanical loads during phases of unloading do not prevent IVD volume changes (104, 157, 158). Daily treadmill running under negative body pressure partially negated altered disc morphology during spine deconditioning over a 28 d unloading period but the daily 45 min protocol failed to reduce expansion of the lower lumbar IVD (39). Exercise with *high*-frequency, *high*-amplitude vibrations (amplitude approximately 3.5–4 mm,

acceleration approximately 5.1-10.9 g) (g is equivalent to the gravitational acceleration of the Earth, 9.81 m s^{-2}) reduced IVD height extension from 8 wks of bed rest (21). However, vibrations must be applied cautiously as back pain is noted at vibration exposure frequencies between 3 and 15 Hz at the acceleration of 0.6-2.8 g (26).

These studies suggest that an efficacious countermeasure does not necessarily need to be large in magnitude. An insight to the reasoning may lie in the daily loading history of the skeleton. In a study by Fritton et al. (75), the number of occurrences of minute strains exhibited by weightbearing and non-weightbearing bones of several species of animals occurs 2-3 orders of magnitude more times than large strains. Cavanagh et al. (44) measured the foot forces of astronauts on Earth and on the International Space Station. Similar to the Fritton study, on earth, there are more occurrences of low magnitude forces derived from daily activity than high magnitude forces derived from walking or exercise. Cavanagh et al. also showed that despite strenuous daily exercise during microgravity not only are the foot forces decreased but the number of low magnitude forces is decreased. Therefore, reintroducing a portion of the ground reaction forces lost during unloading may retard its detrimental effects.

A previous study (96) described the use of low-level vibrations as a countermeasure to IVD alterations from long term bed rest. Healthy human subjects of astronaut age (35±7 yrs, 18 males, 11 females) without a history of back pain were randomly assigned to a control (CTR, n=11) or a low-magnitude mechanical signal intervention (WBV, n=18) group. All subjects underwent continuous 6º head-down bed rest for 90 d followed by a 7 d reambulation period. While maintaining a supine position, WBV subjects were exposed to short durations (10 min/day) of low-magnitude mechanical signals at a frequency of 30 Hz and an acceleration

magnitude of either 0.3 g (n=12) or 0.5 g (n=6). The vibrations were introduced into the axial skeleton through the plantar surface of the feet by means of an upper-body harness that was coupled to the vibrating plate through linear springs. Subjects received spinal MRI scans (n=7 for CTR, n=17 for WBV) at 0 d, 60 d, 90 d and after completion of bed rest (90+7 d). Computed tomography scans of the lumbar spine (n=11 for CTR, n=18 for WBV), were taken at 0 d and 90 d of bed rest to analyze the cross-sectional area of the erector spinae including transversospinal muscles. Symptom complaint logs were available for 29 subjects (n=11 for CTR, n=18 for WBV).

While WBV spinal length increased significantly during the 90 d bed rest protocol, this increase was significantly less than in CTR subjects at 60 d (3.2 mm) and 90 d (1.8 mm). In contrast to CTR subjects, spinal length of WBV subjects returned to baseline levels upon 7 d of reambulation. Bed rest in control subjects increased IVD volume (averaged between L1 and S1) by 15% over 90 d. Importantly, even seven days after completion of the bed rest trial, CTR subjects still showed 8% greater IVD volumes relative to baseline. Vibrations attenuated IVD expansion during bed rest to 10% after 90 d, which is an expansion typical of overnight bed rest (158). In WBV subjects, 7 d of re-ambulation, without WBV treatment, returned IVD volumes to baseline, a response that was significantly different from CTR subjects. IVD convexity, a measure of spinal health, showed a similar effect to bed rest and vibrations.

While the muscle atrophy in subjects treated with vibrations was 6.6% (a non-significant 9.0% smaller loss than in untreated subjects), disc expansion across all subjects was negatively correlated with muscle atrophy (R^2=0.50). Subjects with lower back pain were also afflicted with greater muscle atrophy (-5.9% vs -7.8%). After 90 d of bed rest and 7 d of reambulation, 46% fewer WBV subjects experienced lower back pain than CTR subjects. The potential benefit

of these low magnitude mechanical signals was not confined to the bed rest period *per se*, but extended into the immediate re-ambulation period. The improved reambulation effect is important as reambulation alone does not curb the biochemical and genetic expressions changes noted in the annulus fibrosus after unloading (241).

Harmful Vibrations

While data exist on the benefits of whole-body vibrations, their application must be carried on with caution. Chronic vibrations in helicopter pilots, automotive drivers, and construction workers (135) are associated with LBP (31) and occur in the resonant frequency range of several anatomical structures. The application of vibrations at the resonant frequency of a tissue is dangerous because the displacement of the tissue at that frequency is largest. The resonant frequency of the spine is 4-8 Hz (135, 183, 202) and must therefore be avoided. In response, the International Standards Organization has established exposure limits to vibrations, incorporating acceleration, frequency, duration of exposure, and direction. Harmful effects on the musculoskeletal system occur with vibration accelerations exceeding 1g (1).

Loading Response of Intervertebral Disc

The IVD and other weight-bearing cartilages are constantly subjected to static and dynamic loads. The disc's ability to withstand such varying stresses is dependent upon, but not limited to, the IVD's cellular and molecular response. Static compression inhibits the disc's biosynthesis of proteoglycan, aggrecan, collagen type II, and other proteins (36, 178, 197). The inhibition can occur as quickly as 1 h after the application of compression (197). For example, Kim et al. (131) reported an inhibition of GAG biosynthesis of 25% and after statically loading cartilage at 50% compression for 12 h, 2.5 days were necessary before the aggrecan biosynthesis levels were at

free-swelling levels. Although high levels or duration of static compression have been shown to lead to the inhibition of protein biosynthesis and cell apoptosis (153, 221), all static compressions are not catabolic. The biosynthesis of GAGs and other proteins may also depend on the static stress level and duration of the load (103, 105, 178).

Dynamic compression can stimulate cellular and matrix synthesis (130, 132), but its efficacy is dependent on the amplitude and frequency of the load (25, 197, 221). Large, dynamic compressions (1-5% strain) of the extracellular matrix cause deformation of cells and matrix (37, 192), hydrostatic pressure gradients and interstitial fluid flow (80, 130), physicochemical changes such as streaming potentials, altered osmotic pressures and disc water content (46, 130, 225), all of which may initiate GAG biosynthesis in the IVD. Large, cyclic compression dramatically affects the proteoglycan synthesis in the distal regions of the extracellular matrix (192) and up-regulates aggrecan gene expression (36).

Although there is compelling evidence of the importance of compression-induced fluid movement in the stimulation of chondrocyte biosynthesis (25, 38, 192), the separation of the effects of the fluid flow from the deformation of the cell/matrix is complex. Dynamic compression is comprised of a concert of changes including variations in volume, shear stresses, and fluid flow (130). However, none of these alterations (besides shear stress changes) should occur in a poroelastic tissue under shear. Experiments aimed at distinguishing the stimulation of protein biosynthesis by cell and ECM deformation rather than fluid flow were carried out with significant increases of GAG and collagen markers (25% and 41%, respectively) (73, 118). In a related but separate experiment, biosynthesis comparisons were made at the inner core and

lamellar rings of the AF to show no significant differences (132) suggesting that matrix deformation, not fluid flow, was attributed to the stimulation.

Matrix deformation is the unlikely culprit in the Holguin et al. (96) IVD study as the amplitude of the signal was extremely small (~165 μm). The strain in the IVD due to low-magnitude vibrations is unknown but unlikely similar to the large deformations encountered during postural and dynamic loading (108, 161, 210, 230). Wang et al. (230) using axial images showed no deformation occurred in the NP of the disc and O'Connell et al. (173) using sagittal images of axial compressions of the human cadaveric spines showed that regions of zero deformation (transitions from compression to tension) exist throughout the IVD. Therefore if habitual weightbearing manages to maintain discal integrity and health regardless of regions of low deformation, a mechanism unrelated to strain must also exist.

In bone, low-magnitude vibrations induce anabolic but extremely low strains of ~10 με (122) and due to the inability of bone cells to sense these small strains (242), it seems secondary events, e.g. fluid flow shear stress, may play a more pressing role in motivating these cells during low-magnitude stimuli. For instance, the application of short-duration, interstitial fluid flow in the absence of bone strain inhibited hindlimb unloading-induced bone loss (137). However, the application of low-magnitude vibrations in rodents shows a differential response between a 45Hz and 90Hz signal in attenuating bone loss (122). The differential response suggests that fluid flow may not be the anabolic cause as the stress magnitudes between the two interventions may be similar (231). Similarly, gene expression of bone cells to high-frequency, low-magnitude vibrations is frequency dependent with greater expressions at increasing frequencies, but is also unrelated to the fluid shear stress generated by the

vibrations as the estimated magnitude was several orders of magnitude below known stimulatory levels (141).

The mechanism for large loads may include deformation and stimulation of the IVD and its incumbent viscoelastic cells (216). However, low-magnitude, high-frequency vibrations must employ a different mechanism as cells stimulated at high frequencies stiffen increasingly and non-linearly, resisting deformation (147). Therefore, the detection of the signal by the cells of the intervertebral disc may involve a sensitivity to the applied frequency (57). One proposed frequency-dependent mechanism is the acceleration of the nucleus of the cell within the cytoskeleton (12). For example, vibration amplitudes an order of magnitude below those imposed in the Holguin et al. study can stimulate chondrocyte proliferation and proteoglycan synthesis (126, 152). However, this does not preclude the involvement of additional factors which may contribute to the activity of cells, such as the morphology of the cell or IVD. In addition, high-frequencies may have the added benefit of serving as a surrogate to the low strains produced by muscle contractions above 20Hz (98). Other stimulatory modalities to IVD cells and chondrocytes that do not require matrix deformation include ultrasound and pulsed electromagnetic fields (55, 116).

Summary

Hypo-physiologic loading conditions may accelerate degradation of intervertebral discs. Excessive degradation of the morphology and biochemical composition of the intervertebral disc is typical of disc degeneration and may, ultimately, lead to back pain and/or herniation of the nucleus pulposus. Short-periods of ambulation, with and without exercise, are incapable or minimally capable of normalizing the morphology of the IVD during and after unloading.

Although exposure to large magnitude chronic vibrations can be damaging to the musculo-skeletal system, extremely low-magnitude, high-frequency vibratory signals have been shown to attenuate the morphological changes of the IVD during extended bed rest despite the low amplitude of the signal.

II

HYPOTHESIS AND SPECIFIC AIMS

No study has effectively utilized a countermeasure to the compromised intervertebral discs (IVD) of animals subjected to hindlimb unloading. *Here, the hypothesis is that low-magnitude, high-frequency vibrations will mitigate the IVD alterations from hindlimb unloading.* The proposed study will examine morphological (**Hypothesis 1-3**), sulfated-glycosaminoglycan (sGAG) and collagen content (**Hypothesis 1 and 2**), and biomechanical (**Hypothesis 3**) disruptions of the IVD of hindlimb unloaded rats and their prevention by low-magnitude vibrations applied in the prone or upright position. Secondary tissues will include paraspinal muscle and vertebral bone.

Hypothesis 1: Ambulation, with or without low-magnitude, high-frequency vibrations applied in prone postural rats will not maintain the lumbar IVD morphology and composition during hindlimb unloading.

Hypothesis 2: Low-magnitude, high-frequency vibrations applied in erect postural rats will mitigate the unloading-induced hypotrophy of the nucleus pulposus and annulus fibrosus

Hypothesis 3: Low-magnitude, high-frequency vibrations applied in erect postural rats will mitigate the altered biomechanical properties of the lumbar intervertebral discs of hindlimb unloaded rats.

III

EFFECT OF BRIEF AMBULATION, WITH OR WITHOUT WHOLE BODY VIBRATIONS, ON RAT DISC HEALTH DURING HINDLIMB UNLOADING

ABSTRACT Changes in intervertebral disc (IVD) morphology and biochemistry have been characterized only incompletely in the rat hindlimb unloading (HU) model. Here, we present preliminary data on the differential effects of short periods of weight-bearing with or without low-level whole-body vibrations (WBV) on the lumbar rat IVD during HU. Rats were subjected to HU and exposed to daily periods (15min/d) of either ambulatory activities (HU+AMB) or whole body vibrations superimposed upon ambulation (HU+WBV; WBV at 45Hz, 0.3g). At the end of the 4 wk experimental period and compared to age-matched control rats (AC), the lumbar IVD of HU+AMB had a 22% smaller glycosaminoglycans/collagen ratio, 12% smaller posterior IVD height, 13% smaller cross-sectional area, 9% greater ratio of height/area, and a 24% smaller volume of the surrounding muscle tissue. Compared to HU+AMB rats, the addition of low-level vibratory loading did not significantly alter IVD biochemistry, posterior height, area, or volume but curbed the loss of muscle volume (-8% versus AC) and maintained (-3% versus AC) the IVD height/area ratio. Relative to AC, superposition of the vibratory stimulus onto ambulation had a greater effect on IVD area than on IVD height. IVD volume and IVD posterior height of HU+WBV rats remained 13% and 16% smaller than in normal controls. Even though neither intervention was successful in preventing hindlimb unloading induced changes in IVD volume, compared to ambulation alone, very low-level whole-body vibrations resulted in diminished loss of total back and abdominal muscle volume and directionally altered IVD geometry.

Introduction

Decreasing the level of mechanical loading is detrimental for the function of the IVD. For instance, bed rest increases the compressibility of the spine (154), an indicator of reduced stiffness and IVD degeneration (89). Similarly, spaceflight increases the incidence of nucleus pulposus herniations (119). Both prolonged bed rest and spaceflight induce low back pain (102, 233). Neither the etiology and pathophysiology of IVD degeneration initiated by altered mechanical loading, nor efficacious countermeasures have been identified, in part because many important assays of IVD health are restricted to animal models. Unfortunately, a standard animal model of lumbar unloading that replicates human disc physiology as well as degenerative outcomes has not been established (211).

HU, the most commonly used animal model to simulate musculoskeletal, cardiovascular, orthostatic and metabolic changes due to microgravity and unloading (168, 187), reduces sulfated-glycosaminoglycan (sGAG) in the IVD (241) similar to rodent spaceflight studies (70, 187, 206). Interestingly, sGAG content, as a biochemical indicator of IVD health, is reduced even though HU subjects the spine to tensile forces, rather than unloading per se. A greater expression of molecules associated with catabolism, increased chondrocyte apoptosis, low intradiscal pressure, as well as muscle atrophy and disrupted back muscle recruitment provide further evidence that the change in the IVD mechanical environment with HU might present a signal similar to spinal unloading (87, 241). Even though HU may replicate some specific outcomes of altered loading of the IVD, others, including changes in IVD morphology, have been investigated only incompletely.

Several studies have tested mechanical countermeasures of IVD degradation generated by altered spinal loading. Short-periods of ambulation, with and without loaded backpacks, were incapable or only minimally capable of normalizing the morphology of the IVD after bed rest (104, 145). Forty-five minutes of treadmill exercise under negative body pressure was also not completely effective at mitigating IVD morphological changes in the lower lumbar of bed rest subjects (39). Similarly, in rats subjected to HU, reambulation only partially recovered sGAG-related changes emphasizing the need for preventive measures (241). While (re)ambulation can certainly (restore) prevent changes to the IVD (after) during unloading to some extent (104, 145), locomotory activities alone do not appear to be an efficacious countermeasure.

In contrast to the relatively low loading frequencies typically associated with physical exercise, increasing the frequency of the applied mechanical signals may provide benefits to the IVD during unloading. For instance, brief applications of whole-body vibrations (WBV) with (21) or without (96) resistive exercise maintain IVD morphology and may reduce muscle atrophy during long-term bedrest. While the physical mechanisms by which vibrations may be beneficial to the IVD are unknown, vibrations have been shown to modulate cellular activity (238), improve neuromuscular function (220), and reinforce lumbar proprioception (72). Here, using an animal model of altered spinal loading, we asked whether hindlimb unloading, interrupted by short periods of ambulation with or without superimposed low-level WBV, can maintain IVD morphology and biochemistry relative to normal ambulatory age-matched control rats.

Materials and Methods

Animals

This study was reviewed and approved by the Institutional Use and Care Committee of Stony Brook University. Eighteen female Sprague-Dawley rats were used in this study of which six ambulatory rats serves as age-matched control animals (AC). All rats had free access to a standard rat chow and water.

Equipment

A vibrating plate generated vertical oscillations at 45Hz and 0.3g (236). *In vivo* micro-computed tomography (μCT) images were captured with a VivaCT 75 scanner (Scanco Medical AG, Brüttisellen, Switzerland) at a resolution of 78μm (45kV, 177μA, 200ms integration time). A solution of Hexabrix (Mallinckrodt Inc, St Louis, MO) enhanced the contrast of IVD for e*x vivo* μCT imaging on a MicroCT 40 scanner (Scanco Medical AG) at a resolution of 20μm (45kV, 177μA, 300ms integration time). Biochemical data were collected using a 1,9-dimethylmethylene blue (Sigma-Aldrich, St. Louis, MO) and hydroxyproline assay (Sigma-Aldrich).

Procedures

Twelve rats (10wk of age) were subjected to hindlimb unloading (HU) for 4 wk according to the Morey-Holton method (168). Once a day, for 15min/d, six of the unloaded rats were removed from unloading and allowed normal ambulatory activities in their cages (HU+AMB). The other six rats were also removed from unloading but their cages in which they were allowed to freely ambulate were placed on a vertically oscillating plate (HU+WBV).

At baseline and 4 wk, the lumbar region between the superior planes of L1 and S1 was scanned *in vivo* by μCT. An automated algorithm (123) segmented muscle from bone and quantified total abdominal muscle volume including the multifidus, lumbar erector spinae,

quadratus lumborum, psoas, rectus abdominis, and anterolateral abdominal muscles. The sensitivity of muscle to resistive exercise with whole-body vibrations may differ between specific muscle groups (21) but the scans did not allow the separation of individual muscle groups. The apparent volumetric mineral density of the L1-S1 spinal segment was determined *via* calibrated phantoms (163). After sacrifice, the lumbar spine (n=5/group) was excised of extraneous tissue, soaked in a 40%/60% solution of Hexabrix/0.15 M PBS for 1hr to enhance contrast (182), and imaged *ex vivo* by μCT.

The volume, area and height of each lumbar IVD were determined by a semi-automated algorithm that segmented the IVD by density. The ratio of IVD height/area, a variable that has been associated with IVD degeneration (189) as well as mechanical parameters including the apparent elastic modulus and hydraulic permeability (61, 79), was computed. Mediolateral (ML) and anteroposterior (AP) lengths and anterior (ANT) and posterior (POS) disc heights were determined directly from the 3D tomographies (**Figure 1**). AP length was computed as the average of the left, center, and right anteroposterior lengths. ML was computed as the mediolateral length with the greatest distance between the medial and lateral aspects. ANT height was computed as the average IVD height of the anterior half of the IVD while POS weight corresponded to the average height of the posterior half of the IVD.

Following scanning and rehydration, IVD samples (n=5/group) were evaluated for sGAG content by a 1,9-dimethylmethylene blue assay and for collagen (Col) content by a hydroxyproline assay (93). All outcome variables were calculated for each individual IVD as well as averaged across the lumbar IVD of each spine, resulting in a single IVD value for any given rat.

Statistics

One-way ANOVA with protected post-hoc Fisher's LSD tests were used to compare differences between the three groups. A two-way ANOVA was used to examine interactions between *group* (HU+AMB vs HU+WBV) and *direction* (area vs height) as well as for interactions between *group* and *disc level* (L1-L2 through L6-S1). For the analysis testing the interaction between group and direction, each data area and height measurement within the two experimental groups was normalized to the respective AC mean. Data were expressed as mean ± standard deviation. Relative differences between sample means were denoted as percent difference ± standard deviation of the sampling distribution of the relative difference (relative standard error of the difference). Statistical significance was considered at $p \leq 0.05$.

Results

After 4 wk of HU and compared to age-matched control rats, HU+AMB rats weighed less (-25±4%), $p<0.001$) and had smaller apparent vertebral bone density (-9±2%, p=0.002) (**Table I**) and muscle volume (-24±3%, p=0.001) (**Figure 2**). Averaged across disc levels, IVD sGAG/Col content was 22±6% (p=0.009) less and volume was 18±5% smaller (p=0.005) in HU+AMB rats than in AC (**Figure 2**). For individuals discs, the volume of the L3-L4 (-23±9%, p=0.017), L4-L5 (-21±8%, p=0.015), and L5-L6 (-24±4%, p=0.001) IVD were smaller in HU+AMB than in AC (**Figure 3**). IVD volume at L1-L2 (-12±9%, F=0.93, p=0.421), L2-L3 (-2±6%, F=0.48, p=0.633), and L6-S1 (-18±6%, F=3.11, p=0.082) did not show significant differences. Posterior IVD height of HU+AMB rats was 12±5% smaller (p=0.005) than of controls but the differences in average disc height (-5±4%, F=3.39, p=0.068) and anterior disc height (-3±3%, F=2.59, p=0.117) were not significant between groups (**Figure 4**). IVD area was 13±4% smaller (p=0.004), AP length was 8±3% smaller

(p=0.023) while ML length (-4±2%, F=1.50, p=0.262) did not show significant differences between the two groups (**Figure 5**). The ratio of IVD height to area was 9±5% greater in HU+AMB than in controls but the p-value only approached significance (p=0.055) (**Figure 6**).

At sacrifice, the body mass of HU+WBV rats was 16±7% greater (p=0.023) than the body mass of HU+AMB but 14±4% smaller (p=0.009) than that of AC rats (**Table I**). The apparent vertebral bone density of HU+WBV was not different from HU+AMB (-3±3%, p=0.246) but 12±2% less (p<0.001) than of AC. In contrast, muscle volume of HU+WBV was 21±9% greater (p=0.018) than in HU+AMB rats and not different (-8±7%, p=0.187) from AC rats (**Figure 2**). IVD sGAG/Col content of HU+WBV rats was not significantly different from HU+AMB (12±9%, p=0.303) or AC (-13±7%, p=0.067) rats (**Figure 2**). The average IVD volume of HU+WBV rats was not different from HU+AMB (3±6%, p=0.694) and 16±5% smaller (p=0.010) than in AC rats (**Figure 2**). When individual discs were compared, the L4-L5 IVD volume of HU+WBV rats was not different from HU+AMB (3±8%, p=0.779) but 19±8% smaller (p=0.025) than in AC. L5-L6 IVD volume of HU+WBV was not different (1±9%, p=0.898) from HU+AMB but 24±5% smaller (p=0.001) than of AC (**Figure 3**). Further, L1-L2 (4±9%, -8±11%; F=0.93, p=0.421), L2-L3 (-6±9%, -7±8%; F=0.48, p=0.633), L3-L4 (10±10%, p=0.386; -16±8%, p=0.086) and L6-S1 (4±10%, -15±9%; F=3.11, p=0.082) IVD volumes of HU+WBV rats did not show significant differences to either HU+AMB or AC groups.

When HU+WBV was compared to both HU+AMB and AC, differences in average IVD height (-5±3%, -9±4%; F=3.39, p=0.068) and anterior height (-3±2%, -6±3%; F=2.59, p=0.117) were non-significant (**Figure 4**). Posterior IVD height of HU+WBV rats was not different (-1±3%, p=0.901) from HU+AMB but 13±5% smaller (p=0.018) than in AC rats. IVD area (7±5%, p=0.126;

-7±3%, p=0.085), AP length (3±4%, p=0.454; -6±3%, p=0.093), and ML length (3±2%, 0±2%; F=1.50, p=0.262) of HU+WBV rats were not significantly different from HU+AMB or AC (**Figure 5**). The ratio of IVD height/area in HU+WBV rats was 10±4% (p=0.005) smaller than in HU+AMB but not different (-3±4%, p=0.216) from AC (**Figure 6**). A two-way ANOVA demonstrated that the effect of WBV, when compared to ambulation alone, was significantly different (p=0.039) between IVD area and IVD height (**Figure 4,5**). In other words, WBV altered IVD morphology in a directional manner when compared to ambulation, with a significantly greater benefit (relative to AC) for IVD area than for IVD height. No interaction existed between disc level and group for any given outcome variable.

Discussion

The purpose of this study was to contrast the ability of brief periods of ambulation, with or without low-level whole body vibrations, to curb the geometric and biochemical changes of the rat IVD during HU. Hindlimb unloading interrupted by brief periods of ambulation led to degradation of IVD morphology and biochemistry as well as muscle volume. Superimposing whole body vibrations upon the brief ambulation periods partially prevented the decrease in lumbar muscle volume but not IVD volume, posterior disc height, area, anteroposterior length and sGAG/Col content, and lumbar spine bone density. In addition, the low-level vibratory signals provided a directional benefit for the lumbar IVD hypotrophied by altered spinal loading, normalizing the ratio of IVD height/area to that of normal age-matched controls. While the IVD height-to-area ratio has been linked to disc health (189), further studies are needed to define the benefits of whole body vibrations on the morphological, biochemical, and mechanical properties of the IVD in this rat model.

Statistically significant differences were detected between all three groups but, inherently, the relatively low statistical power of this study may have masked differences that more highly powered studies may detect in the future. Also, physical activity levels were not measured and it is conceivable that the two HU groups received different levels of locomotory derived stimuli. The hindlimb unloaded rat was used as the animal model for this study because of its extensive use in the literature to simulate altered loading in a variety of biologic systems including the IVD. Because of its quadrupedal nature, it is by no means an ideal model for the erect human spine. Nevertheless, it may aid in understanding human spinal mechanics because it is also predominantly loaded in the axial direction (208) and when normalized to disc geometry, the lumbar discs of rodents reveal similar mechanical properties to human lumbar IVD (61). And while there are cell population disparities between the IVD of rats and humans (222), chondrocyte-like cells dominate the cell population of the IVD in both species (99). Together, the rat may serve as a model to test specific hypotheses involving IVD degradation but postural and cellular differences to humans need to be considered when interpreting and extrapolating the results to humans.

Hindlimb unloading subjects the tail to a tensile load of 50% body-weight (88), distributed to vertebrae, IVD, ligaments and zygapophysial joints. Considering that HU, unlike space travel or bedrest, does not remove *loading* per se, the associated hypotrophy of the rat IVD, rather than hypertrophy commonly seen in bedrest and human spaceflight studies (145, 233), may not appear surprising. Short-term, five-day, spaceflight, did not alter IVD height in rats (206). However, the annuli of IVD of rats had significantly *less* wet and dry weights after 14 days of spaceflight (187) and because of the link between disc size and water content, likely a lesser

IVD volume. Compared to 14 days of spaceflight, 14 days of HU did not alter the wet or dry weight of the annulus compared to the same control rats used for the spaceflight analysis and these two IVD properties were greater than in rats flown in space (187). Even though this study did not include measurements of the highly hydrated nucleus pulposus, their data suggests that the signal associated with HU is not analogous to that of spaceflight for the rat IVD and, together with our data, indicates that neither HU nor spaceflight in rodents replicate the IVD morphological changes induced by gravitational unloading in humans.

Six-degree head-down bed rest is the most commonly used method for simulating microgravity on Earth, producing greater morphological changes in the inferior lumbar IVD (20). Despite the hypo/hyper-trophy IVD disparity between the effect of HU and 6^{o} head-down bed rest, HU in the rat also led to greater morphological changes in the inferior lumbar IVD (L3-L6), somewhat in contrast to horizontal bed rest during which no consistent interactions between disc level and disc height or area were observed across different time points (21). Even though changes in IVD morphology after long-term spaceflight are not available on a disc-specific level and HU decreases the size of the IVD while bed rest increases the size of the IVD, it is interesting to note that both rodent HU and human 6^{o} head-down bed rest models alter the size of the lumbar IVD in a similar disc-level dependent manner.

The lack of a group of HU animals that did not receive any intervention (HU alone) precluded any conclusions regarding the effect of ambulation by itself. Nevertheless, short periods of weightbearing did not ablate the change in IVD morphology and biochemical content compared to AC rats, largely consistent with previous data. For instance, short-duration ambulation with or without additional loading via backpacks did not inhibit changes to altered

IVD morphology from one day of bed rest (104). Similarly, 1-6wk of reambulation that followed ≥12wk of bed rest did not ablate the changes in IVD morphology (96, 145). On the other hand, short periods of reambulation following 5wk bed rest attenuated the change in IVD size (145). In rats, reambulation following HU only partially normalizes sGAG-related changes (241). Even though reambulation alone may eventually normalize the morphology of the IVD, such as after short periods of spaceflight (145), early preventive measures are important as the risk of IVD damage remains high immediately upon reambulation under normal weightbearing (119). Interestingly, best rest studies have indicated that the application of vibrations may achieve, at least in part, this goal (21, 96).

The reduced ratio of sGAG/Col content and increased ratio of IVD height/area in rats in which HU was interrupted by 15min/d of weightbearing suggests a degraded matrix. In both experimental groups, the degradation of IVD height was focused on the posterior aspect perhaps because compared to the anterior region, the posterior region is weaker under uniaxial tension (3), suffers greater deformations in degenerated discs (247), and shows greater expansion during 6^{o} head-down bed rest (20). By attracting less fluid, the reduced sGAG/Col ratio reduces disc stiffness, intradiscal pressure, and mechanical support. Further, lower intradiscal pressure and a concomitant increase in the height/area ratio may negatively impact the disc's natural anisotropy by disorganizing the collagenous annulus (84) and reduce fluid movement, and consequently nutrition, to the radial periphery of the disc (79). While alterations to disc height or shape do not necessarily assert a degenerated disc, their appearance can mark the onset of degeneration and aging (79, 189).

Low level vibrations can both stimulate bone formation and reduce bone resorption (236). Here, in tandem with ambulation, WBV was not more successful than ambulation alone in stemming the decrease in the apparent density of the lumbar vertebrae during HU. The low resolution of the μCT scans which was optimized for determining muscle volume did not allow the quantification of trabecular morphology and benefits to the trabecular structure cannot be excluded. It is also possible that the vertically applied signal was dampened to a degree that, while being partially anti-catabolic to IVD and muscle, it became ineffective in calcified tissue. Nevertheless, the results are entirely consistent with data from a recent study in which low-level whole body vibrations also did not attenuate bone loss in the proximal tibia of HU mice but preserved osteoprogenitor cell populations in the marrow and enhanced recovery of bone mass during reambulation (181).

The mechanism(s) by which the IVD and lumbar musculature receives and responds to high-frequency mechanical signals is unclear. Here, whole body vibrations were applied in a vertical direction and with exception of the limited time that the rats spent on their hindlimbs, no compressive gravitational load acted in the axial direction of the spine during the 15min/d of treatment. Similar to previous data suggesting that low-level vibrations can be anabolic to muscle (237), here, rats that received vibrations in addition to ambulatory periods lost less muscle volume than those that were only subject to ambulation. Thus, the geometric changes to the IVD may have been related to increased paraspinal muscle activity during vibrations (49) and/or greater muscle volume that conferred stronger contractions and forces onto the disc during suspension. Clearly, alternatives to a muscle loading hypothesis exist. For instance, the directional response of the IVD to the vertically applied mechanical intervention that

normalized the height/area ratio may have been modulated by cells within the IVD that responded directly to the oscillatory accelerations (238), rather than to deformation per se. Further work is required to elucidate the mechanism by which vibratory loading can affect disc health.

In summary, interrupting HU by 15min/d of weight bearing did not maintain the composition or the geometry of the IVD. Similarly, the superposition of low-level WBV onto ambulation did not prevent the loss of sGAG/Col content, disc area, disc anteroposterior length, disc volume, and lumbar bone density during unloading. Instead, the vertically applied oscillatory signal attenuated the loss of total lumbar and abdominal muscle volume, exerted a greater effect on IVD area than on IVD height and normalized the IVD height-to-area ratio to normal control levels. The mechanism by which muscle and IVD responded to the mechanical signal and whether vibrations applied in the axial direction of the spine can more completely inhibit IVD degradation remain to be investigated.

List of Tables

Table 1. Body mass and apparent vertebral bone density of the lumbar spine of AC, HLU+AMB, and HLU+WBV groups

Group	Body Mass at 0 wk [g]	Body Mass at 4 wk [g]	Bone Density at 4 wk [mgHA/cm^3]
AC	231.8±21.8	345.2±12.4	493±17
HLU+AMB	215.2±16.7	257.8± 30.2†	447±23†
HLU+WBV	222.8±34.8	297.8± 34.3†‡	433±21†

Mean±standard deviation of body mass and apparent vertebral bone density of the lumbar spine in the three groups (n=6 each). Significantly different from AC: † $p<0.01$. Significantly different between HLU+AMB and HLU+WBV: ‡ $p<0.05$.

List of Figures

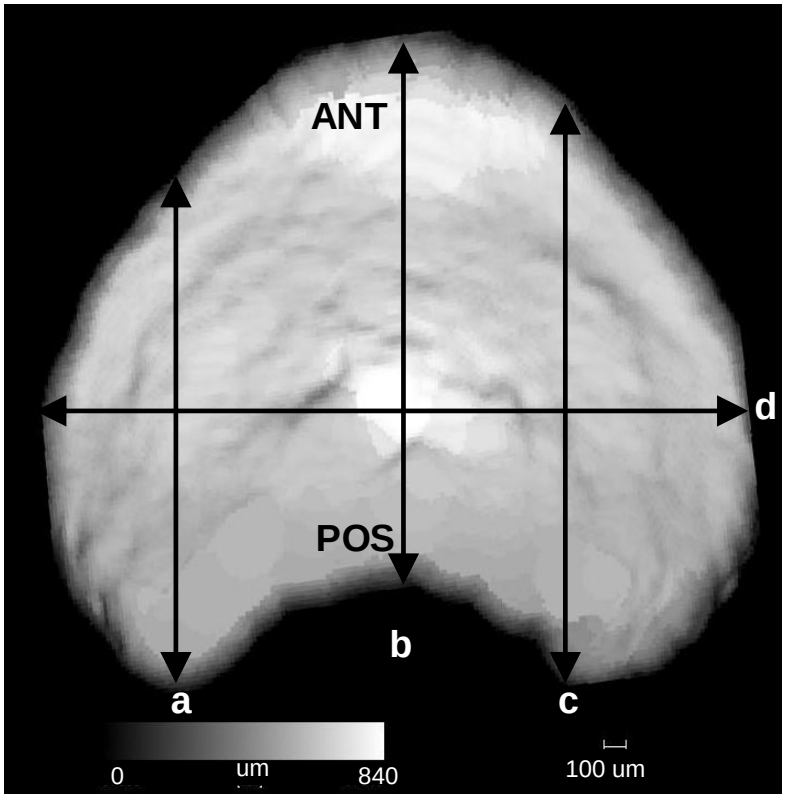

Figure 1. *Height map of an IVD illustrating the (a) left, (b) center and (c) right anteroposterior length, and the (d) mediolateral length. ANT corresponded to the average IVD height of the anterior half of the IVD while POS corresponded to the average IVD height of the posterior half of the IVD.*

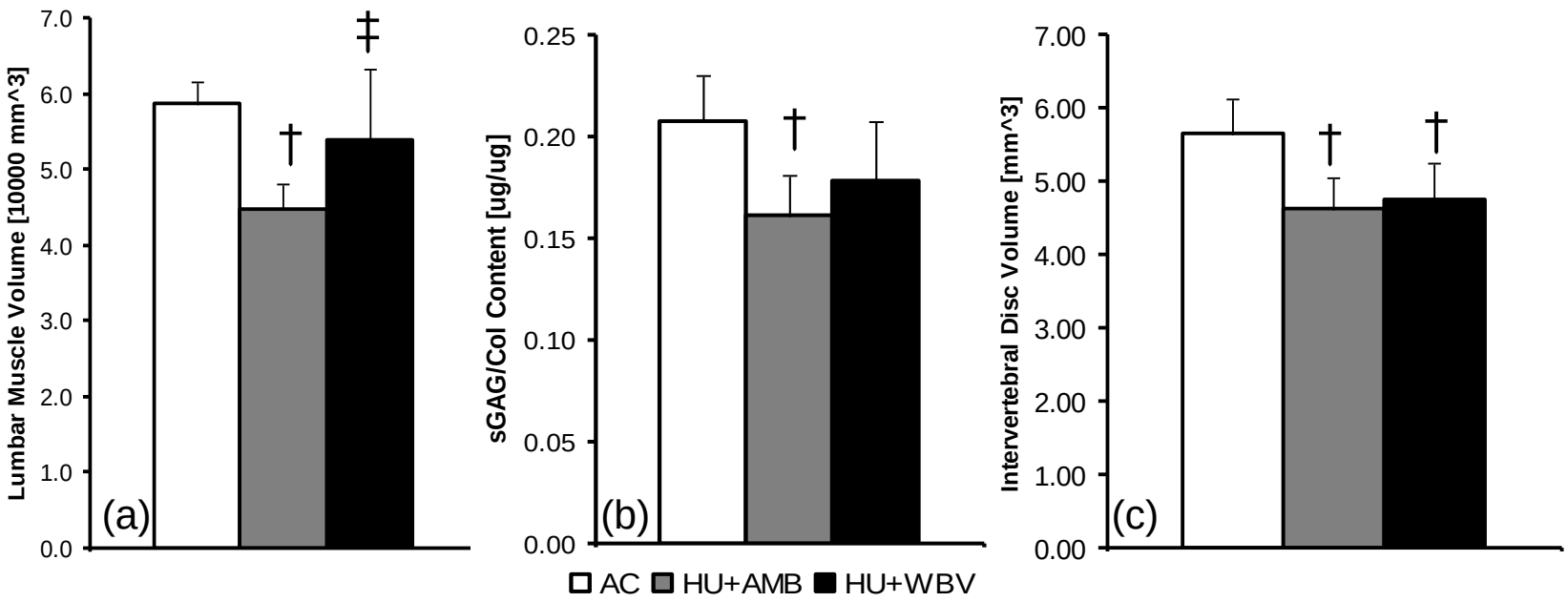

Figure 2. *(a) Lumbar muscle volume, (b) sGAG/Col content, and (c) IVD volume of age-matched control (AC), hindlimb unloaded interrupted by ambulation (HU+AMB), and hindlimb unloaded interrupted by ambulation plus WBV (HU+WBV) rats after 4 wk of HU; mean+SD (n=5-6 each). † p<0.05 compared to AC, ‡ p<0.05 compared to HLU+AMB.*

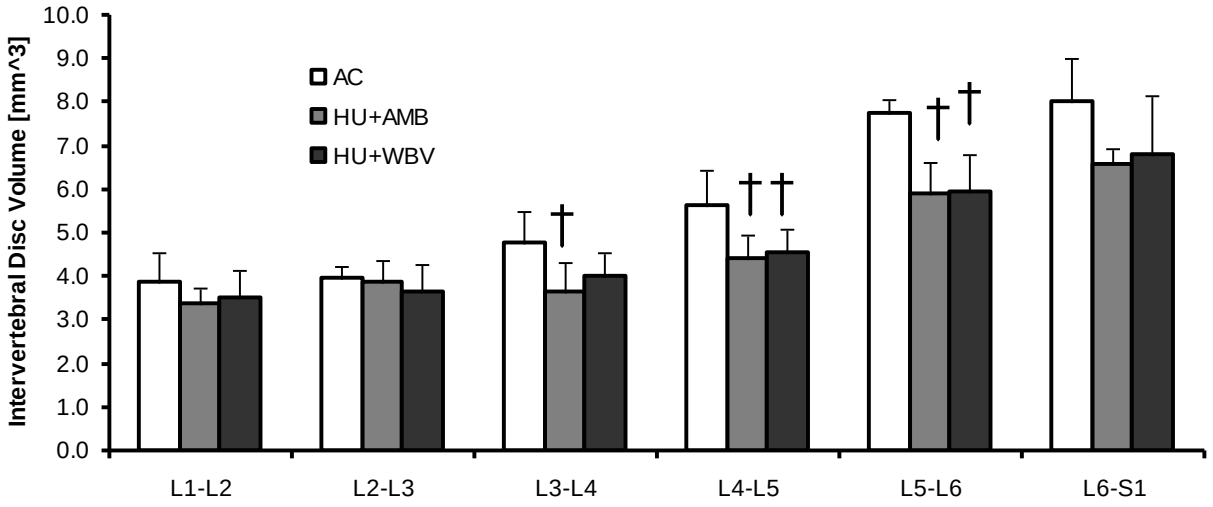

Figure 3. *Volume of each lumbar IVD of AC, HU+AMB, and HU+WBV rats at 4 wk; mean+SD (n=5 each).* † *p<0.05 compared to AC.*

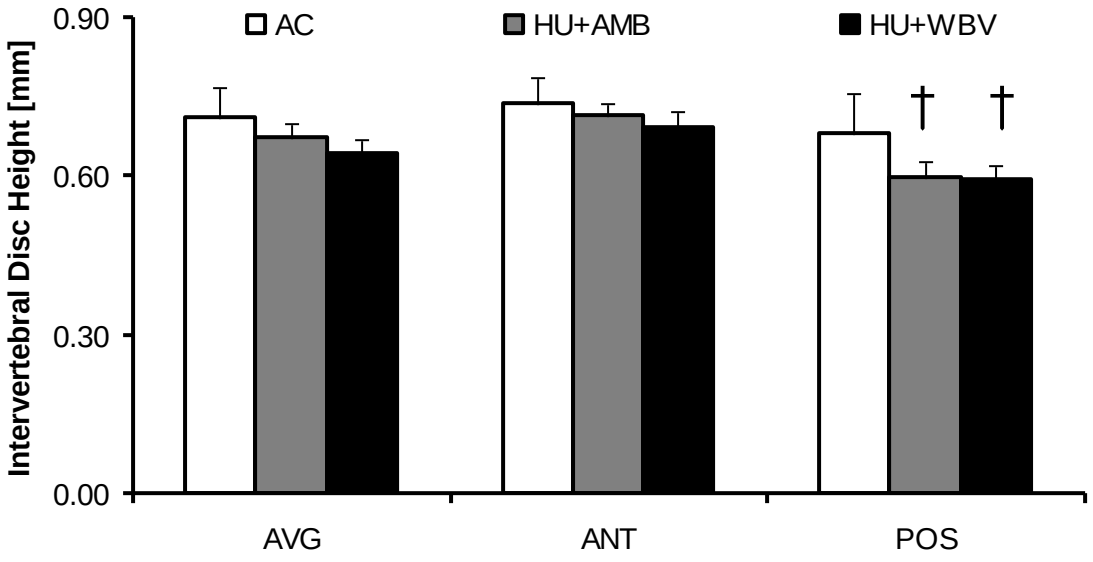

Figure 4. *Average (AVG), anterior (ANT) and posterior (POS) height of the IVD of AC, HU+AMB and HLU+WBV at 4 wk; mean+SD (n=5 each). † p<0.05 compared to AC.*

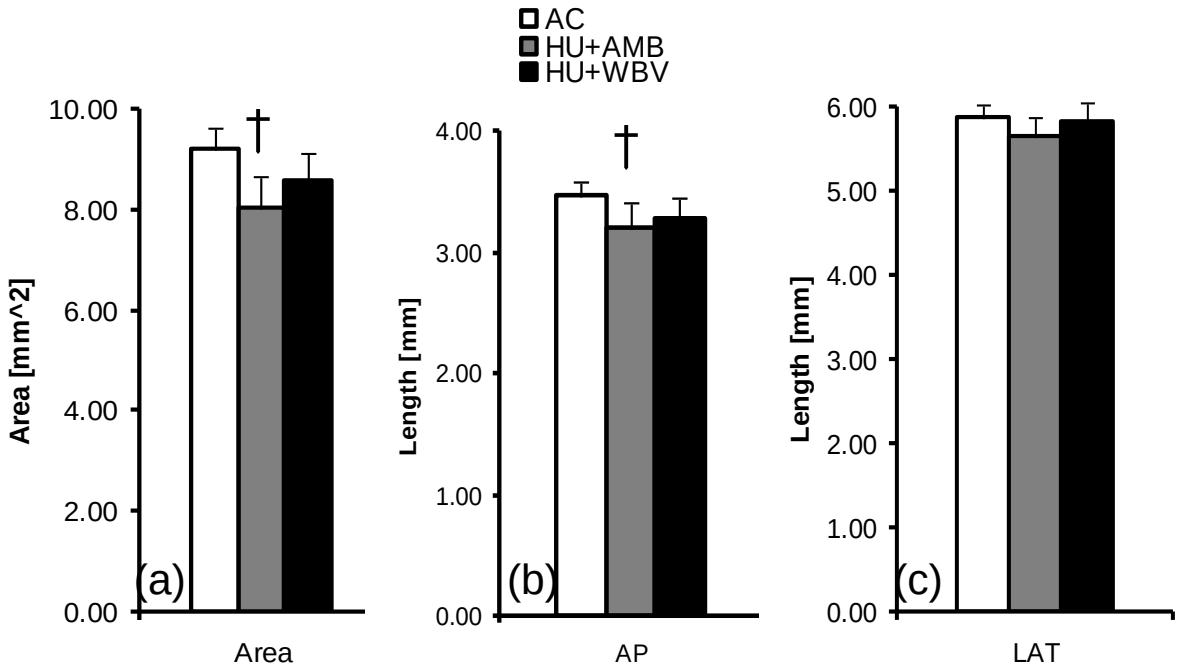

Figure 5. *(a) Area, (b) anteroposterior (AP) length and (c) mediolateral (ML) length of IVD of AC, HLU+AMB and HLU+WBV at 4 wk; mean+SD (n=5 each). † p<0.05 compared to AC.*

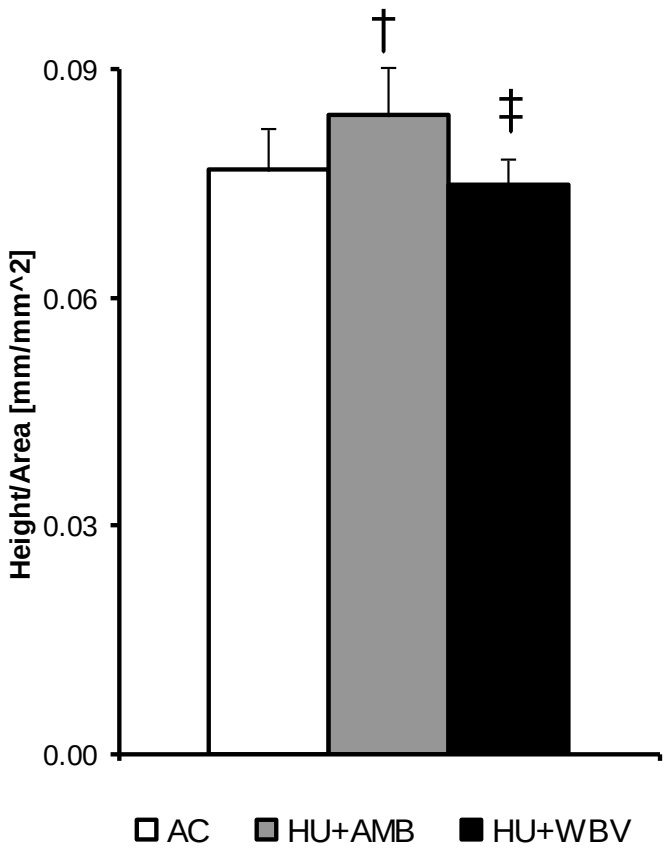

Figure 6. *Height-to-area ratio of IVD of AC, HLU+AMB and HLU+WBV at 4 wk; mean+SD (n=5 each). † p=0.055 compared to AC, ‡ p<0.05 compared to HLU+AMB.*

IV

BRIEF VIBRATIONS APPLIED IN ERECT POSTURAL RATS MITIGATE HINDLIMB UNLOADING-INDUCED DEGRADATION OF THE NUCLEUS PULPOSUS AND ANNULUS FIBROSUS

ABSTRACT Hindlimb unloading causes hypotrophy of the intervertebral disc (IVD) in the form of reduced height and glycosaminoglycan content, both characteristic of disc degeneration. Here, we tested the hypothesis that low-magnitude, vibrations will mitigate IVD hypotrophy and biochemical deterioration during hindlimb unloading in the rat. Four groups of Sprague-Dawley rats (4.5mo, n=11/group) were hindlimb unloaded (HU) for 4 wks. In two HU groups, unloading was interrupted for 15min/d by placing rats in an upright posture on a vertically oscillating plate (0.2g) at either 45Hz or 90Hz (HU+45 or HU+90). Sham control rats stood on an inactive plate (HU+SC). Compared to normally ambulating age-matched controls (AC), four weeks of unloading with or without brief upright posture (HU±SC) caused an 8% smaller IVD area, a 10% smaller average height, and a 19% smaller volume. Similarly, the IVD of HU±SC had less glycosaminoglycans in the nucleus pulposus (21%), anterior annulus fibrosus (16%) and posterior annulus fibrosus (19%). The application of the 90Hz, but not 45Hz, mechanical signal provided significant morphological and biochemical benefits. Compared to HU±SC, the IVD of HU+90 had 8% larger average height and 19% larger IVD volume. Similarly, the IVD of HU+90 had more glycosaminoglycans in the nucleus pulposus (24%), anterior annulus fibrosus (17%) and posterior annulus fibrosus (19%). These data suggest that low-magnitude vibrations, when applied at high frequencies, may play a role in maintaining disc health.

Introduction

Reduced spinal loading during immobilization, sedentary lifestyle or spaceflight may produce disc degradation and ultimately low back pain (154, 196, 211, 233), and may concurrently induce bone loss, muscle atrophy, cardiovascular changes, orthostatic intolerance and metabolic alterations. Astronauts returning from spaceflight also show disrupted IVD structure and nucleus pulposus (NP) herniations at a greater incidence than the general population and army aviators population (119, 233). Spinal unloading during prolonged bed rest induces greater changes in posterior disc height and back pain (19), potentially by straining innervated zygapophysial joints (107). While the specific etiology of back pain remains unknown, disc degeneration is largely implicated as a source because of the extensive changes to the disc which may cause pain for other reasons. For example, stimulating the nociceptive nerves of the annulus fibrosus (AF) and anterior dura mater (52, 200) may, in moderately degenerated discs, originate from reduced disc height, reduced water content or low intradiscal pressure and, in severely degenerated discs, originate from radial tears and rim lesions (29, 199). In the nucleus pulposus (NP), degradation may initiate release of nerve-stimulating cytokines (113). In addition, degeneration of the IVD precedes herniation of the NP, which typically occurs in the weaker, more deformable posteriolateral region of the disc (3, 247).

Avoiding the progression of mechanically induced disc degeneration to back pain and to identify potential countermeasures requires a more complete understanding of how specific mechanical signals preserve IVD health. A standard small-animal model for altered spinal loading without biochemical or surgical disruption is yet to be established (204). Hindlimb unloading is commonly used to simulate the effects of weightlessness on the musculoskeletal,

cardiovascular and orthostatic systems. In the IVD, HU reduces the hydrostatic pressure (87), increases the expression of catabolic sulfated-glycosaminoglycan (sGAG)-related proteins (241), and induces chondrocyte apoptosis (15). These changes are congruous to changes leading to disc degeneration in humans even though HU imposes tensile loading on the rodent spine rather than unloading per se. As a reflection of the differences in the mechanical environment, disc height is reduced during hindlimb unloading (95), contrasting with the increase in IVD height during bedrest.

Short-duration exercise without weightbearing which is high in magnitude and low in frequency can restore the height of the IVD (170) but high-frequency, low-magnitude mechanical signals may also influence remodeling in the IVD (92). High-frequency, low-magnitude vibrations may preserve the morphology of the IVD and reduce the incidence of back pain exacerbated by prolonged bed rest (96). While the mechanism(s) of the mechanical signals remain(s) unclear, the benefits of vibrations include improvement of IVD (95) and bone (122) morphology, neuromuscular adaptation (220) and lumbar proprioception rehabilitation (72). Here, using HU to alter spinal mechanical loading, it our aim was: (1) to determine the spatially dependent geometric and biochemical changes of the rat IVD and (2) to test the efficacy of two vibration frequencies applied in the longitudinal direction of the rat spine to prevent the IVD degradation during hindlimb unloading.

Materials and Methods

Experimental Design.

This study was reviewed and approved by the Institutional Use and Care Committee of Stony Brook University. Female Sprague-Dawley rats (18wks, n=44) were hindlimb unloaded (HU)

(**Figure 7**) for 4 wk according to the Morey-Holton method (168). A subset of HU rats (n=11 per group) stood on a vertically oscillating plate in an upright position that was maintained via vertical plastic cylinders (height: 30.5 cm, inner diameter: 10.2 cm). The signal was applied for 15min/d at a peak acceleration of 0.2g at either 45Hz (HU+45) or 90Hz (HU+90). Sham control (HU+SC) rats stood in an upright position in the cylinder without receiving vibrations. HU rats received no intervention. Baseline (BC) rats of the same animal cohort and age-matched (AC) rats were used as controls. Animals had access ad libitum to standard rat chow and water.

Transmission Measurement.

Lumbar spine displacements were measured in two additional rats during upright vibrations using computer-aided speckle interferometry (45). Silicon carbide speckles were sprinkled onto double sided tape adhered to the shaved rat back and were recorded with a Redlake Motion Scope high speed camera (Del Imaging systems, Cheshire, CT) at 250 fps. Images (~14mm^2) of the vibrating plate and animal oscillating at either 45Hz and 90Hz (0.2g each) were partitioned into 30 sections. The displacement of each section from consecutive images was averaged for the entire image and across 0.06s, used to create a signal profile. The transmission measurements from the L5 region at 0Hz, 45Hz and 90Hz were averaged for the two rats.

Micro Computed Tomography.

Before sacrifice, an *in vivo* scout view (41µm resolution) for 5 animals in each group (VivaCT 75; Scanco, Bassersdorf, Switzerland) was used to determine the *in vivo* lumbar length from superior L1 to superior S1. After sacrifice, the spine was stored *en bloc* at – 20^{o}C. Following storage, the lumbar spine was excised of extraneous tissue, soaked in a 40%/60% solution of Hexabrix (Mallinckrodt Inc, St. Louis, MO) and 0.15 M PBS for 1h to enhance contrast (182) and

imaged by *ex vivo* microCT (MicroCT 40; Scanco) at a resolution of 20µm (45kV, 177µA, 300ms integration time) for IVD, as well as L2 and L5 trabecular morphology. A scout view at a resolution of 8µm was used to measure the *ex vivo* lumbar length from superior L1 to superior S1.

Each lumbar IVD was segmented by density and the volume, area and height were determined. The lumbar IVD of each spine were averaged to represent the overall IVD geometry. The anterior (ANT) and posterior (POS) disc height were measured directly from the 3D tomography (**Figure 8**). ANT corresponded to the average IVD height of the anterior half-area of the IVD while POS corresponded to the height of the remaining half. The ratio of IVD height/area represents a modified Farfan index (66) and has been proposed as a measure a disc health (189). For the trabecular region of the L2 and L5 vertebra, bone volume fraction (BV/TV), trabecular separation (Tb.Sp), trabecular thickness (Tb.Th), trabecular number (Tb.N), connectivity density (Conn.D), and trabecular tissue mineral density (Tb.TMD) were determined from the ex vivo µCT scans (121). Following scanning, all of the discs were resoaked in PBS with protease inhibitors for 1 hr and then returned to -20^{o}C.

Biochemical Analysis.

Once thawed, the NP of each IVD from five lumbar spines of each group was sectioned with a 1.5-mm dermal biopsy punch (Miltex Instrument Comp., Bethpage, NY) and the remaining AF was sectioned medially to represent the anterior and posterior AF. All samples were dried at 65^{o}C for 18 hr to determine dry weight. The samples were digested in papain (Sigma-Aldrich, St. Louis, MO) for 18h at 60^{o}C and sGAG content was estimated by a 1,9-dimethylmethylene blue assay (Sigma-Aldrich). Upon hydrolysis in HCl for 18h at 110 ^{o}C collagen (Col) content was

determined by a hydroxyproline assay (93). The sGAG and Col epitope content were expressed with dry weight (DW) as a referent (106).

Statistics.

In vivo and *ex vivo* lumbar lengths were compared with a t-test. One-way ANOVAs with protected post-hoc Tukey tests were used to compare differences among the 4 wk groups. T-tests were used to compare the four week age difference between AC and BC. A two-way ANOVA was used to test for interactions between animal group and disc level in determining sGAG and collagen content. Linear regressions were used to determine associations between posterior sGAG content and posterior disc height within each animal group since the posterior IVD is weaker than its counterpart. Data were expressed as mean ± standard deviation. Relative differences between sample means were denoted as percent difference [SD] of the sampling distribution of the relative difference (relative standard error of the difference). Statistical significance for all tests was considered at $p<0.05$ (SPSS 18; SPSS Inc., Chicago, IL).

RESULTS

Signal Transmissibility

The measured frequency and amplitude of the plate at 45Hz was 46[2]Hz and 51.1[0.2]µm and 87[4]Hz and 14.9[0.5]µm at 90Hz, matching the physically predicted plate displacement of 48µm at 45Hz and 12µm at 90Hz (**Figure 9**). Video recordings of the L5 spinal regions revealed that the displacement of the signal was dampened by 36[4]% and 35[3]% and the frequency was unaffected (47[0]Hz; 90[6]Hz). The static signal at 0Hz did not generate displacement of the of the L5 region.

Sham Loading

T-tests demonstrated that no outcome variable was significantly different between HU and HU+SC groups. In an effort to preserve statistical power (and avoid raising the probability of committing a type II error) these two groups were pooled and referred to as HU±SC.

Animals

The average initial weight of each group was 291[16]-293[17] grams (min[SD]-max[SD]). After 4 wk, the weight of the AC rats increased by 7[3]% (mean[SD]) (p<.001), of the HU±SC rats decreased by 3[2]% (p=.005), of the HU+45 rats decreased by 2[2]% (p=.027) and of the HU+90 rats did not change (2[2]%, p=.093). Compared to AC, the change in body weight was less in HU±SC, HU+45 and HU+90 rats by 128[15]-139[13]% (p<.001). Neither the weight at 4 wk nor the change in weight was different among the HU groups. No complications arose during the hindlimb unloading protocol.

Extraction Effect on Lumbar Spine Length

Comparison of the ex vivo and in vivo lumbar length for the mean of all animals shows that the excision of the lumbar spine from the body increased the lumbar length from 44.9[1.0]mm to 45.7[1.1]mm (p<.001). However, the percent difference between the ex vivo and in vivo lumbar length was not different among individual groups (p=.41).

Geometric and Biochemical Changes of the IVD and Trabecular Bone Changes during HU

Compared to AC, the IVD of rats subjected to 4 wk of unloading (±sham loading) were smaller by 10[3]% (p<.001) for AVG height (**Figure 10**), 10[3]% (p=.001) for ANT height, 10[3]% (p=.009) for POS height, 8[2]% (p=.008) for area (**Table 2**), and 19[3]% (p<.001) for mean IVD volume. Compared to AC, the individual IVD volume of HU±SC were 20[7]% (p=.024) smaller at L2-L3, 19[5]% (p=.007) smaller at L3-L4 and 20[4]% (p=.001) smaller at L4-L5. The 4 wk age difference

between age-matched and baseline control rats was associated with a 10[3]% (p=.013) greater posterior disc height (**Figure 10**) and a 8[2]% (p=.032) smaller height/area (**Table 2**). No differences existed at L1-L2 or L6-S1 (p≥.225)

Although the effect of unloading on the total sGAG content of the IVD was not statistically different to that of AC, by region, the sGAG content of the IVD of HU±SC was less by 21[8]% (p=.004) in the NP, 16[7]% (p=.035) in the AAF and 19[5]% (p=.008) in the PAF (**Figure 11, Table 3**). Across IVD, compared to AC, PAF sGAG content of HU±SC IVD was less by 35[8]% (p<.001) at L4-L5. No difference in PAF sGAG content occurred at L1-L2, L2-L3 or L6-S1 (p≥.114). Despite greater sGAG content, a negative relationship existed between posterior sGAG content and posterior disc height of AC animals (R^2=.79, p=.049). No relationship existed between posterior sGAG content and posterior disc height of any unloaded animals (R^2≤.61, p≥.161). After 4 wk, compared to BC, total sGAG content (**Figure 10**) of the IVD of AC was greater by 37[5]% (p<.001). Across specific regions of the IVD, compared to BC, the sGAG content of the IVD of AC was greater by 28[11]%-37[10]% (p=.001-.029). Compared to BC, PAF sGAG content of AC IVD was greater by 67[20]% (p=.024) at L5-L6. By contrast, differences in the collagen content of the IVD among groups were predominately age-dependent (**Table 3, 5**).

Compared to AC, the L2 vertebra of HU±SC rats showed less Tb.Th by 11[2]% (p<.001) and less Tb.TMD by 2[1]% (p=.053) (**Table 6**). Compared to AC rats, the L5 vertebrae of HU±SC rats showed less Tb.Th by 14[3]% (p<.001) and less Tb.TMD by 3[1]% (p<.001). The 4 wk difference in age (AC vs BC) affected the BV/TV (+24[10]%, p=0.024) and Conn.D (+19[9]%, p=0.037) of the L2 vertebra and the L5 vertebrae of the AC group showed greater BV/TV,

ConnD., Tb.N and Tb.Th by 39[9]% (p=.001), 27[12]% (p=0.031), 21[5] (p=.026)and 10[3]% (p=.043).

Efficacy of 45Hz vs 90Hz Vibrations

The ability of the two interventions to attenuate the unloading-induced hypotrophy of the lumbar IVD was differential. Overall, while the response from the 45Hz signal was minimal, the application of 90Hz vibrations partially preserved IVD morphology and sGAG content. Geometrically, compared to HU±SC, IVD of HU+90 were larger by 8[2]% (p=.022) in average height, 9[2]% (p=.011) in anterior height and 15[4]% (p=.029) in volume, but not different in posterior IVD height (7[3]%, p=.156) or area (6[2]%, p=.108) (**Figure 10**, **Table 2**). Individually, IVD volumes of the HU+90 were not statistically different (p≥.149) (**Figure 11**). The only geometric benefit of the 45Hz vibrations to the geometry of the IVD occurred in the anterior height; compared to HU±SC, the anterior height was greater by 10[2]% (p=.006) (**Figure 10**). The overall morphologic ineffectiveness of the 45Hz signal was evident in the 16[3]% (p=.008) smaller IVD volume compared to those of AC rats (**Table 2**). Furthermore, the individual IVD of HU+45 was less than of AC by 16[6]% (p=.035) at L4-L5 (**Figure 11**).

Biochemically, compared to HU±SC, the sGAG content of the IVD of HU+90 was greater by 12[4]% (p=.002) in TOTAL, by 24[8]% (p=.008) in NP, by 17[4]% (p=.05) in AAF and by 19[6]% (p=.034) in PAF (**Figure 12**, **Table 3**). Individually, sGAG content of the PAF IVD of HU+90 was greater than of HU±SC by 13[4]% (p=.015) at L4-L5 (**Figure 13**, **Table 4**). In terms of the interaction of vibration treatment and disc level, superior lumbar discs of HU+90 discs had greater sGAG content in the PAF than inferior lumbar discs (p=.008). The sGAG content of mean IVD subjected to the 45hz signal was not different to HU±SC in any region (**Figure 12**). At L4-L5,

sGAG content of PAF of the IVD of HU+45 was less than HU±SC by 40[10]% (p=.010) and AC by 42[9]% (p=.014) (**Figure 13**). Furthermore, a comparison between the vibration treatments showed that the sGAG content of TOTAL, AAF and L3-L4 PAF of HU+45 was less than HU+90 by 15[6]% (p<.001), 18[7]% (p=.029) and 87[21]% (p=.002), respectively (**Figure 12,13 and Table 3,4**).

The L2 and L5 trabecular morphology of HU+90 or HU+45 was not different to HU±SC in any variable (p>.05) (**Table 6**). Compared to AC, the L2 vertebrae of HU+45 and HU+90 rats showed less Tb.Th by 12[3]% (p<.001) and 12[2]% (p<.001). Compared to AC, the L5 vertebrae of HU+45 and HU+90 rats showed less Tb.Th (15[3]%, p<.001) and 15[3]%, p<.001) and less Tb.TMD (5[1]%, p<.001) and 3[1]%, p<.001). Compared to age-matched controls, the L5 vertebrae of HU+45 rats showed less BV/TV (8[7]%, p=.026) and the L5 vertebrae of HU+90 rats showed greater Conn.D (43[17]%, p=.017).

DISCUSSION

The purpose of the study was to show (1) the effect of hindlimb unloading, a model of disc degeneration, on the overall and regional morphology and biochemistry of lumbar IVD and (2) the ability of two low-level vibration interventions with distinct frequencies (45Hz and 90-Hz) to attenuate the unloading-induced changes in the IVD. Four weeks of unloading, regardless of the reintroduction of short periods of upright postural weight bearing, induced morphological and compositional degradation of the intervertebral discs. By contrast, superimposing very low-magnitude, 90Hz vibrations on the short period of upright weight bearing partially prevented the degradation of the intervertebral disc, irrespective of the disc region, while the 45Hz signal provided few benefits. The predilection of the IVD to higher frequency oscillations indicates

that the induction of disc remodeling was not sensitive to the larger amplitude but rather on characteristics particular to the higher frequency of the vibrations.

The “unloading” of the quadruped spine is not an ideal analog of the bipedal human and as such the rodent does not exhibit the four spinal curvatures (2 lordotic and 2 kyphotic) but this animal choice offered some advantages and similarities to the human spine. The shorter life span of the rat allows age dependent changes to occur more rapidly. Indeed, changes in the IVD height/area ratio occurred here in as little as 4 wk even though the animals were considered “adults”. Biomechanically, when normalized by the height/area, the lumbar IVD of rodents are similar to those of humans (61). Cellularly, while the adult rat IVD retains notochordal cells that disappear by adulthood in humans, unlike other species and similar to humans, chondrocyte-like cells of the rat IVD dominate the cell population of the IVD (99). Lastly, the spine of each animal was extracted in order to obtain higher resolution scans and biochemical data of the IVD. The extraction of the spine from the body led to the expansion of the lumbar spine which was most likely concentrated to the extremely hydrated IVD (155) and likely due to lost endogenous tension. The distension may have masked the true amount of disc narrowing. Nevertheless, the expansion of the lumbar spine occurred equally across all the groups, suggesting that the expansion was not engendered by aging or loading disparities among the groups. Overall, the rat may be used as a model of disc degeneration but the cellular and postural disparities, and handling must be acknowledged when interpreting the effects of loading.

The HU group showed a smaller average discal height than the AC group due to the ~50% body weight tail-traction which likely stressed the IVD, ligaments, bone, muscle,

zygapophysial joints and fasciae (88). Therefore, the approximate traction stress on the lumbar intervertebral discs was about 130kPa. While some level traction has preventative capabilities to the progressive degradation of inferior IVD, these beneficial effects are eliminated by traction magnitudes similar to those engendered here during HU (175kPa) (138). Comparable to studies of immobilization, HU and spaceflight (71, 109, 187), HU depleted the sGAG content while the collagen content of the IVD was predominately affected by aging rather than unloading. While degenerated IVD have 32%-45% less GAG than healthy IVD with a greater loss in the NP than AF(11), hindlimb unloading-induced sGAG depletion of the IVD was indiscriminant of the region. Further, the 20% sGAG difference from unloading was similar to aging 20 years during mature adulthood (227). In gravitationally unloaded rats, the wet weight of the IVD is smaller and combined with the reduced sGAG content (187) may explain the reduced size of the IVD of unloaded rats. While the posterior sGAG content of AC IVD was greater than of HU IVD, unloading disrupted the negative relationship that existed in the IVD of AC animals between posterior IVD height and posterior sGAG content indicating that the HU IVD are not simply smaller. A study of similar experimental design shows that the sGAG depletion of both the nucleus pulposus and annulus fibrosus can occur after 3 weeks of unloading and further shows that the sGAG content of the annulus fibrosus remains depleted after 3 weeks of reloading (241). Similarly, in humans, reambulation after long term bed rest incompletely rescues the morphology of the IVD (96).

Low-level mechanical countermeasures to disc changes are effective if applied in the direction of habitual spinal loading (95, 96) and coupled with a compressive load (76). Here, the rats assumed a bipedal stance during the stimuli but the short periods of upright loading

provided neither a benefit nor a detriment to the IVD compared to unloading alone. Upright posture for feeding in orchidectomized rats partially prevents vertebral bone loss (240) but 15min/d of upright posture had no impact on bone loss. In that study, the amount of time spent upright was unnoted. Furthermore, here, the erect stance was supported by cylinders, but the raised-cage animals solely exerted their own musculature for posture. Large compressions alone may not be the root cause of the observed disc degeneration with bipedalism (149) as illustrated by a comparison of the time spent upright between quadrupedal (26 min/d) and bipedal (19 min/d) rats (13). Firstly, indicating that the 15min/d of upright posture in this study was well below the time spent upright by normal quadrupeds or bipedal rats. Secondly, suggesting that the reduced ground reaction forces from the limb amputation led to the degraded state of the disc. Similarly, despite rigorous exercise, bone loss persists in astronauts on the International Space Station who receive less low-magnitude forces typical of forces engendered from daily living activities on Earth (43). Ultimately, reintroducing a portion of the ground reaction forces lost during HU may retard its detrimental effects.

Few studies have investigated the consequences of applying high-frequency, low-magnitude vibrations on the IVD. Here, the introduction of high-frequency vibrations in rats performing a squat-like stance partially maintained the height and volume of the IVD during hindlimb unloading. Whole-body vibration of rats, rather than applying the signal in the direction of the spine, directionally altered the geometry of the IVD during HU by showing a greater benefit to the area than the height of the IVD (95). In humans, vibrations with and without exercise partially maintain IVD height (21, 96). High-frequency oscillations can increase the sGAG synthesis of chondrocytes *in vitro* (217). The altered integrity and expression of anti-

catabolic molecule, TIMP1, found during disc degeneration in humans and during HU (228, 241), may be stimulated with this type of loading (235, 241). In addition, low-magnitude oscillations can suppress the genetic expression of matrix metalloproteinases (238) by activating signaling pathways via ATPs (239). The anabolic, anti-catabolic and catabolic repertoire of high-frequency vibrations also extends to collagenous remodeling and may do so with and without the precondition of a compromising event such as HU (124, 236).

The level of dampening observed here is similar to previous data that demonstrated a 60% transmission of >25Hz vibrations to the L4 vertebrae of human subjects with 20^{o} knee flexion (195). Whether different discs experience significantly different levels of stimulation remains unclear. Site-specificity of the IVD is of particular interest as the posterior annulus is biomechanically weaker than the anterior annulus and, during standing, is loaded in compression, in contrast to the tensile load on the anterior annulus (3, 230). Compared to the lower lumbar IVD, the posterior annulus of the upper lumbar IVD of rats subjected to 90Hz signals demonstrated a greater sGAG content than the 45Hz treated and unloaded/sham animals. Despite the reduced transmissibility of high-frequency vibrations to the hip and head, the upper lumbar discs may sense more acceleration than the lower lumbar discs because the upper lumbar discs do not share the loading experience with the dampening structure of the hip(34). This may be further exhibited by the reduction in sGAG content of the PAF of the upper most lumbar disc which neighbors the dampening structure of the ribcage. Secondly, the transmission of vibratory signals is more likely to occur through the posterior aspect of the vertebra rather than the anterior because regardless of the level of degeneration of the

intervertebral disc greater compression occurs in the posterior section of the vertebral body than the anterior(7), allowing for improved transmission via the posterior section.

Even though no benefits of vibrations were conferred to the vertebrae in the current study, a preferential response of the 90Hz over the 45Hz signal was demonstrated in the tibia of ovariectomized rats(122). While the mechanism for large loads may include deformation and stimulation of the IVD and its incumbent viscoelastic cells (216), low-magnitude, high-frequency vibrations likely employ a different mechanism as cells stimulated at high frequencies stiffen increasingly and non-linearly, resisting deformation (147). Therefore, the detection of the signal by the cells of the intervertebral disc may involve a sensitivity to the applied frequency (57). One proposed frequency-dependent mechanism is the acceleration of the nucleus of the cell within the cytoskeleton (12). Vibration amplitudes an order of magnitude below those imposed here can stimulate chondrocyte proliferation and proteoglycan synthesis (126, 152). However, this does not preclude the involvement of additional factors which may contribute to the activity of cells, such as the morphology of the cell or IVD. In addition, high-frequencies may have the added benefit of serving as a surrogate to the low strains produced by the endogenous muscle contractions occurring above 20Hz (98).

Relatively large and dynamic loads are typically considered critical to maintain the compositional and metabolic health of the IVD (235). In contrast, the current study employed low-magnitude, high-frequency mechanical signals applied for brief periods every day to inhibit morphological and biochemical deterioration associated with hindlimb unloading. Similar to a previous data on the skeleton (122), the IVD distinguished between the two vibratory signals: 45Hz or 90Hz, with 90Hz being more effective than 45Hz. Whether this differential sensitivity

was directly modulated by cells (i.e., higher sensitivity at higher frequencies) remains to be determined. Together, these data emphasize the ability of the IVD to respond to low-level mechanical signals and pose vibrations as a potential venue for addressing the maintenance of IVD health.

List of Tables

Table 2. Intervertebral disc morphology of the five groups of rats

Group	Height/Area [mm^{-1}]	Area [mm^2]	Volume [mm^3]
BC	.072(.002)	10.9(.7)	6.4(1.2)
AC	.066(.004)*	11.7(.6)	6.9(.4)
HU±SC	.069(.005)	10.8(.8)†	5.6(.8)†
HU+45	.067(.005)	11.1(.7)	5.8(.6)†
HU+90	.066(.004)	11.4(.4)	6.5(.6)‡

Values are mean(SD)
* Age-matched (AC) vs. baseline (BC) controls, $p<.05$
† Vs. age-matched controls (AC), $p<.01$
‡ Vs. hindlimb unloading with/without sham loading (HU±SC), $p<.05$

Table 3. Mean sGAG and collagen content for lumbar IVD of rats

Group	sGAG				Col			
	TOTAL	**NP**	**AAF**	**PAF**	**TOTAL**	**NP**	**AAF**	**PAF**
BC	.09(.01)	.52(.07)	.11(.01)	.11(.01)	.28(.06)	.22(.03)	.36(.06)	.30(.06)
AC	.13(.01)*	.67(.11)*	.15(.02)*	.15(.01)*	.41(.07)*	.40(.13)*	.54(.11)*	.45(.09)*
HU±SC	.12(.01)	.53(.09)†	.13(.01)†	.12(.01)†	.45(.09)	.33(.13)	.55(.11)	.43(.07)
HU+45	.11(.02)†	.57(.04)	.12(.02)†	.12(.02)	.39(.10)	.27(.13)	.47(.13)	.36(.11)
HU+90	.13(.01)‡§	.66(.07)‡	.15(.01)‡§	.14(.01)‡	.48(.13)	.31(.18)	.59(.11)	.45(.08)

Each value was the µg of epitope / mg of dry weight
Each TOTAL (n=10-11) and regional (n=5) sGAG and collagen content data point was the average of 6 lumbar IVD; mean(SD).
HU±SC sample size for TOTAL sGAG was n=22, TOTAL collagen was n=20 and regional content was n=10
* Age-matched (AC) vs. baseline (BC) controls
† Vs. AC,
‡ Vs. HU±SC
§ Vs. HU+45, $p<.05$

Table 4. Mean sGAG content of the PAF of lumbar IVD of rats

Group	L1-L2	L2-L3	L3-L4	L4-L5	L5-L6	L6-S1
BC	.36(.07)	.26(.01)	.23(.02)	.25(.05)	.17(.02)	.17(.01)
AC	.47(.29)	.29(.11)	.33(.06)*	.29(.05)	.29(.08)*	.25(.04)*
HU±SC	.31(.06)	.29(.08)	.32(.08)	.19(.02)†	.22(.05)	.20(.04)
HU+45	.31(.06)	.29(.08)	.19(.04)†‡	.22(.04)	.22(.09)	.21(.07)
HU+90	.37(.09)	.37(.07)	.36(.08)**§**	.27(.02)‡	.19(.03)	.21(.02)

Each value was the µg of epitope / mg of dry weight
Each TOTAL (n=10) and regional (n=5) collagen content data point was the average of 6 lumbar IVD; mean(SD).
* Age-matched (AC) vs. baseline (BC) controls
† Vs. AC
‡ Vs. HU±SC
§ Vs. HU+45, $p<.05$

Table 5. Total and regional collagen content of IVD after 4 weeks to baseline [%]

Group	TOTAL	NP	AAF	PAF
BC	100.0(21.2)	100.0(13.3)	100.0(17.6)	100.0(20.9)
AC	146.4(23.4)*	180.7(58.3)*	148.9(30.2)*	150.5(30.6)*
HU±SC	160.2(32.5)	152.5(58.4)	150.2(31.3)	142.3(24.4)
HU+45	137.9(39.3)	123.4(58.1)	130.1(36.2)	122.1(37.3)
HU+90	170.0(45.4)	141.9(81.9)	161.9(29.7)	149.0(25.4)

Each TOTAL (n=10) and regional (n=5) collagen content data point was the average of 6 lumbar IVD; mean(SD).
* Age-matched (AC) vs. baseline (BC) controls, $p<.05$

Table 6. Trabecular morphology of L2 and L5 vertebrae of the five groups of rats

L2	BV/TV [%]	Conn.D [mm^{-3}]	Tb.N [mm^{-1}]	Tb.Th [µm]	Tb.TMD [mg HA/cm^3]
BC	32.0(5.8)	59(10)	3.80(.44)	91.0(7.4)	778(15)
AC	39.8(9.4)*	67(27)	4.52(1.04)*	94.4(6.1)	791(17)
HU±SC	34.6(6.0)	80(19)	4.37(.62)	83.8(5.6)†	768(14)†
HU+45	33.9(5.2)	81(37)	4.21(.79)	83.2(5.9)†	768(21)
HU+90	35.5(6.9)	91(27)	4.55(.88)	83.5(4.8)†	768(19)
L5	BV/TV [%]	Conn.D [mm^{-3}]	Tb.N [mm^{-1}]	Tb.Th [µm]	Tb.TMD [mg HA/cm^3]
BC	28.3(4.7)	52(12)	3.62(.31)	86.3(6.6)	779(11)
AC	39.3(6.9)*	66(18)*	4.36(.52)*	94.5(7.5)*	780(16)
HU±SC	33.9(7.3)	87(23)	4.43(.64)	81.1(7.8)†	765(15)†
HU+45	31.1(6.4)†	83(29)	4.10(.63)	81.0(7.6)†	765(16)†
HU+90	33.3(6.4)	94(29)†	4.48(.73)	80.4(6.6)†	765(16)†

Values are presented as mean(SD).
* Age-matched (AC) vs. baseline (BC) controls
† Vs. AC, $p<.05$

List of Figures

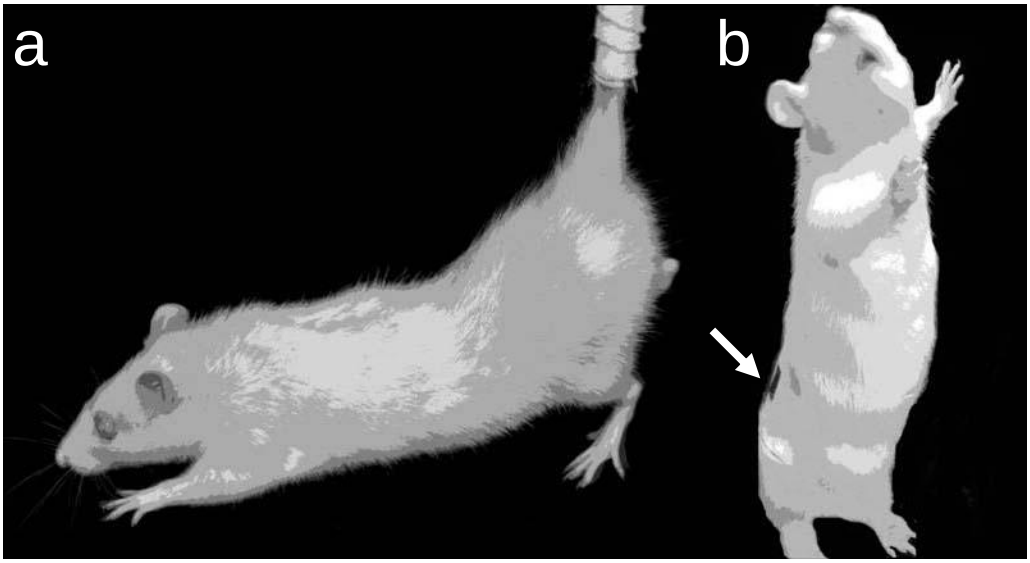

Figure 7. *Posture of an animal during (a) hindlimb unloading during which the angle between the torso and the ground was about 30^{o} (88). (b) For 15min/d rats were released from HU and placed into an upright position in an acrylic tube (height: 30.5 cm, inner diameter: 10.2 cm) in which they received a low-level, vertical vibratory signal (45Hz or 90Hz) or sham loading (0Hz). The white arrow points to where the motion at L5 was measured in two rats.*

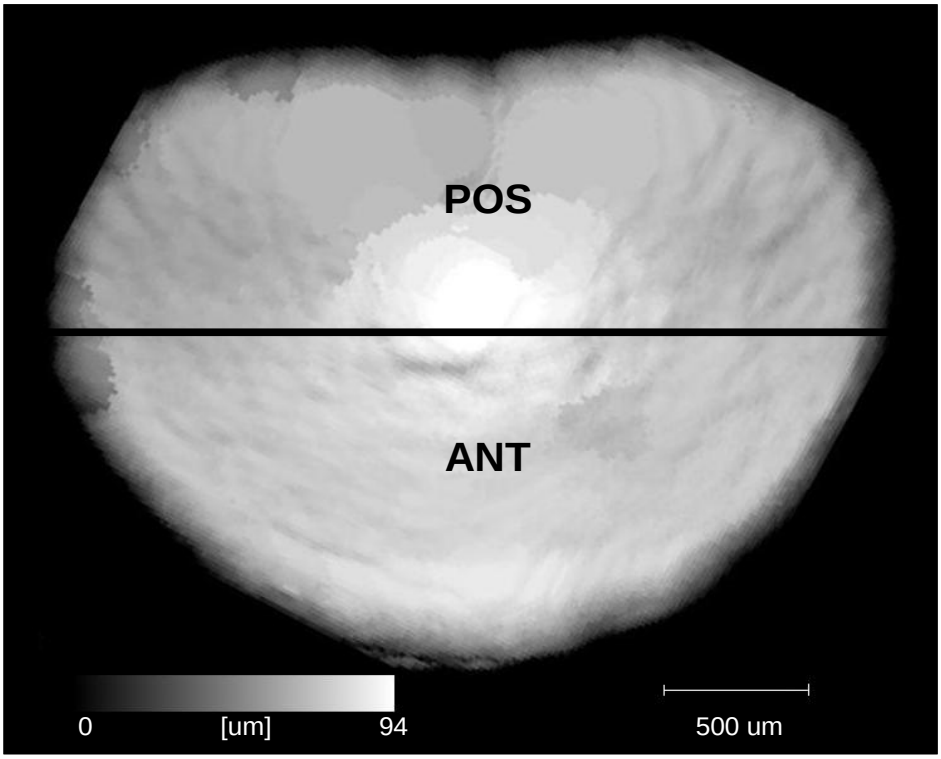

Figure 8. *Height map of an IVD. ANT corresponded to the average IVD height of the anterior half of the IVD while POS corresponded to the average IVD height of the posterior half of the IVD.*

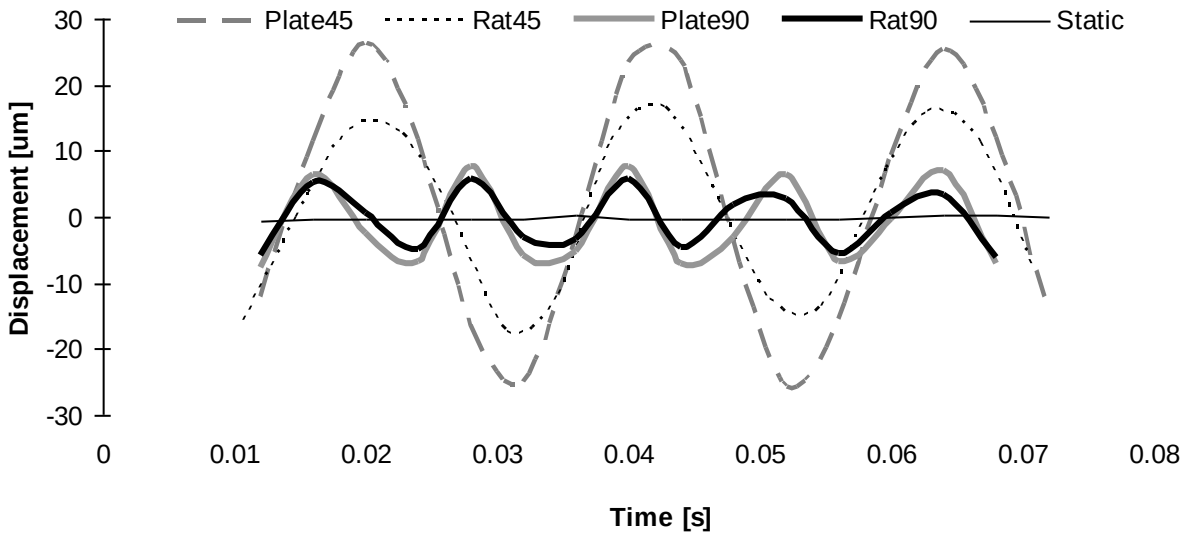

Figure 9. *Displacements of the vibrating plate (0.2g) at 45Hz (grey dashed) and 90Hz (grey) and of the rat L5 region at 0Hz (solid), 45Hz (dotted) and 90Hz (bold) vibrations. Compared to the vibrating plate, the measured frequency at L5 was maintained in the upright rat but the amplitude was dampened by ~35% at both frequencies.*

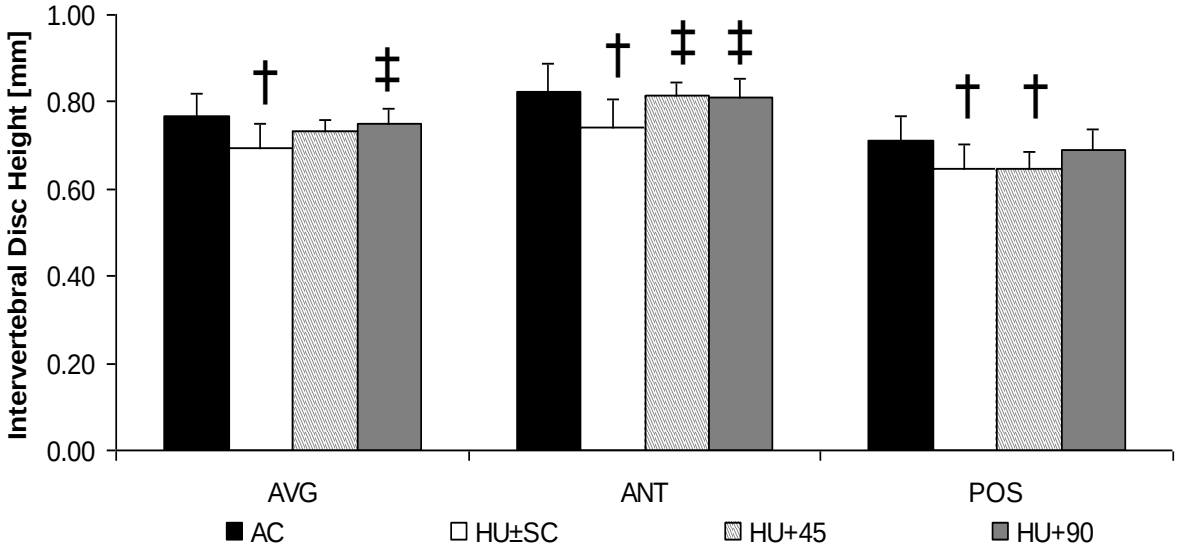

Figure 10. *Average (AVG), anterior (ANT) and posterior (POS) height of the IVD of AC (n=11), HU±SC (n=22), HU+45 (n=11) and HU+90 (n=11); mean+SD. IVD of HU±SC had less AVG, ANT and POS IVD height than of AC. Vibrations at 90Hz maintained AVG and ANT IVD height, while vibrations at 45Hz maintained ANT but not POS IVD height. † compared to AC, ‡ compared to HU; p <0.05*

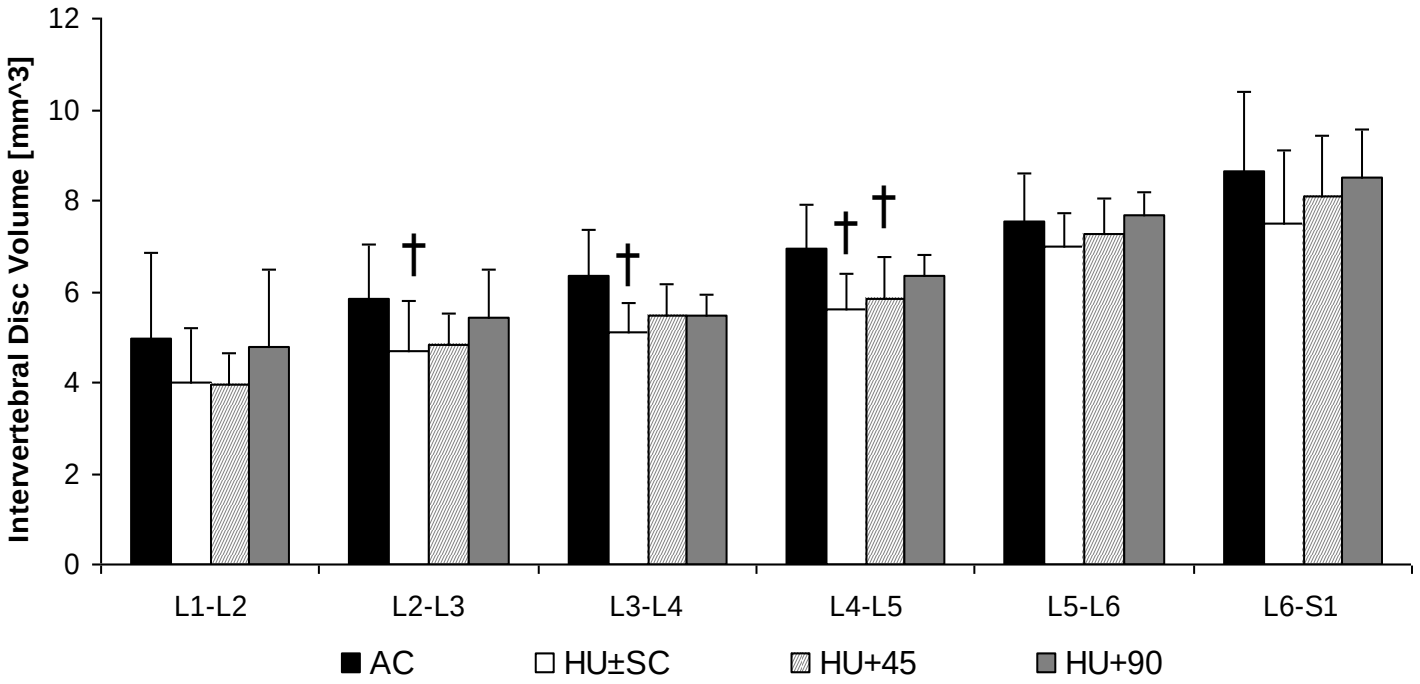

Figure 11. *Volume across lumbar discs of AC (n=11), HU±SC (n=22), HU+45 (n=11) and HU+90(n=11); mean+SD. Compared to AC, hindlimb unloaded IVD, with or without upright posture, had less volume between L2 and L5. Vibrations at 45Hz did not maintain the IVD volume at L3-L4 compared to AC. † compared to AC; p <0.05*

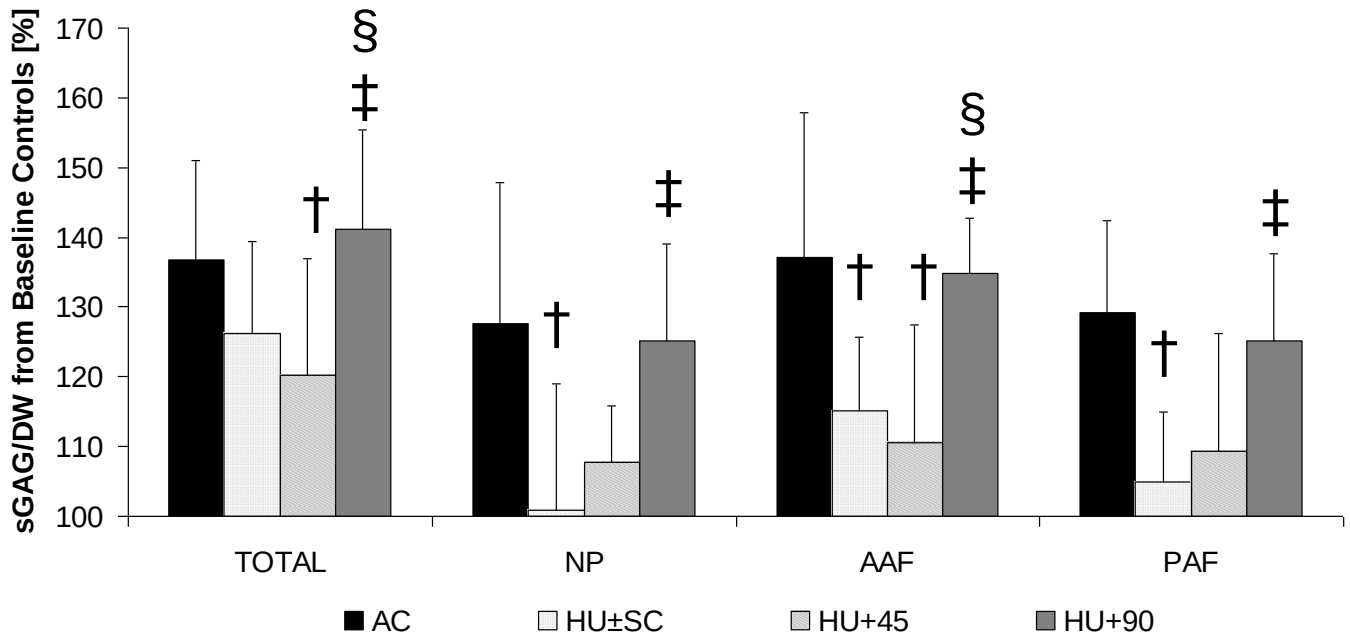

Figure 12. *Sulfated-glycosaminoglycan (sGAG) content of the whole IVD (TOTAL), nucleus pulposus (NP), anterior annulus fibrosus (AAF) and posterior annulus fibrosus (PAF) of BC (TOTAL n=11; Region n=5), AC (TOTAL n=11; Region n=5), HU±SC (TOTAL n=22; Region n=10), HU+45 (TOTAL n=11; Region n=5) and HU+90 (TOTAL n=11; Region n=5); mean+SD. IVD of HU±SC had less sGAG content than of AC at every region. TOTAL and AAF of HU+45 IVD was less than of AC. Compared to HU±SC, vibrations at 90Hz maintained sGAG content at every region, and was greater than of HU+45 at AAF. Overall, the total content of HU+90 IVD was greater than of HU±SC and HU+45.* † *compared to AC,* ‡ *compared to HU,* **§** *compared to HU+45; p <0.05*

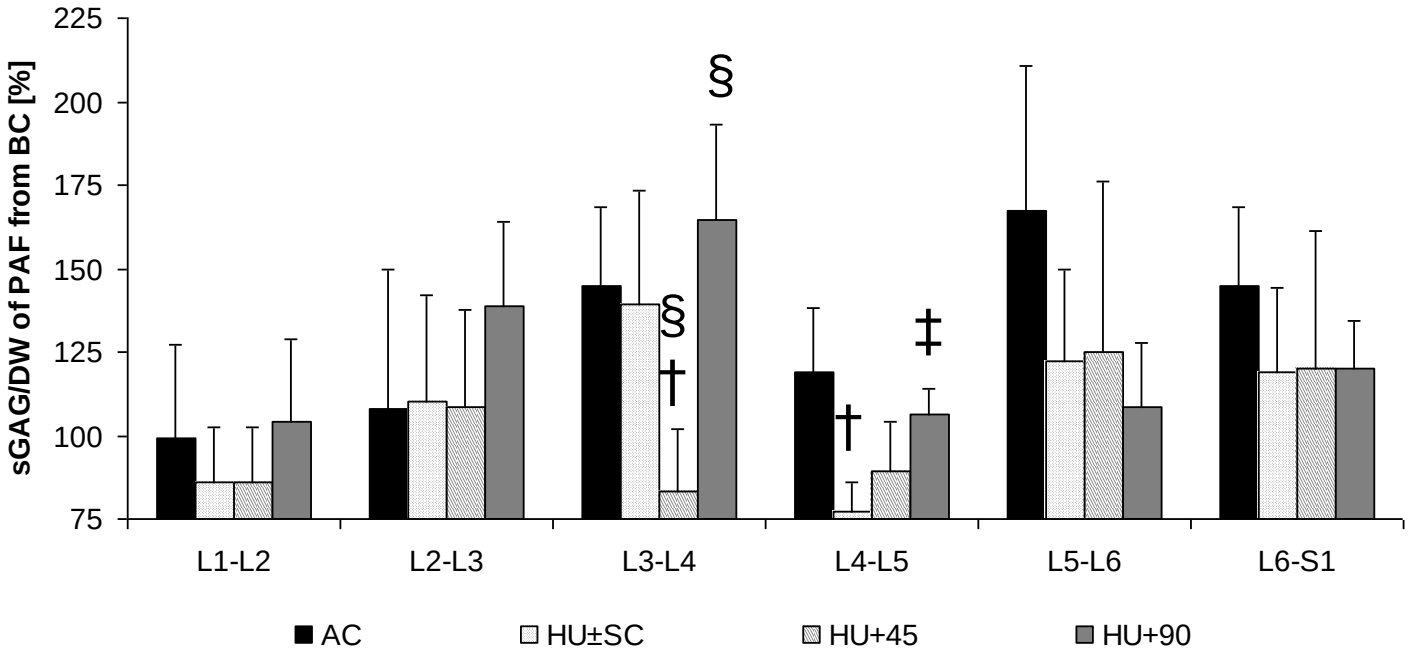

Figure 13. *sGAG content of the PAF of individual lumbar discs from AC (n=5), HU±SC (n=10), HU+45 (n=5) and HU+90 (n=5) animals; mean+SD. At L4-L5, sGAG content of PAF IVD of HU±SC was less than of AC but 90Hz vibrations maintained it. Contrarily, at L3-L4, PAF of HU+45 IVD had less sGAG content than of AC, HU±SC and HU+90 IVD. Lastly, the interaction of disc level and vibration application was greater in the cephalic PAF of HU+90 IVD than of HU+45 or HU±SC. † compared to AC, ‡ compared to HU,* **§** *compared to HU+45; p <0.05*

V

Brief Vibrations Applied in Upright Rats Partially Prevent Muscle Changes and Maintain Mechanical and Morphological Properties of L4-L5 Motion-Segment during Hindlimb Unloading

ABSTRACT Reduced spinal loading degrades the intervertebral disc (IVD) and alters muscle size. To determine if low-magnitude, high-frequency vibrations maintain IVD biomechanics, morphology and their relationship, and prevent muscle changes during hindlimb unloading, three groups of Sprague-Dawley rats (4.5mo, n=8/group) were hindlimb unloaded (HU). In two HU groups, unloading was interrupted for 15min/d of upright posture on a vertically oscillating plate (0.2g, 90Hz) (HU+90) or inactive plate (HU+SC). After four weeks and compared to normally ambulating age-matched controls (AC), L4-L5 IVD of HU±SC had less height change, 39% smaller nucleus pulposus area, 26% greater compressive modulus, 76% less tension-compression neutral zone (NZ) modulus, 133s greater time constant, 25% and 19% greater elastic damping modulus and stiffness, 26% less torsional NZ stiffness, and a weaker relationship between tension-compression NZ modulus and posterior height change. Psoas area of HU±SC had increased 15% where of AC had not and, compared to AC, change in paraspinal area was 305% less. Exogenously introduced oscillations maintained IVD morphology, axial properties, and psoas muscle area. Compared to HU±SC, IVD of HU+90 had greater height change, 35% greater nucleus pulposus area, 18% smaller compressive modulus, 339% greater tension-compression NZ modulus, 16% smaller elastic damping stiffness and a maintained relationship between tension-compression NZ modulus and posterior height change but no difference in time constant, elastic damping modulus, or torsional NZ stiffness. Psoas area of HU+90 was unchanged but paraspinal area loss was unabated. Very brief, small mechanical signals partially protected the spine, positioning these signals as potential load contributors.

Introduction

Reduced dynamic loading as occurs with immobilization, bed rest, microgravity, or prolonged inactivity may lead to altered morphology and mechanics of the spinal musculoskeletetature and to discogenic back pain (30, 78, 140, 145, 146, 232, 233). Although the etiology of back pain remains unclear and may be the result of several factors (24, 125), degeneration of the disc remains one of the most implicated causes due to the extensive compositional changes the disc undergoes (84). Consequently, degenerated IVD exhibit biomechanically compromised motion segments and, in turn, spines (172, 245). Even short periods of unloading may affect the mechanics and morphology of the spine (232) but concern arises following prolonged periods of reduced loading which can disrupt the molecular and biomechanical properties of the IVD (109, 154, 156, 206).

Animal models of degeneration offer unique opportunities to test countermeasures of discal degeneration and individually test the functionality of an IVD via invasive procedures. Here, the model can produce degradative IVD changes by simulating the physically altered discal environment without compromising the mechanism by which the disc can recover as may occur in chemically or surgically induced degradation (204). Hindlimb unloading is a widely utilized animal model for simulating musculoskeletal changes from diminished functional weightbearing (168). Although hindlimb unloading tenses the tail, similar to degenerated discs, HU discs show decreased hydrophilic glycosaminoglycan content, decreased discal hydrostatic pressure, increased collagen content and disorganization, chondrocytic apoptosis and persistent expression of catabolic molecules during the recovery period (15, 87, 160, 241). HU discs demonstrate larger collagen fiber diameters in the posterior region (160), making the IVD

more suited for tension, but less capable of recoverable creep (185) and more susceptible to damage typical of that weaker region (3). Therefore, the effect of hindlimb unloading on the biomechanical function of the IVD and on the relationship between biomechanics and changing morphology remains speculative.

IVD may remodel in response to low-frequency, high-magnitude loads but the contrary, high-frequency, low-magnitude vibrations, may also preserve the morphology of the IVD and reduce the incidence of back pain exacerbated by prolonged spinal unloading (96). While the mechanism(s) of the mechanical signals remain(s) unclear, the benefits of vibrations include improvement of musculoskeletal (95, 122, 237) morphology, neuromuscular adaptation (220) and lumbar proprioception rehabilitation (72). Despite the low magnitude of the signal, high-frequency vibrations can traverse the longitudinal axis of the spine (186, 195). While high-frequency vibrations with or without resistive exercise delivered in a squat-like posture maintain IVD morphology and may prevent muscle changes during spinal unloading (21, 96), the effect of high-frequency oscillations remains unknown for the biomechanical function and musculoskeletal morphology of and surrounding a middle segment (L4-L5) of the lumbar spine during hindlimb unloading.

Materials and Methods

Experimental Design.

This study was reviewed and approved by the Institutional Use and Care Committee of Stony Brook University. Following two weeks of acclimatization, female Sprague-Dawley rats (18wks of age, n=24) were hindlimb unloaded (HU) for 4 wks according to the Morey-Holton method (168). One group (n=8/group) of HU rats stood on a vertically oscillating plate (15min/d, peak

acceleration of 0.2g) in an upright position that was maintained via vertical plastic cylinders (height: 30.5 cm, inner diameter: 10.2 cm) at 90Hz (HU+90) because the signal requires a compressive load for transmission (195) and facilitation of potential deformations (77). Sham control (HU+SC) rats stood upright in the cylinder without receiving vibrations. HU rats received no intervention. Baseline (BC) and normally ambulatory age-matched (AC) rats were used as controls. Animals had access ad libitum to standard rat chow and water.

Micro Computed Tomography of Muscle and Bone.

At baseline and 4 wk, the inferior L5 vertebra to the superior L4 vertebra region (approximate L4-L5 motion segment length) was imaged by VivaCT 75 (Scanco, Bassersdorf, Switzerland) at a resolution of 78µm (45kV, 177µA, 300ms integration time). An automated algorithm (123) segmented muscle from bone to determine spinal bone and muscle volume which included the erector spinae, multifidus, quadratus lumborum (paraspinal), and psoas. Since both unloading and vibrations coupled with resistive exercise differentially alter the spinal musculature (21), the psoas and paraspinal muscles were contoured in 3 consecutive images at inferior L4 and L5. At baseline and 4 wk, scout views (41µm) were used to determine vertebral bone length as the average of the anterior, center and posterior length. After sacrifice, the lumbar spine was stored *en bloc* at -20^{o}C.

Mechanical Testing.

Combinatorial loads perpetually stress the IVD but in order to measure the fundamental faculties of the inhomogeneous and viscoelastic IVD, it must be tested in controlled mechanical tests. Therefore, similar to other studies (32, 33, 62), a 3-part (tension-compression, creep and torsion) mechanical testing protocol was performed on the L4-L5 segment. A cycle of ex vivo

tension-compression of the L4-L5 segment has three phases: (1) in the tensile region, only the annulus fibrosus is subjected to axial tension, (2) in the NZ region, the bulk of the annulus may resist buckling, but in concert with the pressurized nucleus pulposus loads may begin uncrimping annulus fibers and removing macroscopic slack, and (3) in the compressive region, the annulus predominately bears the load as circumferential stress from the radial loads originating from incompressible fluid of the nucleus (24). Creep testing elucidates fluid-dependent properties from elastic properties of the IVD. Lastly, torsion stresses the annulus by producing interlaminar shear and tension, where the linear region results from stretching lamellae oriented in the direction of rotation and the NZ results from laminar transitioning.

Prior to mechanical testing, the L4-L5 bone-disc-bone segment was excised of extraneous tissue, soaked and thawed in 1X PBS for 18 hr. Briefly, the L4 vertebra was gripped by customized microvises and the L5 vertebra was fixed in container of PMMA, attached to a platform, to avoid applying torsion. Once secure, the sample was immersed in 1X PBS. An Instron 5542 testing system (Instron, Canton, MA) applied a 0.1 Hz frequency of -6N to 3N, so that the tensile load surpassed the neutral zone in order to determine the zero-load point. After twenty cycles of compression-tension, a 1-s ramp from 0 to 6N was achieved and maintained at 6N for 1hr for the creep test Immediately following creep testing and superimposed on the 6N axial load, a stepper-motor (AM15E0045; Faulhaber, Clearwater, FL) applied 10 cycles of torsion, where each cycle consisted of a $\pm 8^{o}$ rotation at 1.6^{o}/s.

IVD Geometry.

Following mechanical testing, the L4-L5 IVD was bisected and imaged using a stereomicroscope (Leica MZ6, Bannockburn, IL). The horizontal image was analyzed using a custom Matlab

algorithm (174) to determine the anteroposterior width for the entire disc (W_{AP}) and nucleus pulposus (N_{AP}), mediolateral width for the entire disc (W_{ML}) and nucleus pulposus (N_{ML}), and area for the annulus fibrosus and nucleus pulposus. In vivo scout views (41µm) were used to determine the anterior, center, posterior and average IVD height. Average IVD height was calculated as the mean of anterior, center and posterior height. Assuming the nucleus pulposus supports negligible torsion, the polar moment of inertia (J) of the IVD was calculated as $J = \pi/64 \left[W_{ML}^3 W_{AP} + W_{AP}^3 W_{ML} - N_{ML}^3 N_{AP} + N_{AP}^3 N_{ML} \right]$ (61). Widths and regional heights were used for normalization.

Mechanical Data Analysis.

Data analysis from each test was performed on custom Matlab programs. Data from the preconditioned 20th cycle of compression-tension was analyzed using the trilinear fit model (33, 198) to measure the compressive, tensile and neutral zone stiffness of the L4-L5 motion segment. Briefly, the compressive and tensile loading curves were isolated and a 5th order polynomial was fit. The minimum slope of the curve represented the neutral zone stiffness. The slope of the linear fit through the data points between 80% and 100% of the compressive load constituted the compressive stiffness, and respectively for tension. Compressive range of motion (ROM) was normalized to height. Similarly, the preconditioned 10th cycle of torsion was fit with a trilinear model to obtain neutral zone (K_{NZ}) and linear region (K) stiffnesses. Apparent torsional neutral zone modulus (G_{NZ}) and linear region modulus (G) was calculated as $G_i=K_ih/J$ (MPa/^{o}) where h was the IVD height and J was the polar moment of inertia. After the 1-s step load of 6N (F_C), 1hr of creep displacement was fit to a rheological model (17, 128): $d\ t \,/\, F_C = 1/S_1 \ 1-e^{-S_1 t/\eta_1} \ + \ 1/S_2 \ 1-e^{-S_2 t/\eta_2} \ + 1/S_3$ where $S_{1,2}$ are the elastic damping

coefficients, S_3 is the instantaneous elastic stiffness, $\eta_{1,2}$ are the viscous damping coefficients, and $\tau_{1,2}$ are the time constants. Each stiffness and damping coefficient was normalized to determine the apparent elastic and viscoelastic moduli (MPa) by multiplying each to the IVD geometry (height/area).

Statistics.

Paired and unpaired t-tests were used for longitudinal, BC vs AC, and slopes of regression line comparisons (243). One-way ANOVAs with post-hoc Tukey tests were used to compare the 4 wk groups. Two-way ANOVAs were used to test the interaction between group and regional disc height. Linear regressions within each group were run between the neutral zone modulus and change in posterior IVD height and between lumbar muscle volume and L4-L5 length, and across groups were run between the average muscle area and average mechanical property. One-sample t-tests with a significance threshold of 0.01 were used to remove outliers from each group. Data were expressed as mean ± standard deviation (mean[SD]). Relative differences between sample means were denoted as percent difference [SD] of the sampling distribution of the relative difference (relative standard error of the difference). Statistical significance was considered at $p \leq 0.05$ (SPSS 18; SPSS Inc., Chicago, IL), unless otherwise stated.

Results

Sham Loading

T-tests demonstrated that no outcome variable except torsional modulus was significantly different between HU and HU+SC groups. In every figure and table, the mean HU and HU+SC are presented to show their similarity. In an effort to preserve statistical power (and avoid

raising the probability of committing a type II error) these two groups were pooled and referred to as HU±SC.

IVD Geometry

Baseline mean IVD height of rats from AC was 0.79[0.05]mm, HU±SC was 0.83[0.07]mm and HU+90 was 0.82[0.07]mm and not different (p=0.860). Compared to AC, change of IVD height from baseline of the HU±SC IVD was less by 96[24]% (p=0.005) (**Figure 14**) but IVD height did not change from baseline in each group (p≥0.056). Compared to AC, area of the nucleus pulposus of HU±SC discs was less by 39[8]% (p<0.001) (**Figure 15**) and, compared to BC, the same of AC discs was greater by 25[10]% (p=0.023). Annulus fibrosus area was not different among the groups (p=0.949). High-frequency vibrations partially prevented changes to IVD morphology. Change in mean height of HU+90 IVD was greater than of HU±SC by 2052[893]% (p=0.016) (**Figure 14**). Compared to HU±SC, nucleus pulposus area of HU+90 discs were greater by 35[12]% (p=0.016) (**Figure 15**).

Tension-Compression Properties

Compressive, tensile and neutral zone modulus of the baseline group was 6.5[0.8], 2.6[0.5] and 0.3[0.2] MPa, respectively. The four-week age difference between BC and AC rats did not significantly alter any elastic properties of the L4-L5 motion segment (p≥0.115). Hindlimb unloading with or without brief erect stance disrupted the mechanical properties of the L4-L5 motion segment. Compared to AC, compressive modulus of HU±SC IVD was greater by 26[8]% (p=0.020) and tension-compression NZ modulus of HU±SC discs was less by 60[23]% (p=0.043) (**Figure 16**). A similar increase was noted with the tension-compression NZ but not with the compressive stiffness (**Table 7**). Tensile modulus was not different among the 4 wk

groups (p=0.304). When noting the relationship between neutral zone modulus and change in posterior disc height, the AC group showed a negative, moderate (R^2=0.60, p=0.040) relationship (**Figure 17**). Compared to AC, the same relationship for the HU group (R^2=0.00, p=0.905) was less (p=0.022).

The introduction of 90Hz vibrations quelled the altered elastic properties of the L4-L5 IVD from unloading with or without brief, upright posture. Compared to HU±SC, compressive modulus of HU+90 IVD was less by 18[9]% (p=0.047) and NZ modulus of HU+90 IVD was greater by 185[74]% (p=0.012) (**Figure 16**). The intervention provided a similar protection for the respective structural properties (**Table 7**). Additionally, the linear regression between neutral zone modulus and change in posterior height of HU+90 discs was negatively related (R^2=0.65, p=0.028) and more related than of HU±SC (p=0.006) discs (**Figure 17**).

Creep Properties

Upon a compressive load of 6N for 1 hr, the viscoelastic creep response of each group showed an instantaneous deformation of ~.10mm followed by a relaxed creep deformation of ~.40mm (**Figure 18**). Compared to AC, long time constant τ_2 of HU±SC IVD was greater by 101[32]s (p=0.009) and instantaneous elastic modulus S_3 was greater by 25[8]% (p=0.008) (**Table 8**). The stiffness of S_3 was similarly greater (**Table 7**). Compressive range of motion, short time constant τ_1, S_1 nor S_2 were different among the 4 wk groups (p≥0.303). Compared to BC, short time constant τ_1 of AC discs was greater by 3.6[1.3]s (p=0.017). No differences in compressive range of motion or moduli $S_{1\text{-}3}$ existed between BC and AC (p≥0.262).

Superposition of 90Hz mechanical signals provided few benefits to creep or torsional property changes derived by hindlimb unloading. Vibrations did not mitigate the greater τ_2 of

HU±SC IVD (p=0.858) and was not different to the τ_2 of AC (85[42]s, p=0.067) (**Table 8**). Contrarily, instantaneous elastic stiffness of HU+90 IVD was less by 16[5]% p=0.004) (**Table 7**) but the modulus was not different to that of HU±SC (p=0.278) or AC (p=0.305) IVD.

Torsional Properties

NZ torsional stiffness K_{NZ} of AC IVD was less than of HU±SC IVD by 25[6]% (p<0.001) (**Table 7**) but NZ torsional modulus G_{NZ} (p=0.059) and torsional modulus G (p=0.608) of the L4-L5 IVD were not different among the 4 wk groups (**Table 8**). G_{NZ} and G of AC discs were not different to BC discs (p≥0.085). NZ torsional stiffness K_{NZ} of HU+90 IVD was not different to that of HU±SC (p=0.161) IVD and, compared to AC, K_{NZ} of HU+90 IVD was less by 37[8]% (p<0.001) (**Figure 19**).

Paraspinal Muscle and Vertebral Bone Morphology

Baseline muscle areas were not different (**Table 9**). Four weeks of aging did not alter the psoas or paraspinal muscle area at L4 or L5 for the AC rats (p≥0.086) (**Figure 20, Table 7**). Contrarily, HU±SC rats gained 17[15]% (p<0.001) and 12[20]% (p=0.038) psoas muscle area at L4, and lost 14[9]% (p<0.001) paraspinal area at L4. Compared to AC, HU±SC rats lost 353[80]% (p<0.001) paraspinal muscle area at L4 but not at L5 (p=0.220). Change in area of the psoas muscle at L4 (p=0.078) and L5 (p=0.658) was not different among the 4 wk groups. Overall, every group had increased lumbar muscle volume over 4 wk (p≤0.002) (**Table 16**).

90Hz vibrations provided partial benefits to the paraspinal muscles of the unloaded rats. HU+90 animals did not gain psoas muscle area at either vertebral level (p≥0.138) (**Figure 20**). However, HU+90 rats lost 17[2]% and 16[2]% paraspinal muscle area at L4 and L5 (p<0.001). Compared to HU±SC, HU+90 rats lost 74[38]% more paraspinal muscle area at L5 (p=0.029).

Compared to AC, the change in paraspinal muscle area at L4 and L5 of HU+90 rats was less by 425[71]% and 591[87]% ($p<0.002$). Across the groups, mean paraspinal muscle area was highly related ($R^2=0.99$, $p<0.001$) to NZ torsional stiffness of the L4-L5 IVD (**Figure 19**).

After 4 wk, the AC group gained 4.2[2.2]% ($p=0.003$) bone volume (**Table 10**). Every unloading group, regardless of loading, lost bone volume ($p<0.001$) and HU+90 rats lost more bone volume than HU±SC ($p=0.050$) rats. Although mean vertebral bone length of every group increased from baseline ($p\leq0.002$), increases in vertebral bone length of HU±SC and HU+90 groups were less than of AC ($p\leq0.037$). Change in the motion segment length was not different among the groups ($p=0.147$). Furthermore, change in L4-L5 length and change in muscle volume were excellently related in the AC ($R^2=0.99$, $p<0.001$) and HU+90 ($R^2=0.91$, $p<0.001$) groups and were moderately related in the HU±SC ($R^2=0.48$, $p=0.006$) group (**Figure 21**). The relationships were not different among the groups ($p\geq0.058$).

DISCUSSION

The aim of this study was to assess the biomechanical and morphological quality of the L4-L5 spinal segment and lumbar spinal muscle of rats that were unloaded with and without intermittent erect posture, and unloaded plus brief bouts of low-level vibrations superimposed on erect posture. Vibrations partially countered the morphological degradation of the IVD and muscle but not bone, and partially countered the disruption of the axial but not torsional properties of the L4-L5 segment during four weeks of hindlimb unloading. These data suggest that low-magnitude, high-frequency vibrations may be important mechanical contributors to the maintenance of the spine.

Rats are quadrupedal but, like humans, rat spines are loaded axially (208, 243) and, when normalized to geometry, behave mechanically similar (61, 62). Normal upright posture in humans dictates that the anterior region of the IVD is loaded in tension while the posterior region in compression (230). Surprisingly, a rat disc may be loaded in a similar fashion as suggested by thinner collagen fibers in the posterior region (160), where thin fibrils are needed to promote recoverable creep (185). The musculoskeletal response to (un)loading may differ among species (54, 204, 246). IVD-cell populations differ between rats and humans (222) but chondrocytes dominate the IVD of both (99). The mechanical results did not allow complete extrapolation to the human condition because the intention of the mechanical tests was to compare the resistance of the IVD across the loading groups and therefore required removal of the zygapophysial joints. While the zygapophysial joints may contribute to the biomechanical response of the spine during large, complex loads and thus would affect the determination of the elastic regions, their absence was much less important during determinations of NZ properties as minimal contact would occur between the articulating surfaces - underscoring the sensitivity of the NZ of the spine to the IVD (2, 5). Together, the rodent spine may serve to test IVD-related hypotheses but animal model disparities make extrapolation to the human condition difficult.

Similar to the effect of discal fluid alterations in humans, after 4 wk of unloading, IVD of HU±SC rats were geometrically smaller and functionally weaker than of AC rats. HU±SC discs were smaller and displayed weaker axial NZ moduli, which corroborated a loss of glycosaminoglycan content (33, 94) and is associated with minor injury (180) and disc degeneration (90). Therefore, hydration loss may increase the laxity of the disc during low-

magnitude loads, by loading the nucleus pulposus with less involvement of the solid matrix. Associatively, despite a statistically insignificant difference in compressive ROM, when compared to the greater mean IVD compressibility of subjects post bedrest (59[33]%), HU±SC segments had physiologically greater (49[20]%) compressive ROM than AC segments (154). Similar to the relationship between fluid loss and greater aggregate or compressive modulus of nondegenerate IVD (23, 139), the negative relationship between NZ modulus and change in posterior height of AC discs was weakened with unloading suggesting a disruption of the internal constituency of the posterior disc and not a scaled-down version of the region.

Hindlimb unloading further altered the mechanical behavior of the IVD in response to large loads and torsion. After 4 wk, short time constant τ_1, corresponding to the movement of unbound fluid, was greater in AC discs likely due to greater hydration and not different among the 4 wk groups. Similar to degenerated discs (128, 224), the compressive modulus and τ_2, corresponding to the movement of fluid through a resistant volume, was greater in HU±SC IVD. The hindered ability to relax was also evident in instantaneous elastic modulus of HU±SC discs and is consistent with the increased resiliency of gravitationally unloaded rat IVD (206). Additionally, IVD of HU±SC animals had weaker NZ torsional stiffness K_{NZ} but modulus G_{NZ} was not different from that of AC discs suggesting a similar distribution of torsional load in the annulus fibrosus but less resistance in an absolute sense. Together, hindlimb unloading morphologically and mechanically degraded the IVD.

Muscular loading is a predominate source of axial load to the rodent spine and therefore muscle morphology may provide insight to the mechanical loading conditions of HU discs. Four weeks of normal ambulatory aging caused no change to any muscle area. HU±SC

rats had increased psoas muscle area and, at L4, decreased paraspinal muscle area. Compared to AC, change in paraspinal area of HU±SC spines was less. Altered spinal loading has the ability to not only atrophy the back muscles (19) and disrupt their recruitment (127) but, as shown here, muscle-dependently affect area. Similarly, bed rest increases psoas area and decreases multifidus area (20) and since bed rest and hindlimb unloading oppositely affect IVD height, spinal length changes are unlikely direct causes to the disparate muscle area changes. Therefore the muscle areas changes were likely borne by the need to recruit alternate muscle fiber types to accommodate altered loading demands (41, 85, 169).

The introduction of 90Hz oscillations superimposed on intermittent periods of squat-like posture benefitted the height, nucleus pulposus area, NZ modulus, compressive modulus and instantaneous elastic stiffness of the L4-L5 IVD and was ineffectual to instantaneous elastic modulus, τ_2 and neutral zone stiffness K_{NZ}. In other words, vibrations benefited the properties sensitive to alterations of the nucleus pulposus rather than the annulus. In humans, vibrations with and without exercise maintain IVD height during spinal unloading to, at most, overnight bed rest levels (21, 96). In rodents, low-level vibrations help maintain IVD size and composition (94). While the relationship between glycosaminoglycan content and posterior height may not be maintained with 90Hz vibrations at L4-L5, the posterior glycosaminoglycan content is greater in HU+90 than HU±SC discs (94) which may explain a maintained relationship between NZ modulus and change in posterior height of HU+90 discs, and a greater relationship than of HU±SC discs. Similar to the present animal unloading study, bed rest studies show that maintenance of the morphology of the IVD by mechanical signals may also retard mechanical degradation of the IVD (39, 154).

Vibrations prevented a change in psoas muscle area but were ineffectual to the paraspinal area. Both muscles groups are involved with spinal compression but the multifidus is additionally involved with torso rotation (24). Corroboratively, paraspinal area and K_{NZ} were highly related (R^2=0.99) and therefore, maintenance of either may depend on the other. The differential impact of the countermeasure to the muscle areas may be due to dampening and therefore, proximity to the point of application. Low-magnitude, high-frequency vibrations applied at the plantar surface can improve soleus muscle area (237). Contrarily, increasing the magnitude of the vibrations may prevent muscular changes near and far from the point of application (21, 65), but strenuous exercise regimes must be applied cautiously as they may promote back pain (18).

The relationship between change in muscle volume and approximate spinal unit length illustrated the sensitive balance among the musculoskeletal tissues. For AC animals, the change in muscle volume between L4 and L5 was excellently related to the length (R^2=0.99), where muscle volume, L4-L5 length, vertebral length and bone volume all grew over 4 wk. Hindlimb unloading, regardless of upright posture, had a moderate relationship (R^2=0.48) by retardation of growth and loss of tissues, where muscle volume increased and bone volume decreased and, compared to AC, unloaded spines had less change in L4-L5 length and vertebral length. Vibrations protected the relationship between the change in muscle volume and segment length (R^2=0.91), but the tissue magnitudes were not different from HU±SC rat. These results suggest that maintenance of IVD height significantly contributed to the excellent relationship between change in muscle volume and segment length, potentially maintaining spinal load distribution. However, change in bone volume was less than HU±SC segments. Effectual

maintenance of rat vertebral bone volume may necessitate a larger magnitude during high-frequency vibrations (186, 201) but the results were consistent with the ineffectual prevention of tibial bone loss of HU mice (181).

Low-level, high-frequency mechanical signals partially maintained the function and morphology of a spinal motion segment, and prevented a loss in the relationship between IVD mechanics and morphology and between muscle volume and lumbar length during degradative spinal loading. The inability of the signal to completely protect the musculoskeletature of the lumbar spine from the detrimental effects of immobilization acknowledges the need to incorporate various exercise regimes (21, 39, 154). Although possible, it is unlikely that the paraspinal muscles indirectly (49) maintained the IVD since paraspinal area remained atrophied in the vibration group. Furthermore, greater muscle volume alone did not generate protective effects since L4-L5 muscle volume were similar between HU±SC and HU+90. Regardless of the mechanism(s), the results may highlight extremely low amplitude signals as a fundamental portion of treatment regimes or even daily loading (75). The efficacy of vibratory signals to prevent or treat muscle atrophy, back pain or disc degeneration of the immobilized due to prolonged bed rest, neuromuscular diseases or spinal cord injuries requires further study.

LIST OF TABLES

Table 7. Structural mechanical properties of motion segment L4-L5

Group	S_{COM} [N/mm]	S_{TEN} [N/mm]	S_{NZ} [N/mm]	Com ROM [mm]	S_1 [N/mm]	S_2 [N/mm]	S_3 [N/mm]	G_{NZ} [N/mm^o]	G [N/mm^o]
BC	97(5)	41(5)	4.6(2.6)	.31(.26)	34(5)	17(2)	466(40)	.30(.11)	1.1(.4)
AC	89(11)	40(3)	6.8(3.6)	.21(.06)	39(4)	18(1)	447(41)	.31(.05)	1.6(.3)*
HU±SC	99(11)	37(5)	2.3(1.8)†	.28(.11)	36(7)	18(1)	534(59)†	.23(.03)†	NA
HU§ HU+SC§	96 102	35 39	1.5 3.1	.32 .23	34 38	18 18	542 526	.23 .23	1.3 1.7
HU+90	82(13)‡	40(5)	6.7(4.3)‡	.28(.13)	38(6)	17(2)	447(50)‡	.20(.05)†	1.4(.2)

Values are presented as mean(SD) where n=7 for BC, AC and HU+90 and n=14 for HU±SC
§ Mean values for HU and HU+SC
NA – Not pooled due to significant t-test
* AC vs. BC
† Vs. AC
‡ Vs. HU±SC; $p<0.05$

Table 8. Material mechanical properties of motion segment L4-L5

Group	Com ROM [mm/mm]	S_1 [MPa]	S_2 [MPa]	S_3 [MPa]	τ_1 [s]	τ_2 [s]	G_{NZ} [kPa/^{o}]	G [kPa/^{o}]
BC	0.27 (0.19)	3.1 (0.6)	1.7 (0.4)	41.8 (5.1)	16.3 (2.4)	792 (74)	19.1 (6.3)	80.4 (22.1)
AC	0.24 (0.04)	3.3 (0.5)	1.6 (0.2)	38.4 (5.7)	19.8 (2.5)*	768 (76)	18.5 (3.0)	104.5 (25.8)
HU±SC	0.36 (0.17)	3.6 (0.9)	1.6 (0.2)	48.0 (7.2)†	18.9 (4.2)	900 (55)†	15.9 (3.0)	NA
HU§ HU+SC§	0.39 0.32	3.1 4.0	1.5 1.7	46.4 49.5	19.0 18.7	903 899	14.8 17.2	96.9 111.5
HU+90	0.31 (0.15)	3.5 (1.0)	1.7 (0.2)	43.4 (4.5)	19.5 (4.4)	884 (81)†	14.2 (3.5)	99.8 (12.0)

Values are presented as mean(SD) where n=7 for BC, AC and HU+90 and n=14 for HU±SC
Note $\eta=S_i \cdot \tau_i$
§ Mean values for HU and HU+SC
NA – Not pooled due to significant t-test
* AC vs. BC
† Vs. AC, $p<0.05$

Table 9. Baseline psoas and paraspinal muscle area of AC, HU±SC and HU+90 rats [cm^2]

Muscle-Location	AC	HU±SC	HU+90
Psoas-L4	0.62(0.04)	0.65(0.05)	0.68(0.05)
Psoas-L5	0.84(0.09)	0.81(0.07)	0.84(0.07)
Paraspinal-L4	2.67(0.18)	2.67(0.16)	2.63(0.19)
Paraspinal-L5	2.57(0.10)	2.39(0.24)	2.44(0.24)

Values are presented as mean(SD) where n=7 for AC and HU+90 and n=14 for HU±SC

Table 10. Muscle and bone volume, and vertebral bone and L4-L5 length of rats

	AC	HU±SC	HU+90
Muscle Volume [cm^3]			
Baseline	91.4(2.3)	93.4(2.8)	92.7(3.2)
4 wk	94.5(2.4) *	95.7(3.3) *	95.7(2.9) *
Percent [%]	*3.7(2.1)*	*1.9(1.1)*	*3.2(2.1)*
Bone Volume [cm^3]			
Baseline	22.4(0.7)	22.5(0.5)	23.3(1.0)
4 wk	23.3(0.8) *	21.0(1.1) *	20.8(0.8) *
Percent [%]	*4.1(2.2)*	*-6.8(4.2)* †	*-10.7(2.0)* †
Mean Vert. Length [mm]			
Baseline	6.4(0.2)	6.6(0.4)	6.8(0.2)
4 wk	6.9(0.1) *	6.9(0.2) *	6.9(0.2) *
Percent [%]	*8.4(3.3)*	*4.3(4.1)* †	*2.4(1.1)* †
L4-L5 Length [mm]			
Baseline	15.1(0.4)	15.4(0.5)	15.4(0.5)
4 wk	15.6(0.4) *	15.6(0.5)	15.7(0.5) *
Percent [%]	*3.7(2.1)*	*1.5(3.2)*	*1.4(0.8)*

Values are presented as mean(SD) where n=7 for AC and HU+90 and n=14 for HU±SC
* Vs. Baseline
† Vs. AC
‡ Vs. HU±SC; $p<0.05$

FIGURE LEGEND

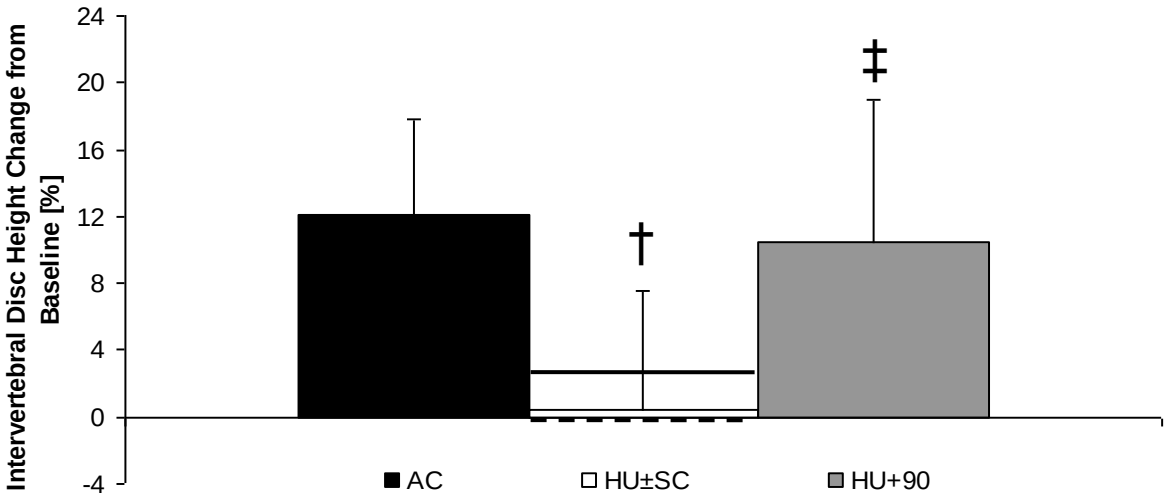

Figure 14. *Change of IVD Height from baseline of AC (n=7), HU±SC (n=14) and HU+90 (n=7); mean+SD. The hashed line was the mean HU value and the solid line was the mean HU+SC value. The introduction of 90Hz mechanical signals to upright posture maintained the change in IVD height. † compared to AC, ‡ compared to HU±SC; p <0.05*

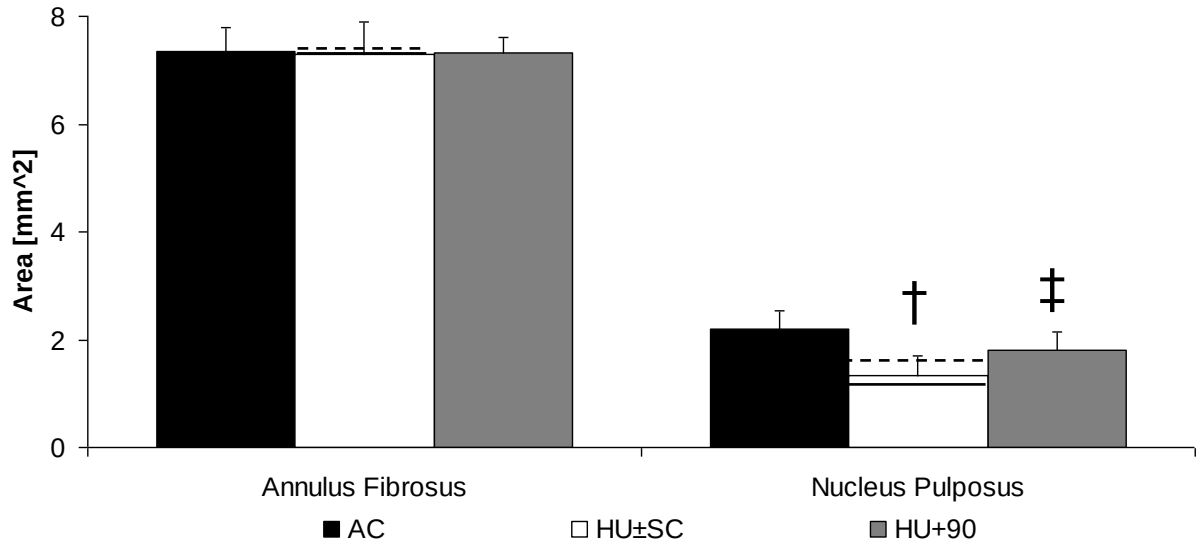

Figure 15. *Nucleus pulposus area of AC (n=7), HU±SC (n=14) and HU+90 (n=7) IVD; mean+SD. The hashed line was the mean HU value and the solid line was the mean HU+SC value. Compared to AC, IVD of hindlimb unloaded, with or without upright loading, animals had less nucleus pulposus area and 90 Hz vibrations maintained the nucleus pulposus area. † compared to AC, ‡ compared to HU+SC; p <0.05*

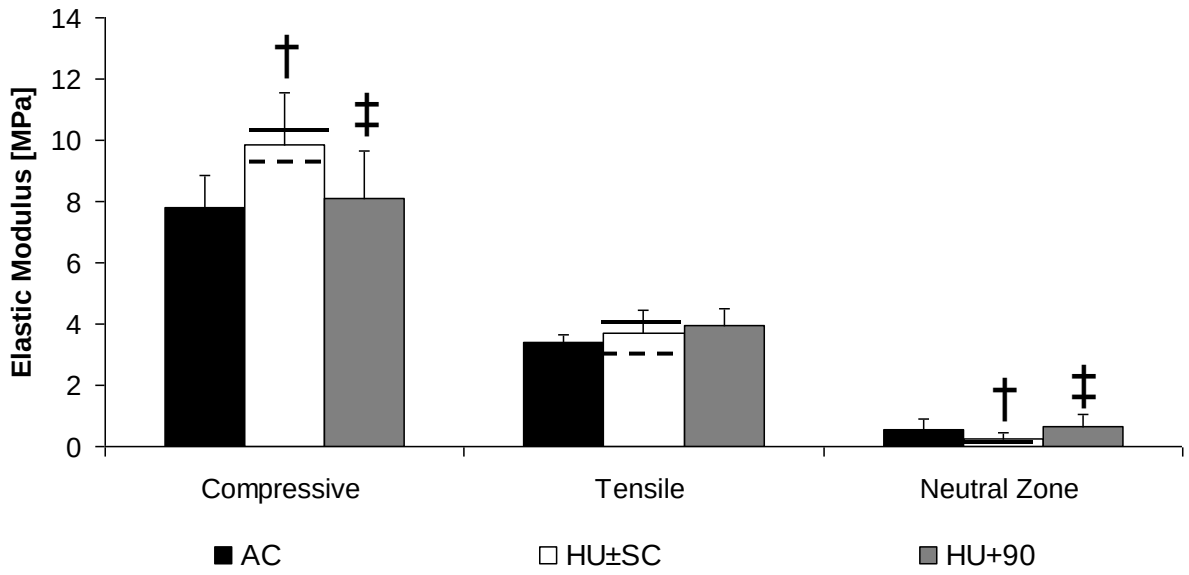

Figure 16. *Compressive, tensile and neutral zone modulus of L4-L5 segment from AC (n=7), HU±SC (n=14) and HU+90 (n=7) animals; mean+SD. The hashed line was the mean HU value and the solid line was the mean HU+SC value. Compared to AC, HU±SC segments had weaker neutral zone moduli and HU+SC segment had greater compressive moduli. HU+90 segments had greater neutral zone moduli and less compressive moduli than HU±SC segments. † compared to AC, ‡ compared to HU±SC; p <0.05*

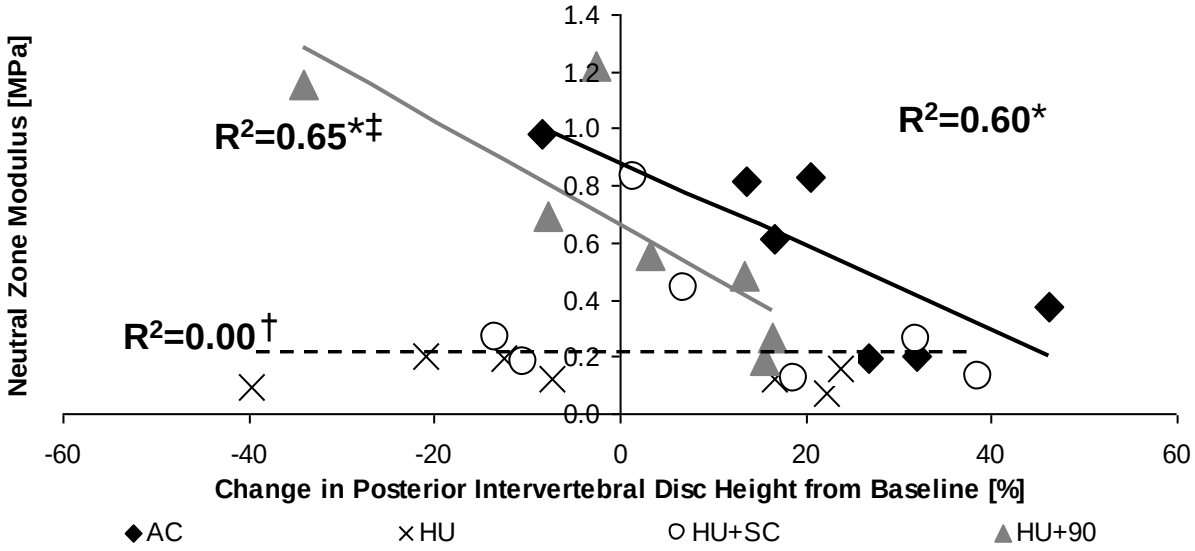

Figure 17. *Group regressions between neutral zone modulus and change in posterior disc height of AC (n=7), HU±SC (n=14) and HU+90 (n=7) animals. The hashed line is the regression for both HU and HU+SC values. High-frequency vibrations prevented a loss in the relationship from hindlimb unloading with or without sham loading. * regression, † compared to AC, ‡ compared to HU±SC; p <0.05*

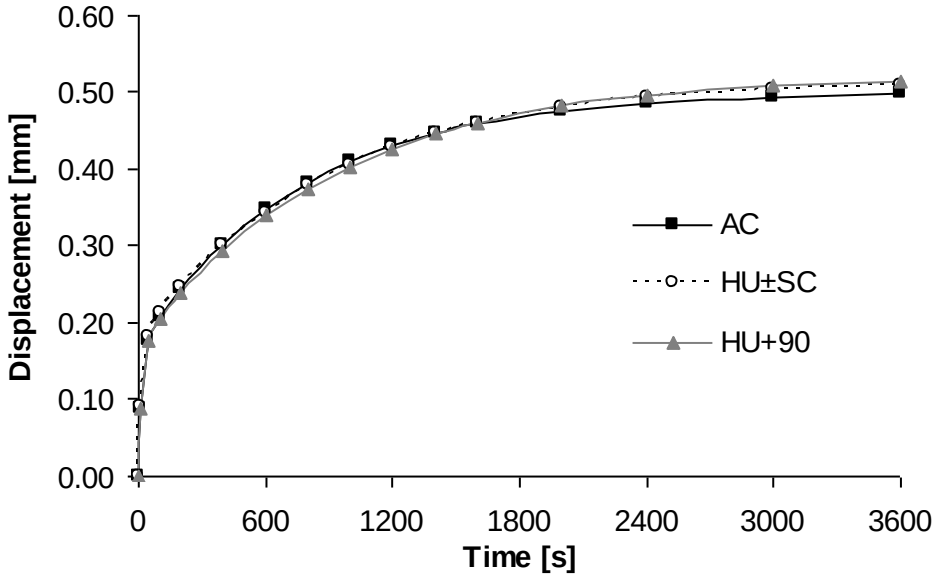

Figure 18. *Using mean values from the polynomial fit, the creep behavior of the AC (n=7), HU±SC (n=14) and HU+90 (n=7) animals were similar.*

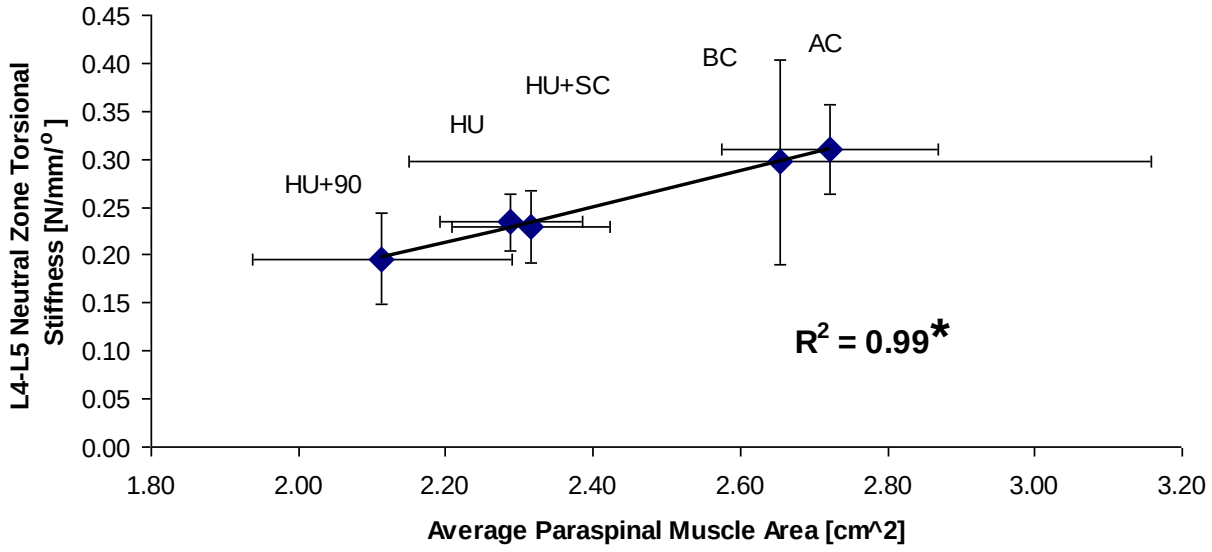

Figure 19. *Excellent regression between neutral zone torsional stiffness and average paraspinal muscle area across the mean of BC (n=7), AC (n=7), HU (n=7), HU+SC (n=7) and HU+90 (n=7).*

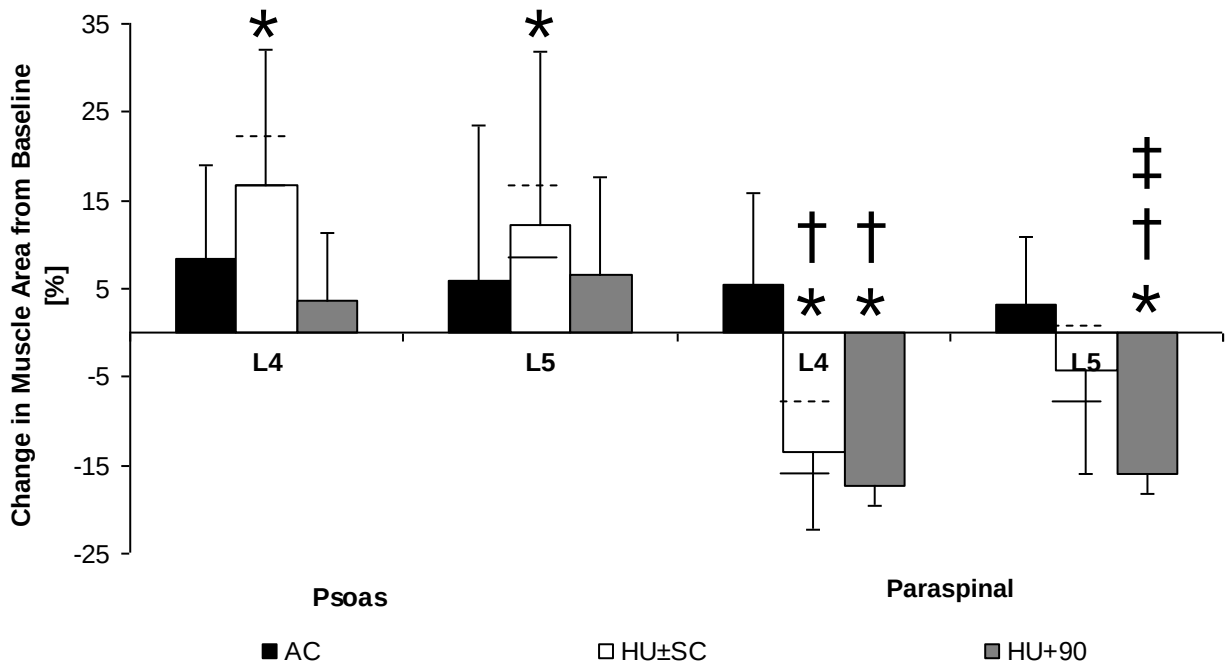

Figure 20. *Change in paraspinal muscle area at L4 and L5 of AC (n=7), HU±SC (n=14) and HU+90 (n=7) animals; mean+SD. The hashed line was the mean HU value and the solid line was the mean HU+SC value. Unloading with and without upright loading increased the psoas area at L4 and L5. At L4, paraspinal area of HU±SC rats was less than of AC rats. At L5, paraspinal area of HU+90 rats was less than of HU±SC and AC rats. * compared to baseline of same animal, † compared to AC, ‡ compared to HU±SC; p <0.05*

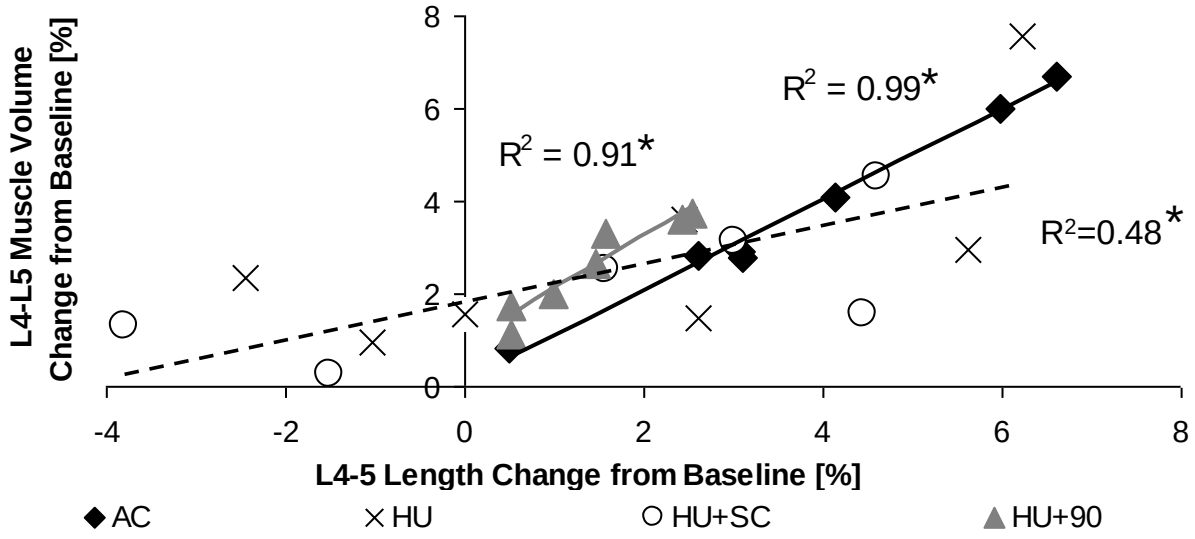

Figure 21. *Regression between change in muscle volume from L4 to L5 and change in L4-L5 length of AC (n=7), HU±SC (n=14) and HU+90 (n=7) animals; mean+SD. Each datum was a rat. Excellent regressions existed for AC rats with growth of lumbar length in every rat. The relationship was moderate for rats that were hindlimb unloaded with or without interruption by brief, upright posture with a few rats experiencing loss of lumbar length. The inclusion of 90Hz vibrations to upright posture maintained the relationship and growth of lumbar length in every rat. * p<.05*

VI

GLOBAL DISCUSSION

Global Discussion

The objective of the dissertation was to simulate the effects of reduced weightbearing on the IVD and counter the alterations with low-magnitude, high-frequency oscillations. Hindlimb unloading from the rat tail induced biochemical, morphological and mechanical changes to the IVD. Comparisons of these changes to those occurring in the IVD during degeneration, human microgravity, extended bed rest and rat microgravity show some similarities and differences and may provide insight to the mechanism of change (**Table 11**). During degeneration of the human IVD induced by aging, loading or genetics there is obvious discal damage with loss of size, hydration, GAG loss, subsequent compressive and viscoelastic stiffening but also increased compressibility (16, 136, 151, 175, 189, 224). Histologically, the IVD appears abnormal with opaqueness due to the abovementioned changes (29, 190). The known effects of human unloading on the intervertebral are few due to limited studies but include increased size and reduced osmotic pressure (96, 102, 145, 213). MRI imaging of bed rest subjects reveals abnormality beyond size (96). Dissimilar from human IVD, space flown rats do not show dimensional size changes but have reduced IVD wet weight (187, 206). No osmotic pressure changes were present but the re-exposure to over 50 hours of normal gravity could have reversed the spaceflight effects (87). Similarly to degenerated discs, hindlimb unloaded IVD are stiffer but appear histologically normal (187, 206).

Hindlimb unloading studies had yet to determine morphological changes to the IVD but similar to the effects of degeneration and microgravity, loss of GAG and osmotic pressure

occurred (87, 106, 187). Contrarily, hindlimb unloading caused no changes in collagen content (187). The IVD also appeared normal (106, 187, 241). First, there appears to be a disparity between the morphological effects from loading on the IVD of rats and humans. Secondly, the effects from hindlimb unloading on the IVD seem to posit the hypothesis that it resembles a slightly degenerated IVD or even an aged one because of the normalcy of the disc's appearance (106, 187, 241). Another type of cartilage resembles this hypotrophy and GAG loss from reduced loading, articular cartilage (133) and similar to the IVD (241), reloading incompletely restores the loss (83, 134).

The mechanism for large loads may include deformation and stimulation of the IVD and its incumbent viscoelastic cells (216). However, low-magnitude, high-frequency vibrations may employ a different mechanism; articular chondrocytes subjected to high oscillatory frequencies stiffen increasingly and non-linearly, resisting deformation (147). Therefore, the detection of the signal by the cells of the intervertebral disc may involve a sensitivity to the applied frequency (57). One proposed frequency-dependent mechanism is the acceleration of the nucleus of the cell within the cytoskeleton (12). Low-magnitude, high-frequency oscillations of annulus cells can suppress the genetic expression of matrix metalloproteinases (238) by activating signaling pathways via ATPs (239) but the study (238) also noted a decrease in aggrecan expression but did not measure changes to other, smaller GAGs. Although aggrecan is the dominant GAG in providing mechanical support to the IVD it is possible that the high-frequency vibrations may have increased the content of smaller GAGs, such as versican and decorin (56). Decorin is a pericellular GAG that decreases with age (205) and its expression is

reduced with the application of 40Hz vibrations but elevated at 80Hz (56). The composition of pericellular matrix may affect the delivery of mechanical signals to cells.

The vibrations may also have prevented fluid loss during hindlimb unloading by utilizing the viscoelasticity of the disc rather than by stimulating cellular production; an IVD with solid and fluid constituents will exude less fluid at higher frequencies. Additionally, the mechanism of unloading-induced degradation may also have been mechanical in nature where the tension of the suspension may have exuded the fluid. Furthermore, presupposing that rat discs mimic the tension-compression disparity in the anterior-posterior region of human discs (230), it is likely that the anterior region would maintain its morphology more readily than the posterior region because fluid more easily traverses the disc radially (79) and the force disparity could be 'sucking' fluid in the anterior direction. Brief periods of upright posture with 45Hz and 90Hz showed an improvement in the anterior and not the posterior region but the posterior height of the 90Hz group animals showed a trend towards maintenance. The 90Hz signal may allow the disc to stiffen more than the 45Hz, thereby retaining more fluid and size. The addition of an animal group that was only vibrated would help determine whether the vibrations were acting "anabolically" or "anti-catabolically" to the IVD but the mechanism affecting changes to the IVD from application of vibrations in a normally ambulating rat may differ. An ex vivo experiment could help elucidate the effect of one bout of vibration by measuring the wet weight at several time points prior to and following tensile load.

The mechanical properties changes of the IVD provide further insight to the structural make-up the unloading and unloaded plus vibrated IVD. High-frequency mechanical signals exclusively maintained properties closely related to hydration as noted by mechanical

properties and the maintained discal height, nucleus pulposus area and sGAG content. Decreased hydration may reduce the NZ modulus (245). In a well hydrated IVD, loads are transferred to the nucleus pulposus which radially displaces load to the annulus, which in turn begins to remove crimp from annulus fibers and remove macroscopic slack. In a dehydrated IVD, more axial motion is required to engage the annulus fibers, leading to a lower tension-compression NZ modulus. Even though the annulus has collagen fibers that can stretch ~4% (51), has collagen fibers bonds that can be strained to comprise the elasticity of the annulus and has elastin fibers, the magnitude of motion is still limited. Greater axial compressive motion compromises the limit of radial motion of the annulus in response to compressive loads. Therefore, although vibrated IVD exhibited a similar compressive of ROM as unloaded IVD, vibrated IVD had greater tension-compression NZ modulus which likely helped in maintaining a normal compressive modulus.

Other than hydration alterations, changes to the solid matrix quality of the annulus fibrosus may offer other hypotheses concerning the effect of hindlimb unloading on the IVD and maintenance of the IVD by low-magnitude vibrations. Despite unaltered collagen content during hindlimb unloading, inchoate collagen, as occurs during gravitational unloading (70), may have increased the compressive modulus during hindlimb unloading by compromising the low elongation capability of collagen. Disorganized collagen may also increase the hydraulic resistance of the IVD, thereby reducing fluid exudation and increasing initial damping. More collagen content could contribute to similar mechanical behavior but unloading does not increase collagen content (94, 160). Greater cross-linking would theoretically increase compressive modulus (48) and torsional stiffness (14) but since K_{NZ} was lower in HU±SC IVD,

greater cross-linking was unlikely. Overall, lower K_{NZ} during hindlimb unloading was corroborated by the paraspinal atrophy of torsion-related muscles and loss of glycosaminoglycans, which including hydrophilic capabilities also help bind lamellae (51).

Despite an unchanged annulus fibrosus area, the net hydraulic permeability could be reduced by a change in fluid-pore size of the annulus matrix. Hindlimb unloaded discs demonstrate altered fibril diameters to accommodate for the tail traction (160). The increased diameter of the posterior fibrils may reduce the transport of fluid from the spinal cord. The inability of the vibration treatment to prevent viscoelastic properties of the IVD may be borne from altered collagen organization. Whole-body vibrations applied orthogonal to the spine during unloading benefited the area of the IVD, rather than the height of the IVD, which could mean a modulation of collagen orientation. However, vibrations applied in an upright stance did not prevent changes to the long time constant τ_2 or instantaneous elastic modulus S_3, indicating that the benefit of vibrations did not include the annulus.

The similarities of the effects of human spinal unloading and rat hind limb unloading in mechanical properties of the intervertebral disc and muscular area changes increase the likelihood that the biochemical changes measured here also occur during. Low-magnitude vibrations applied in humans (96) and rats mitigated morphology change. Therefore, it is also possible that the benefit of vibrations to the intervertebral disc was indirect since increased glycosaminoglycan content, which could swell the rat disc, would not reduce the hyper-swelling of the disc during reduced spinal loading. Since vibrations can be beneficial to connective tissue (148, 166), maintained ligamentous tension from vibrations could attenuate swelling in humans and in rats provide healthy dynamic loading. Whether the intervertebral disc responds to high-

frequency, low-magnitude mechanical signals directly or indirectly through endogenous loading requires further investigation.

In conclusion, hindlimb unloading hypotrophies the intervertebral disc, reduces the glycosaminoglycan content and functionally disrupts the lumbar motion segment. Neither brief ambulation nor the addition of low-magnitude, high frequency vibrations applied orthogonal to the rat spine ablates the alterations from hindlimb unloading. Vibrations applied in the longitudinal axis of the rat spine partially maintained the physique of the lumbar spine and its surrounding spinal musculature. Whether the beneficial extent of these vibrations in humans is similar or whether vibrations can recover discal damage also remains to be investigated.

List of Table

Table 11. Comparison of the effects of degeneration, human and rats spinal unloading, and hindlimb unloading on the IVD

Compared to Vivarium Control	Human Disc Degeneration	Reduced Weight Bearing		HU	Holguin-HU
		Human Microgravity & Bed Rest	Rat Microgravity		
Disc Thickness	▼(189)	▲(102)	●(206)	~	▼
Disc Area	~	▲(145)	~	~	▼
Disc Volume	▼(189)	▲(97)	~	~	▼
Wet Weight	▼(218)	~	●(206) - ▼(187)	●(187)	~
Osmotic Pressure	▼(199)	▼(213)	●(87)	▼(87)	~
GAG	▼(151)	~	▼(187, 206)	▼(106, 187)	▼
H-proline	▲(223)	~	▲(187, 206)	●(187)	●
Stiffness	▲(136, 224)	~	▲(206)	~	▲
Histology or MRI	Abnormal(29, 190)	Normal(97)	Normal(187)	Normal (106, 187, 241)	~
Compressibility	▲(175)	▲(154)	~	~	▲

▲ Increase, ▼ Decrease, ● Same, ~ Not Available

References

1. **Abercromby AF, Amonette WE, Layne CS, McFarlin BK, Hinman MR, and Paloski WH**. Vibration exposure and biodynamic responses during whole-body vibration training. *Medicine and science in sports and exercise* 39: 1794-1800, 2007.

2. **Abumi K, Panjabi MM, Kramer KM, Duranceau J, Oxland T, and Crisco JJ**. Biomechanical evaluation of lumbar spinal stability after graded facetectomies. *Spine (Phila Pa 1976)* 15: 1142-1147, 1990.

3. **Acaroglu ER, Iatridis JC, Setton LA, Foster RJ, Mow VC, and Weidenbaum M**. Degeneration and aging affect the tensile behavior of human lumbar anulus fibrosus. *Spine* 20: 2690-2701, 1995.

4. **Adams MA, and Hutton WC**. The effect of posture on the fluid content of lumbar intervertebral discs. *Spine* 8: 665-671, 1983.

5. **Adams MA, and Hutton WC**. The mechanical function of the lumbar apophyseal joints. *Spine* 8: 327-330, 1983.

6. **Adams MA, McNally DS, and Dolan P**. 'Stress' distributions inside intervertebral discs. The effects of age and degeneration. *J Bone Joint Surg Br* 78: 965-972, 1996.

7. **Adams MA, Pollintine P, Tobias JH, Wakley GK, and Dolan P**. Intervertebral disc degeneration can predispose to anterior vertebral fractures in the thoracolumbar spine. *J Bone Miner Res* 21: 1409-1416, 2006.

8. **Aguiar DJ, Johnson SL, and Oegema TR**. Notochordal cells interact with nucleus pulposus cells: regulation of proteoglycan synthesis. *Experimental cell research* 246: 129-137, 1999.

9. **Akella SV, Regatte RR, Gougoutas AJ, Borthakur A, Shapiro EM, Kneeland JB, Leigh JS, and Reddy R**. Proteoglycan-induced changes in T1rho-relaxation of articular cartilage at 4T. *Magn Reson Med* 46: 419-423, 2001.

10. **Akeson WH, Amiel D, Abel MF, Garfin SR, and Woo SL**. Effects of immobilization on joints. *Clinical orthopaedics and related research* 28-37, 1987.

11. **Antoniou J, Steffen T, Nelson F, Winterbottom N, Hollander AP, Poole RA, Aebi M, and Alini M**. The human lumbar intervertebral disc: evidence for changes in the biosynthesis and denaturation of the extracellular matrix with growth, maturation, ageing, and degeneration. *The Journal of clinical investigation* 98: 996-1003, 1996.

12. **Bacabac RG, Smit TH, Van Loon JJ, Doulabi BZ, Helder M, and Klein-Nulend J**. Bone cell responses to high-frequency vibration stress: does the nucleus oscillate within the cytoplasm? *Faseb J* 20: 858-864, 2006.

13. **Bailey AS, Adler F, Min Lai S, and Asher MA**. A comparison between bipedal and quadrupedal rats: do bipedal rats actually assume an upright posture? *Spine (Phila Pa 1976)* 26: E308-313, 2001.

14. **Barbir A, Godburn KE, Michalek AJ, Lai A, Monsey RD, and Iatridis JC**. Effects of Torsion on Intervertebral Disc Gene Expression and Biomechanics, Using a Rat Tail Model. *Spine (Phila Pa 1976)*.

15. **Basso N, and Heersche JN**. Effects of hind limb unloading and reloading on nitric oxide synthase expression and apoptosis of osteocytes and chondrocytes. *Bone* 39: 807-814, 2006.

16. **Battie MC, Videman T, Kaprio J, Gibbons LE, Gill K, Manninen H, Saarela J, and Peltonen L**. The Twin Spine Study: contributions to a changing view of disc degeneration. *Spine J* 9: 47-59, 2009.

17. **Beckstein JC, Sen S, Schaer TP, Vresilovic EJ, and Elliott DM**. Comparison of animal discs used in disc research to human lumbar disc: axial compression mechanics and glycosaminoglycan content. *Spine* 33: E166-173, 2008.

18. **Belavy DL, Armbrecht G, Gast U, Richardson CA, Hides JA, and Felsenberg D**. Countermeasures against lumbar spine deconditioning in prolonged bed-rest: resistive exercise with and without whole-body vibration. *J Appl Physiol* 2010.

19. **Belavy DL, Armbrecht G, Richardson CA, Felsenberg D, and Hides JA**. Muscle atrophy and changes in spinal morphology: is the lumbar spine vulnerable after prolonged bed-rest? *Spine* 10.1097/BRS.0b013e3181cc93e8: 2010.

20. **Belavy DL, Armbrecht G, Richardson CA, Felsenberg D, and Hides JA**. Muscle Atrophy and Changes in Spinal Morphology: Is the Lumbar Spine Vulnerable After Prolonged Bed-Rest? *Spine (Phila Pa 1976)* 2010.

21. **Belavy DL, Hides JA, Wilson SJ, Stanton W, Dimeo FC, Rittweger J, Felsenberg D, and Richardson CA**. Resistive simulated weightbearing exercise with whole body vibration reduces lumbar spine deconditioning in bed-rest. *Spine* 33: E121-131, 2008.

22. **Berlemann U, Gries NC, and Moore RJ**. The relationship between height, shape and histological changes in early degeneration of the lower lumbar discs. *Eur Spine J* 7: 212-217, 1998.

23. **Best BA, Guilak F, Setton LA, Zhu W, Saed-Nejad F, Ratcliffe A, Weidenbaum M, and Mow VC**. Compressive mechanical properties of the human anulus fibrosus and their relationship to biochemical composition. *Spine* 19: 212-221, 1994.

24. **Bogduk N**. *Clinical Anatomy of the Lumbar Spine and Sacrum*. London: Elsevier, Churchill Livingston, 2007.

25. **Bonassar LJ, Grodzinsky AJ, Frank EH, Davila SG, Bhaktav NR, and Trippel SB**. The effect of dynamic compression on the response of articular cartilage to insulin-like growth factor-I. *J Orthop Res* 19: 11-17, 2001.

26. **Bongers PM, Boshuizen HC, Hulshof CT, and Koemeester AP**. Long-term sickness absence due to back disorders in crane operators exposed to whole-body vibration. *International archives of occupational and environmental health* 61: 59-64, 1988.

27. **Boos N, Rieder R, Schade V, Spratt KF, Semmer N, and Aebi M**. 1995 Volvo Award in clinical sciences. The diagnostic accuracy of magnetic resonance imaging, work perception, and psychosocial factors in identifying symptomatic disc herniations. *Spine* 20: 2613-2625, 1995.

28. **Boos N, Wallin A, Aebi M, and Boesch C**. A new magnetic resonance imaging analysis method for the measurement of disc height variations. *Spine* 21: 563-570, 1996.

29. **Boos N, Weissbach S, Rohrbach H, Weiler C, Spratt KF, and Nerlich AG**. Classification of age-related changes in lumbar intervertebral discs: 2002 Volvo Award in basic science. *Spine* 27: 2631-2644, 2002.

30. **Bortz WM, 2nd**. The disuse syndrome. *The Western journal of medicine* 141: 691-694, 1984.

31. **Bovenzi M, and Hulshof CT**. An updated review of epidemiologic studies on the relationship between exposure to whole-body vibration and low back pain (1986-1997). *International archives of occupational and environmental health* 72: 351-365, 1999.

32. **Boxberger JI, Auerbach JD, Sen S, and Elliott DM**. An in vivo model of reduced nucleus pulposus glycosaminoglycan content in the rat lumbar intervertebral disc. *Spine (Phila Pa 1976)* 33: 146-154, 2008.

33. **Boxberger JI, Sen S, Yerramalli CS, and Elliott DM**. Nucleus Pulposus Glycosaminoglycan Content Is Correlated with Axial Mechanics in Rat Lumbar Motion Segments. *Journal of Orthopaedic Research* 24: 1906-1915, 2006.

34. **Bressel E, Smith G, and Branscomb J**. Transmission of whole body vibration in children while standing. *Clinical biomechanics (Bristol, Avon)* 25: 181-186, 2010.

35. **Buckwalter JA**. Aging and degeneration of the human intervertebral disc. *Spine* 20: 1307-1314, 1995.

36. **Buschmann MD, Gluzband YA, Grodzinsky AJ, and Hunziker EB**. Mechanical compression modulates matrix biosynthesis in chondrocyte/agarose culture. *Journal of cell science* 108 (Pt 4): 1497-1508, 1995.

37. **Buschmann MD, Hunziker EB, Kim YJ, and Grodzinsky AJ**. Altered aggrecan synthesis correlates with cell and nucleus structure in statically compressed cartilage. *Journal of cell science* 109 (Pt 2): 499-508, 1996.

38. **Buschmann MD, Kim YJ, Wong M, Frank E, Hunziker EB, and Grodzinsky AJ**. Stimulation of aggrecan synthesis in cartilage explants by cyclic loading is localized to regions of high interstitial fluid flow. *Archives of biochemistry and biophysics* 366: 1-7, 1999.

39. **Cao P, Kimura S, Macias BR, Ueno T, Watenpaugh DE, and Hargens AR**. Exercise within lower body negative pressure partially counteracts lumbar spine deconditioning associated with 28-day bed rest. *J Appl Physiol* 99: 39-44, 2005.

40. **Carpenter D, LeBlanc A, Evans H, Sibonga J, and Lang T**. Long-term changes in the density and structure of the human hip and spine after long-duration space flight. *Acta Astronautica* 67: 71-81, 2010.

41. **Cassidy JD, Yong-Hing K, Kirkaldy-Willis WH, and Wilkinson AA**. A study of the effects of bipedism and upright posture on the lumbosacral spine and paravertebral muscles of the Wistar rat. *Spine (Phila Pa 1976)* 13: 301-308, 1988.

42. **Cassinelli EH, Hall RA, and Kang JD**. Biochemistry of intervertebral disc degeneration and the potential for gene therapy applications. *Spine J* 1: 205-214, 2001.

43. **Cavanagh PR, Genc KO, Gopalakrishnan R, Kuklis MM, Maender CC, and Rice AJ**. Foot forces during typical days on the international space station. *J Biomech*.

44. **Cavanagh PR, K.O. G, Gopalakrishnan R, Kuklis MM, Meander CC, and Rice AJ**. Foot forces during typical days on the international space station. *J Biomech* doi:10.1016/j.jbiomech.2010.1003.1044, 2010.

45. **Chiang F**. Micro-/nano-speckle method with applications to materials, tissue engineering and heart mechanics. *Strain* 44: 27-39, 2008.

46. **Ching CT, Chow DH, Yao FY, and Holmes AD**. Changes in nuclear composition following cyclic compression of the intervertebral disc in an in vivo rat-tail model. *Medical engineering & physics* 26: 587-594, 2004.

47. **Christe A, Laubli R, Guzman R, Berlemann U, Moore RJ, Schroth G, Vock P, and Lovblad KO**. Degeneration of the cervical disc: histology compared with radiography and magnetic resonance imaging. *Neuroradiology* 47: 721-729, 2005.

48. **Chuang SY, Odono RM, and Hedman TP**. Effects of exogenous crosslinking on in vitro tensile and compressive moduli of lumbar intervertebral discs. *Clinical biomechanics (Bristol, Avon)* 22: 14-20, 2007.

49. **Cochrane DJ, Loram ID, Stannard SR, and Rittweger J**. Changes in joint angle, muscle-tendon complex length, muscle contractile tissue displacement, and modulation of EMG activity during acute whole-body vibration. *Muscle & nerve* 40: 420-429, 2009.

50. **Collacott EA, Zimmerman JT, White DW, and Rindone JP**. Bipolar permanent magnets for the treatment of chronic low back pain: a pilot study. *Jama* 283: 1322-1325, 2000.

51. **Comper WD, and Laurent TC**. Physiological function of connective tissue polysaccharides. *Physiological reviews* 58: 255-315, 1978.

52. **Coppes MH, Marani E, Thomeer RT, and Groen GJ**. Innervation of "painful" lumbar discs. *Spine* 22: 2342-2349; discussion 2349-2350, 1997.

53. **Dabbs VM, and Dabbs LG**. Correlation between disc height narrowing and low-back pain. *Spine* 15: 1366-1369, 1990.

54. **Davidsen PK, Gallagher IJ, Hartman JW, Tarnopolsky MA, Dela F, Helge JW, Timmons JA, and Phillips SM**. High responders to resistance exercise training demonstrate differential regulation of skeletal muscle microRNA expression. *J Appl Physiol*.

55. **De Mattei M, Caruso A, Pezzetti F, Pellati A, Stabellini G, Sollazzo V, and Traina GC**. Effects of pulsed electromagnetic fields on human articular chondrocyte proliferation. *Connective tissue research* 42: 269-279, 2001.

56. **Desmoulin GT, Reno CR, and Hunter CJ**. Free axial vibrations at 0 to 200 Hz positively affect extracellular matrix messenger ribonucleic acid expression in bovine nucleus pulposi. *Spine (Phila Pa 1976)* 35: 1437-1444, 2010.

57. **Desmoulin GT, Reno CR, and Hunter CJ**. Free Axial Vibrations At 0 to 200 Hz Positively Affect Extracellular Matrix Messenger Ribonucleic Acid Expression in Bovine Nucleus Pulposi. *Spine (Phila Pa 1976)* 2010.

58. **Donohue PJ, Jahnke MR, Blaha JD, and Caterson B**. Characterization of link protein(s) from human intervertebral-disc tissues. *The Biochemical journal* 251: 739-747, 1988.

59. **Duke PJ, and Montufar-Solis D**. Exposure to altered gravity affects all stages of endochondral cartilage differentiation. *Adv Space Res* 24: 821-827, 1999.

60. **Edwards WT, Ordway NR, Zheng Y, McCullen G, Han Z, and Yuan HA**. Peak stresses observed in the posterior lateral anulus. *Spine* 26: 1753-1759, 2001.

61. **Elliott DM, and Sarver JJ**. Young investigator award winner: validation of the mouse and rat disc as mechanical models of the human lumbar disc. *Spine* 29: 713-722, 2004.

62. **Espinoza Orias AA, Malhotra NR, and Elliott DM**. Rat disc torsional mechanics: effect of lumbar and caudal levels and axial compression load. *Spine J* 9: 204-209, 2009.

63. **Eyre D BP, BuckwaterJ, et al.** The intervertebral disc: basic science perspectives In: *New pespectives on low back pain*, edited by Frymoyer J GS. Park Ridge (IL): American Academy of Orthopaedic Surgeons, 1989, p. 147-207.

64. **Eyre DR, Wu JJ, and Woods PE**. The cartilage collagens: structural and metabolic studies. *J Rheumatol Suppl* 27: 49-51, 1991.

65. **Falempin M, and In-Albon SF**. Influence of brief daily tendon vibration on rat soleus muscle in non-weight-bearing situation. *J Appl Physiol* 87: 3-9, 1999.

66. **Farfan HF, Cossette JW, Robertson GH, Wells RV, and Kraus H**. The effects of torsion on the lumbar intervertebral joints: the role of torsion in the production of disc degeneration. *The Journal of bone and joint surgery* 52: 468-497, 1970.

67. **Farfan HF, Huberdeau RM, and Dubow HI**. Lumbar intervertebral disc degeneration: the influence of geometrical features on the pattern of disc degeneration--a post mortem study. *The Journal of bone and joint surgery* 54: 492-510, 1972.

68. **Fei QM, Jiang XX, Chen TY, Li J, Murakami H, Tsai KJ, and Hutton WC**. Changes with age and the effect of recombinant human BMP-2 on proteoglycan and collagen gene expression in rabbit anulus fibrosus cells. *Acta biochimica et biophysica Sinica* 38: 773-779, 2006.

69. **Fitzgerald JB, Jin M, Dean D, Wood DJ, Zheng MH, and Grodzinsky AJ**. Mechanical compression of cartilage explants induces multiple time-dependent gene expression patterns and involves intracellular calcium and cyclic AMP. *The Journal of biological chemistry* 279: 19502-19511, 2004.

70. **Foldes I, Kern M, Szilagyi T, and Oganov VS**. Histology and histochemistry of intervertebral discs of rats participated in spaceflight. *Acta biologica Hungarica* 47: 145-156, 1996.

71. **Foldes I, Kern M, Szilagyi T, and Oganov VS**. Histology and histochemistry of intervertebral discs of rats participated in spaceflight. *Acta biologica Hungarica* 47: 145-156, 1996.

72. **Fontana TL, Richardson CA, and Stanton WR**. The effect of weight-bearing exercise with low frequency, whole body vibration on lumbosacral proprioception: a pilot study on normal subjects. *The Australian journal of physiotherapy* 51: 259-263, 2005.

73. **Frank EH, Jin M, Loening AM, Levenston ME, and Grodzinsky AJ**. A versatile shear and compression apparatus for mechanical stimulation of tissue culture explants. *Journal of biomechanics* 33: 1523-1527, 2000.

74. **Freemont AJ, Watkins A, Le Maitre C, Jeziorska M, and Hoyland JA**. Current understanding of cellular and molecular events in intervertebral disc degeneration: implications for therapy. *The Journal of pathology* 196: 374-379, 2002.

75. **Fritton SP, McLeod KJ, and Rubin CT**. Quantifying the strain history of bone: spatial uniformity and self-similarity of low-magnitude strains. *J Biomech* 33: 317-325, 2000.

76. **Fritz M**. Description of the relation between the forces acting in the lumbar spine and whole-body vibrations by means of transfer functions. *Clinical biomechanics (Bristol, Avon)* 15: 234-240, 2000.

77. **Garman R, Gaudette G, Donahue LR, Rubin C, and Judex S**. Low-level accelerations applied in the absence of weight bearing can enhance trabecular bone formation. *J Orthop Res* 25: 732-740, 2007.

78. **Giangregorio L, and McCartney N**. Bone loss and muscle atrophy in spinal cord injury: epidemiology, fracture prediction, and rehabilitation strategies. *The journal of spinal cord medicine* 29: 489-500, 2006.

79. **Gu WY, Mao XG, Foster RJ, Weidenbaum M, Mow VC, and Rawlins BA**. The anisotropic hydraulic permeability of human lumbar anulus fibrosus: influence of age, degeneration, direction, and water content. *Spine* 24: 2449-2455, 1999.

80. **Gu WY, Mao XG, Rawlins BA, Iatridis JC, Foster RJ, Sun DN, Weidenbaum M, and Mow VC**. Streaming potential of human lumbar anulus fibrosus is anisotropic and affected by disc degeneration. *Journal of biomechanics* 32: 1177-1182, 1999.

81. **Guehring T, Nerlich A, Kroeber M, Richter W, and Omlor GW**. Sensitivity of notochordal disc cells to mechanical loading: an experimental animal study. *Eur Spine J* 19: 113-121, 2010.

82. **Guehring T, Wilde G, Sumner M, Grunhagen T, Karney GB, Tirlapur UK, and Urban JP**. Notochordal intervertebral disc cells: sensitivity to nutrient deprivation. *Arthritis and rheumatism* 60: 1026-1034, 2009.

83. **Haapala J, Arokoski J, Pirttimaki J, Lyyra T, Jurvelin J, Tammi M, Helminen HJ, and Kiviranta I**. Incomplete restoration of immobilization induced softening of young beagle knee articular cartilage after 50-week remobilization. *International journal of sports medicine* 21: 76-81, 2000.

84. **Haefeli M, Kalberer F, Saegesser D, Nerlich AG, Boos N, and Paesold G**. The course of macroscopic degeneration in the human lumbar intervertebral disc. *Spine* 31: 1522-1531, 2006.

85. **Haggmark T, Eriksson E, and Jansson E**. Muscle fiber type changes in human skeletal muscle after injuries and immobilization. *Orthopedics* 9: 181-185, 1986.

86. **Handa T, Ishihara H, Ohshima H, Osada R, Tsuji H, and Obata K**. Effects of hydrostatic pressure on matrix synthesis and matrix metalloproteinase production in the human lumbar intervertebral disc. *Spine* 22: 1085-1091, 1997.

87. **Hargens AR, and Mahmood M**. Decreased swelling pressure of rat nucleus pulposus associated with simulated weightlessness. *Physiologist* 32: S23-24, 1989.

88. **Hargens AR, Steskal J, Johansson C, and Tipton CM**. Tissue fluid shift, forelimb loading, and tail tension in tail-suspended rats. *Physiologist* 27: S37-38, 1984.

89. **Haughton V, Lim T, and An H**. Intervertebral disk appearance correlated with stiffness of lumbar spinal motion segments. *Ajnr* 20: 1161-1165, 1999.

90. **Haughton VM, Lim TH, and An H**. Intervertebral disk appearance correlated with stiffness of lumbar spinal motion segments. *Ajnr* 20: 1161-1165, 1999.

91. **Hicks GS, Duddleston DN, Russell LD, Holman HE, Shepherd JM, and Brown CA**. Low back pain. *The American journal of the medical sciences* 324: 207-211, 2002.

92. **Hill TE, Desmoulin GT, and Hunter CJ**. Is vibration truly an injurious stimulus in the human spine? *Journal of biomechanics* 42: 2631-2635, 2009.

93. **Hoemann CD, Sun J, Chrzanowski V, and Buschmann MD**. A multivalent assay to detect glycosaminoglycan, protein, collagen, RNA, and DNA content in milligram samples of cartilage or hydrogel-based repair cartilage. *Analytical biochemistry* 300: 1-10, 2002.

94. **Holguin N, and Judex S**. Brief bouts of low-level vibrations attenuate intervertebral disc degeneration. In: *ORS Annual Meeting*. Las Vegas, NV: 2010.

95. **Holguin N, and Judex S**. Rat Intervertebral Disc Health During Hindlimb Unloading: Brief Ambulation With or Without Vibration *Aviation, space, and environmental medicine* 81: 2010.

96. **Holguin N, Muir J, Rubin C, and Judex S**. Short applications of very low-magnitude vibrations attenuate expansion of the intervertebral disc during extended bed rest. *Spine J* 9: 470-477, 2009.

97. **Holguin N, Rubin C, and Judex S**. Short Applications of Very Low-Magnitude Vibrations Attenuate Expansion of the Intervertebral Disc during Extended Bed Rest. *Spine J* 2009.

98. **Huang RP, Rubin CT, and McLeod KJ**. Changes in postural muscle dynamics as a function of age. *The journals of gerontology* 54: B352-357, 1999.

99. **Hunter CJ, Matyas JR, and Duncan NA**. Cytomorphology of notochordal and chondrocytic cells from the nucleus pulposus: a species comparison. *Journal of anatomy* 205: 357-362, 2004.

100. **Hunter CJ, Matyas JR, and Duncan NA**. The functional significance of cell clusters in the notochordal nucleus pulposus: survival and signaling in the canine intervertebral disc. *Spine (Phila Pa 1976)* 29: 1099-1104, 2004.

101. **Hunter CJ, Matyas JR, and Duncan NA**. The notochordal cell in the nucleus pulposus: a review in the context of tissue engineering. *Tissue engineering* 9: 667-677, 2003.

102. **Hutchinson KJ, Watenpaugh DE, Murthy G, Convertino VA, and Hargens AR**. Back pain during 6 degrees head-down tilt approximates that during actual microgravity. *Aviation, space, and environmental medicine* 66: 256-259, 1995.

103. **Hutton WC, Ganey TM, Elmer WA, Kozlowska E, Ugbo JL, Doh ES, and Whitesides TE, Jr.** Does long-term compressive loading on the intervertebral disc cause degeneration? *Spine* 25: 2993-3004, 2000.

104. **Hutton WC, Malko JA, and Fajman WA**. Lumbar disc volume measured by MRI: effects of bed rest, horizontal exercise, and vertical loading. *Aviation, space, and environmental medicine* 74: 73-78, 2003.

105. **Hutton WC, Toribatake Y, Elmer WA, Ganey TM, Tomita K, and Whitesides TE**. The effect of compressive force applied to the intervertebral disc in vivo. A study of proteoglycans and collagen. *Spine* 23: 2524-2537, 1998.

106. **Hutton WC, Yoon ST, Elmer WA, Li J, Murakami H, Minamide A, and Akamaru T**. Effect of tail suspension (or simulated weightlessness) on the lumbar intervertebral disc: study of proteoglycans and collagen. *Spine* 27: 1286-1290, 2002.

107. **Ianuzzi A, Little JS, Chiu JB, Baitner A, Kawchuk G, and Khalsa PS**. Human lumbar facet joint capsule strains: I. During physiological motions. *Spine J* 4: 141-152, 2004.

108. **Iatridis JC, MaClean JJ, and Ryan DA**. Mechanical damage to the intervertebral disc annulus fibrosus subjected to tensile loading. *Journal of biomechanics* 38: 557-565, 2005.

109. **Iatridis JC, Mente PL, Stokes IA, Aronsson DD, and Alini M**. Compression-induced changes in intervertebral disc properties in a rat tail model. *Spine (Phila Pa 1976)* 24: 996-1002, 1999.

110. **Iatridis JC, Setton LA, Foster RJ, Rawlins BA, Weidenbaum M, and Mow VC**. Degeneration affects the anisotropic and nonlinear behaviors of human anulus fibrosus in compression. *Journal of biomechanics* 31: 535-544, 1998.

111. **Iatridis JC, Setton LA, Weidenbaum M, and Mow VC**. Alterations in the mechanical behavior of the human lumbar nucleus pulposus with degeneration and aging. *J Orthop Res* 15: 318-322, 1997.

112. **Iatridis JC, Weidenbaum M, Setton LA, and Mow VC**. Is the nucleus pulposus a solid or a fluid? Mechanical behaviors of the nucleus pulposus of the human intervertebral disc. *Spine* 21: 1174-1184, 1996.

113. **Igarashi T, Kikuchi S, Shubayev V, and Myers RR**. 2000 Volvo Award winner in basic science studies: Exogenous tumor necrosis factor-alpha mimics nucleus pulposus-induced neuropathology. Molecular, histologic, and behavioral comparisons in rats. *Spine (Phila Pa 1976)* 25: 2975-2980, 2000.

114. **Inkinen RI, Lammi MJ, Lehmonen S, Puustjarvi K, Kaapa E, and Tammi MI**. Relative increase of biglycan and decorin and altered chondroitin sulfate epitopes in the degenerating human intervertebral disc. *The Journal of rheumatology* 25: 506-514, 1998.

115. **Itai Y, Kariya Y, and Hoshino Y**. Morphological changes in rat hindlimb muscle fibres during recovery from disuse atrophy. *Acta physiologica Scandinavica* 181: 217-224, 2004.

116. **Iwashina T, Mochida J, Miyazaki T, Watanabe T, Iwabuchi S, Ando K, Hotta T, and Sakai D**. Low-intensity pulsed ultrasound stimulates cell proliferation and proteoglycan production in rabbit intervertebral disc cells cultured in alginate. *Biomaterials* 27: 354-361, 2006.

117. **Jahnke MR, and McDevitt CA**. Proteoglycans of the human intervertebral disc. Electrophoretic heterogeneity of the aggregating proteoglycans of the nucleus pulposus. *The Biochemical journal* 251: 347-356, 1988.

118. **Jin M, Frank EH, Quinn TM, Hunziker EB, and Grodzinsky AJ**. Tissue shear deformation stimulates proteoglycan and protein biosynthesis in bovine cartilage explants. *Archives of biochemistry and biophysics* 395: 41-48, 2001.

119. **Johnston SL, Campbell MR, Scheuring R, and Feiveson AH**. Risk of herniated nucleus pulposus among U.S. astronauts. *Aviation, space, and environmental medicine* 81: 566-574, 2010.

120. **Johnston SL, Wear ML, Birzele JA, and Hamm PB**. Increased incidence of herniated nucleus pulposus among astronauts and other selected populations [abstract]. *Aviation, space, and environmental medicine* 69: 220, 1998.

121. **Judex S, Donahue LR, and Rubin C**. Genetic predisposition to low bone mass is paralleled by an enhanced sensitivity to signals anabolic to the skeleton. *Faseb J* 16: 1280-1282, 2002.

122. **Judex S, Lei X, Han D, and Rubin C**. Low-magnitude mechanical signals that stimulate bone formation in the ovariectomized rat are dependent on the applied frequency but not on the strain magnitude. *J Biomech* 40: 1333-1339, 2007.

123. **Judex S, Luu YK, Ozcivici E, Adler B, Lublinsky S, and Rubin CT**. Quantification of adiposity in small rodents using micro-CT. *Methods (San Diego, Calif* 2009.

124. **Judex S, Zhong N, Squire ME, Ye K, Donahue LR, Hadjiargyrou M, and Rubin CT**. Mechanical modulation of molecular signals which regulate anabolic and catabolic activity in bone tissue. *Journal of cellular biochemistry* 94: 982-994, 2005.

125. **Kalichman L, Hodges P, Li L, Guermazi A, and Hunter DJ**. Changes in paraspinal muscles and their association with low back pain and spinal degeneration: CT study. *Eur Spine J* 2009.

126. **Kaupp JA, and Waldman SD**. Mechanical vibrations increase the proliferation of articular chondrocytes in high-density culture. *Proc Inst Mech Eng H* 222: 695-703, 2008.

127. **Kawano F, Wang XD, Lan YB, Yoneshima H, Ishihara A, Igarashi M, and Ohira Y**. Hindlimb suspension inhibits air-righting due to altered recruitment of neck and back muscles in rats. *The Japanese journal of physiology* 54: 229-242, 2004.

128. **Keller TS, Hansson TH, Holm SH, Pope MM, and Spengler DM**. In vivo creep behavior of the normal and degenerated porcine intervertebral disk: a preliminary report. *Journal of spinal disorders* 1: 267-278, 1988.

129. **Kershner D, and Binhammer R**. Intrathecal ligaments and nerve root tension: possible sources of lumbar pain during spaceflight. *Aviation, space, and environmental medicine* 75: 354-358, 2004.

130. **Kim YJ, Bonassar LJ, and Grodzinsky AJ**. The role of cartilage streaming potential, fluid flow and pressure in the stimulation of chondrocyte biosynthesis during dynamic compression. *Journal of biomechanics* 28: 1055-1066, 1995.

131. **Kim YJ, Grodzinsky AJ, and Plaas AH**. Compression of cartilage results in differential effects on biosynthetic pathways for aggrecan, link protein, and hyaluronan. *Archives of biochemistry and biophysics* 328: 331-340, 1996.

132. **Kim YJ, Sah RL, Grodzinsky AJ, Plaas AH, and Sandy JD**. Mechanical regulation of cartilage biosynthetic behavior: physical stimuli. *Archives of biochemistry and biophysics* 311: 1-12, 1994.

133. **Kiviranta I, Jurvelin J, Tammi M, Saamanen AM, and Helminen HJ**. Weight bearing controls glycosaminoglycan concentration and articular cartilage thickness in the knee joints of young beagle dogs. *Arthritis and rheumatism* 30: 801-809, 1987.

134. **Kiviranta I, Tammi M, Jurvelin J, Arokoski J, Saamanen AM, and Helminen HJ**. Articular cartilage thickness and glycosaminoglycan distribution in the young canine knee joint after remobilization of the immobilized limb. *J Orthop Res* 12: 161-167, 1994.

135. **Kumar A, Varghese M, Mohan D, Mahajan P, Gulati P, and Kale S**. Effect of whole-body vibration on the low back. A study of tractor-driving farmers in north India. *Spine (Phila Pa 1976)* 24: 2506-2515, 1999.

136. **Kuo YW, and Wang JL**. Rheology of intervertebral disc: an ex vivo study on the effect of loading history, loading magnitude, fatigue loading, and disc degeneration. *Spine (Phila Pa 1976)* 35: E743-752.

137. **Kwon RY, Meays DR, Tang WJ, and Frangos JA**. Microfluidic enhancement of intramedullary pressure increases intersititial fluid flow and inhibits bone loss in hindlimb suspended mice. *J Bone Miner Res*.

138. **Lai A, and Chow DH**. Effects of traction on structural properties of degenerated disc using an in vivo rat-tail model. *Spine (Phila Pa 1976)* 35: 1339-1345.

139. **Lai WM, Hou JS, and Mow VC**. A triphasic theory for the swelling and deformation behaviors of articular cartilage. *Journal of biomechanical engineering* 113: 245-258, 1991.

140. **Lang T, LeBlanc A, Evans H, Lu Y, Genant H, and Yu A**. Cortical and trabecular bone mineral loss from the spine and hip in long-duration spaceflight. *J Bone Miner Res* 19: 1006-1012, 2004.

141. **Lau E, Al-Dujaili S, Guenther A, Liu D, Wang L, and You L**. Effect of low-magnitude, high-frequency vibration on osteocytes in the regulation of osteoclasts. *Bone* 46: 1508-1515.

142. **Le Maitre CL, Frain J, Fotheringham AP, Freemont AJ, and Hoyland JA**. Human cells derived from degenerate intervertebral discs respond differently to those derived from non-degenerate intervertebral discs following application of dynamic hydrostatic pressure. *Biorheology* 45: 563-575, 2008.

143. **LeBlanc A, Rowe R, Schneider V, Evans H, and Hedrick T**. Regional muscle loss after short duration spaceflight. *Aviation, space, and environmental medicine* 66: 1151-1154, 1995.

144. **LeBlanc A, Schneider V, Shackelford L, West S, Oganov V, Bakulin A, and Voronin L**. Bone mineral and lean tissue loss after long duration space flight. *Journal of musculoskeletal & neuronal interactions* 1: 157-160, 2000.

145. **LeBlanc AD, Evans HJ, Schneider VS, Wendt RE, 3rd, and Hedrick TD**. Changes in intervertebral disc cross-sectional area with bed rest and space flight. *Spine* 19: 812-817, 1994.

146. **LeBlanc AD, Schneider VS, Evans HJ, Pientok C, Rowe R, and Spector E**. Regional changes in muscle mass following 17 weeks of bed rest. *J Appl Physiol* 73: 2172-2178, 1992.

147. **Lee B, Han L, Frank EH, Chubinskaya S, Ortiz C, and Grodzinsky AJ**. Dynamic mechanical properties of the tissue-engineered matrix associated with individual chondrocytes. *Journal of biomechanics* 43: 469-476.

148. **Legerlotz K, Schjerling P, Langberg H, Bruggemann GP, and Niehoff A**. The effect of running, strength, and vibration strength training on the mechanical, morphological, and biochemical properties of the Achilles tendon in rats. *J Appl Physiol* 102: 564-572, 2007.

149. **Liang QQ, Zhou Q, Zhang M, Hou W, Cui XJ, Li CG, Li TF, Shi Q, and Wang YJ**. Prolonged upright posture induces degenerative changes in intervertebral discs in rat lumbar spine. *Spine (Phila Pa 1976)* 33: 2052-2058, 2008.

150. **Lim CH, Jee WH, Son BC, Kim DH, Ha KY, and Park CK**. Discogenic lumbar pain: association with MR imaging and CT discography. *European journal of radiology* 54: 431-437, 2005.

151. **Lipson SJ, and Muir H**. 1980 Volvo award in basic science. Proteoglycans in experimental intervertebral disc degeneration. *Spine* 6: 194-210, 1981.

152. **Liu J, Sekiya I, Asai K, Tada T, Kato T, and Matsui N**. Biosynthetic response of cultured articular chondrocytes to mechanical vibration. *Research in experimental medicine* 200: 183-193, 2001.

153. **Loening AM, James IE, Levenston ME, Badger AM, Frank EH, Kurz B, Nuttall ME, Hung HH, Blake SM, Grodzinsky AJ, and Lark MW**. Injurious mechanical compression of bovine articular cartilage induces chondrocyte apoptosis. *Archives of biochemistry and biophysics* 381: 205-212, 2000.

154. **Macias BR, Cao P, Watenpaugh DE, and Hargens AR**. LBNP treadmill exercise maintains spine function and muscle strength in identical twins during 28-day simulated microgravity. *J Appl Physiol* 102: 2274-2278, 2007.

155. **MacLean JJ, Lee CR, Alini M, and Iatridis JC**. The effects of short-term load duration on anabolic and catabolic gene expression in the rat tail intervertebral disc. *J Orthop Res* 23: 1120-1127, 2005.

156. **MacLean JJ, Lee CR, Grad S, Ito K, Alini M, and Iatridis JC**. Effects of immobilization and dynamic compression on intervertebral disc cell gene expression in vivo. *Spine* 28: 973-981, 2003.

157. **Malko JA, Hutton WC, and Fajman WA**. An in vivo magnetic resonance imaging study of changes in the volume (and fluid content) of the lumbar intervertebral discs during a simulated diurnal load cycle. *Spine* 24: 1015-1022, 1999.

158. **Malko JA, Hutton WC, and Fajman WA**. An in vivo MRI study of the changes in volume (and fluid content) of the lumbar intervertebral disc after overnight bed rest and during an 8-hour walking protocol. *Journal of spinal disorders & techniques* 15: 157-163, 2002.

159. **Marchand F, and Ahmed AM**. Investigation of the laminate structure of lumbar disc anulus fibrosus. *Spine* 15: 402-410, 1990.

160. **Maynard JA**. The effects of space flight on the composition of the intervertebral disc. *The Iowa orthopaedic journal* 14: 125-133, 1994.

161. **Michalek AJ, Buckley MR, Bonassar LJ, Cohen I, and Iatridis JC**. Measurement of local strains in intervertebral disc anulus fibrosus tissue under dynamic shear: contributions of matrix fiber orientation and elastin content. *Journal of biomechanics* 42: 2279-2285, 2009.

162. **Midura RJ, Su X, and Androjna C**. A simulated weightlessness state diminishes cortical bone healing responses. *Journal of musculoskeletal & neuronal interactions* 6: 327-328, 2006.

163. **Miller LM, Little W, Schirmer A, Sheik F, Busa B, and Judex S**. Accretion of bone quantity and quality in the developing mouse skeleton. *J Bone Miner Res* 22: 1037-1045, 2007.

164. **Miyazaki T, Kobayashi S, Takeno K, Meir A, Urban J, and Baba H**. A phenotypic comparison of proteoglycan production of intervertebral disc cells isolated from rats, rabbits, and bovine tails; which animal model is most suitable to study tissue engineering and biological repair of human disc disorders? *Tissue Eng Part A* 15: 3835-3846, 2009.

165. **Mizuno H, Roy AK, Vacanti CA, Kojima K, Ueda M, and Bonassar LJ**. Tissue-engineered composites of anulus fibrosus and nucleus pulposus for intervertebral disc replacement. *Spine* 29: 1290-1297; discussion 1297-1298, 2004.

166. **Moezy A, Olyaei G, Hadian M, Razi M, and Faghihzadeh S**. A comparative study of whole body vibration training and conventional training on knee proprioception and postural stability after anterior cruciate ligament reconstruction. *British journal of sports medicine* 42: 373-378, 2008.

167. **Moneta GB, Videman T, Kaivanto K, Aprill C, Spivey M, Vanharanta H, Sachs BL, Guyer RD, Hochschuler SH, Raschbaum RF, and et al.** Reported pain during lumbar discography as a function of anular ruptures and disc degeneration. A re-analysis of 833 discograms. *Spine* 19: 1968-1974, 1994.

168. **Morey-Holton ER, and Globus RK**. Hindlimb unloading rodent model: technical aspects. *Journal of Applied Physiology* 92: 1367-1377, 2002.

169. **Moriggi M, Vasso M, Fania C, Capitanio D, Bonifacio G, Salanova M, Blottner D, Rittweger J, Felsenberg D, Cerretelli P, and Gelfi C**. Long term bed rest with and without vibration exercise countermeasures: Effects on human muscle protein dysregulation. *PROTEOMICS* 10: 3756–3774, 2010.

170. **Nahhas Rodacki CL, Luiz Felix Rodacki A, Ugrinowitsch C, Zielinski D, and Budal da Costa R**. Spinal unloading after abdominal exercises. *Clinical biomechanics (Bristol, Avon)* 23: 8-14, 2008.

171. **Nerlich AG, Schleicher ED, and Boos N**. 1997 Volvo Award winner in basic science studies. Immunohistologic markers for age-related changes of human lumbar intervertebral discs. *Spine (Phila Pa 1976)* 22: 2781-2795, 1997.

172. **Niosi CA, and Oxland TR**. Degenerative mechanics of the lumbar spine. *Spine J* 4: 202S-208S, 2004.

173. **O'Connell GD, Johannessen W, Vresilovic EJ, and Elliott DM**. Human internal disc strains in axial compression measured noninvasively using magnetic resonance imaging. *Spine (Phila Pa 1976)* 32: 2860-2868, 2007.

174. **O'Connell GD, Vresilovic EJ, and Elliott DM**. Comparison of animals used in disc research to human lumbar disc geometry. *Spine (Phila Pa 1976)* 32: 328-333, 2007.

175. **O'Connell GD, Vresilovic EJ, and Elliott DM**. Human intervertebral disc internal strain in compression: The effect of disc region, loading position, and degeneration. *J Orthop Res*.

176. **O'Hara BP, Urban JP, and Maroudas A**. Influence of cyclic loading on the nutrition of articular cartilage. *Annals of the rheumatic diseases* 49: 536-539, 1990.

177. **Oganov VS, Grigor'ev AI, Voronin LI, Rakhmanov AS, Bakulin AV, Schneider VS, and LeBlanc AD**. [Bone mineral density in cosmonauts after flights lasting 4.5-6 months on the Mir orbital station]. *Aviakosmicheskaia i ekologicheskaia meditsina = Aerospace and environmental medicine* 26: 20-24, 1992.

178. **Ohshima H, Urban JP, and Bergel DH**. Effect of static load on matrix synthesis rates in the intervertebral disc measured in vitro by a new perfusion technique. *J Orthop Res* 13: 22-29, 1995.

179. **Olsen BR**. Collagen Biosynthesis. In: *Cell Biology of Extracellular Matrix*, edited by Hay ED. New York: Plenum Press, 1991, p. 177-220.

180. **Oxland TR, and Panjabi MM**. The onset and progression of spinal injury: a demonstration of neutral zone sensitivity. *Journal of biomechanics* 25: 1165-1172, 1992.

181. **Ozcivici E, Luu YK, Rubin CT, and Judex S**. Low-level vibrations retain bone marrow's osteogenic potential and augment recovery of trabecular bone during reambulation. *PLoS One* 5: e11178, 2010.

182. **Palmer AW, Guldberg RE, and Levenston ME**. Analysis of cartilage matrix fixed charge density and three-dimensional morphology via contrast-enhanced microcomputed tomography. *Proceedings of the National Academy of Sciences of the United States of America* 103: 19255-19260, 2006.

183. **Panjabi MM, Andersson GB, Jorneus L, Hult E, and Mattsson L**. In vivo measurements of spinal column vibrations. *The Journal of bone and joint surgery* 68: 695-702, 1986.

184. **Park C, Kim YJ, Lee CS, An K, Shin HJ, Lee CH, Kim CH, and Shin JW**. An in vitro animal study of the biomechanical responses of anulus fibrosus with aging. *Spine* 30: E259-265, 2005.

185. **Parry DA, Barnes GR, and Craig AS**. A comparison of the size distribution of collagen fibrils in connective tissues as a function of age and a possible relation between fibril size distribution and mechanical properties. *Proceedings of the Royal Society of London Series B, Containing papers of a Biological character* 203: 305-321, 1978.

186. **Pasqualini M, Laroche N, Vvanden Bossche A, and Vico L**. Site and Frequency Specific Effects of Whole Body Vibration on Axial and Appendicular Structural Bone Parameters in Aged Rats. In: *J Bone Miner Res* 2010.

187. **Pedrini-Mille A, Maynard JA, Durnova GN, Kaplansky AS, Pedrini VA, Chung CB, and Fedler-Troester J**. Effects of microgravity on the composition of the intervertebral disk. *J Appl Physiol* 73: 26S-32S, 1992.

188. **Peng B, Hao J, Hou S, Wu W, Jiang D, Fu X, and Yang Y**. Possible pathogenesis of painful intervertebral disc degeneration. *Spine* 31: 560-566, 2006.

189. **Pfirrmann CW, Metzdorf A, Elfering A, Hodler J, and Boos N**. Effect of aging and degeneration on disc volume and shape: A quantitative study in asymptomatic volunteers. *J Orthop Res* 24: 1086-1094, 2006.

190. **Pfirrmann CW, Metzdorf A, Zanetti M, Hodler J, and Boos N**. Magnetic resonance classification of lumbar intervertebral disc degeneration. *Spine* 26: 1873-1878, 2001.

191. **Provenzano PP, Martinez DA, Grindeland RE, Dwyer KW, Turner J, Vailas AC, and Vanderby R, Jr.** Hindlimb unloading alters ligament healing. *J Appl Physiol* 94: 314-324, 2003.

192. **Quinn TM, Grodzinsky AJ, Buschmann MD, Kim YJ, and Hunziker EB**. Mechanical compression alters proteoglycan deposition and matrix deformation around individual cells in cartilage explants. *Journal of cell science* 111 (Pt 5): 573-583, 1998.

193. **Roberts N, Hogg D, Whitehouse GH, and Dangerfield P**. Quantitative analysis of diurnal variation in volume and water content of lumbar intervertebral discs. *Clinical anatomy (New York, NY* 11: 1-8, 1998.

194. **Roberts S, Evans H, Trivedi J, and Menage J**. Histology and pathology of the human intervertebral disc. *The Journal of bone and joint surgery* 88 Suppl 2: 10-14, 2006.

195. **Rubin C, Pope M, Fritton JC, Magnusson M, Hansson T, and McLeod K**. Transmissibility of 15-hertz to 35-hertz vibrations to the human hip and lumbar spine: determining the

physiologic feasibility of delivering low-level anabolic mechanical stimuli to skeletal regions at greatest risk of fracture because of osteoporosis. *Spine* 28: 2621-2627, 2003.

196. **Saberi H, Rahimi L, and Jahani L**. A comparative MRI study of upper and lower lumbar motion segments in patients with low back pain. *Journal of spinal disorders & techniques* 22: 507-510, 2009.

197. **Sah RL, Kim YJ, Doong JY, Grodzinsky AJ, Plaas AH, and Sandy JD**. Biosynthetic response of cartilage explants to dynamic compression. *J Orthop Res* 7: 619-636, 1989.

198. **Sarver JJ, and Elliott DM**. Mechanical differences between lumbar and tail discs in the mouse. *Journal of Orthopaedic Research* 23: 150-155, 2005.

199. **Sato K, Kikuchi S, and Yonezawa T**. In vivo intradiscal pressure measurement in healthy individuals and in patients with ongoing back problems. *Spine* 24: 2468-2474, 1999.

200. **Sayson JV, and Hargens AR**. Pathophysiology of low back pain during exposure to microgravity. *Aviation, space, and environmental medicine* 79: 365-373, 2008.

201. **Sehmisch S, Galal R, Kolios L, Tezval M, Dullin C, Zimmer S, Stuermer KM, and Stuermer EK**. Effects of low-magnitude, high-frequency mechanical stimulation in the rat osteopenia model. *Osteoporos Int* 2009.

202. **Seidel H, Bluethner R, and Hinz B**. Effects of sinusoidal whole-body vibration on the lumbar spine: the stress-strain relationship. *International archives of occupational and environmental health* 57: 207-223, 1986.

203. **Sibonga JD, Zhang M, Evans GL, Westerlind KC, Cavolina JM, Morey-Holton E, and Turner RT**. Effects of spaceflight and simulated weightlessness on longitudinal bone growth. *Bone* 27: 535-540, 2000.

204. **Singh K, Masuda K, and An HS**. Animal models for human disc degeneration. *Spine J* 5: 267S-279S, 2005.

205. **Singh K, Masuda K, Thonar EJ, An HS, and Cs-Szabo G**. Age-related changes in the extracellular matrix of nucleus pulposus and anulus fibrosus of human intervertebral disc. *Spine (Phila Pa 1976)* 34: 10-16, 2009.

206. **Sinha RK, Shah SA, Hume EL, and Tuan RS**. The effect of a 5-day space flight on the immature rat spine. *Spine J* 2: 239-243, 2002.

207. **Sivan S, Neidlinger-Wilke C, Wurtz K, Maroudas A, and Urban JP**. Diurnal fluid expression and activity of intervertebral disc cells. *Biorheology* 43: 283-291, 2006.

208. **Smit TH**. The use of a quadruped as an in vivo model for the study of the spine - biomechanical considerations. *Eur Spine J* 11: 137-144, 2002.

209. **Sohn HM, You JW, and Lee JY**. The relationship between disc degeneration and morphologic changes in the intervertebral foramen of the cervical spine: a cadaveric MRI and CT study. *Journal of Korean medical science* 19: 101-106, 2004.

210. **Stokes IA**. Surface strain on human intervertebral discs. *J Orthop Res* 5: 348-355, 1987.

211. **Stokes IA, and Iatridis JC**. Mechanical conditions that accelerate intervertebral disc degeneration: overload versus immobilization. *Spine* 29: 2724-2732, 2004.

212. **Straus BN**. Chronic pain of spinal origin: the costs of intervention. *Spine* 27: 2614-2619; discussion 2620, 2002.

213. **Styf JR, Ballard RE, Fechner K, Watenpaugh DE, Kahan NJ, and Hargens AR**. Height increase, neuromuscular function, and back pain during 6 degrees head-down tilt with traction. *Aviation, space, and environmental medicine* 68: 24-29, 1997.

214. **Styf JR, Hutchinson K, Carlsson SG, and Hargens AR**. Depression, mood state, and back pain during microgravity simulated by bed rest. *Psychosomatic medicine* 63: 862-864, 2001.

215. **Sun DD, and Leong KW**. A nonlinear hyperelastic mixture theory model for anisotropy, transport, and swelling of annulus fibrosus. *Annals of biomedical engineering* 32: 92-102, 2004.

216. **Szafranski JD, Grodzinsky AJ, Burger E, Gaschen V, Hung HH, and Hunziker EB**. Chondrocyte mechanotransduction: effects of compression on deformation of intracellular organelles and relevance to cellular biosynthesis. *Osteoarthritis and cartilage / OARS, Osteoarthritis Research Society* 12: 937-946, 2004.

217. **Takeuchi R, Saito T, Ishikawa H, Takigami H, Dezawa M, Ide C, Itokazu Y, Ikeda M, Shiraishi T, and Morishita S**. Effects of vibration and hyaluronic acid on activation of three-dimensional cultured chondrocytes. *Arthritis and rheumatism* 54: 1897-1905, 2006.

218. **Thompson JP, Oegema TR, Jr., and Bradford DS**. Stimulation of mature canine intervertebral disc by growth factors. *Spine* 16: 253-260, 1991.

219. **Thornton WE, Hoffler GW, and Rummel JA**. Anthropometric changes and fluid shifts In: Biomedical Results from Skylab, NASA, 1977.

220. **Torvinen S, Kannus P, Sievanen H, Jarvinen TA, Pasanen M, Kontulainen S, Jarvinen TL, Jarvinen M, Oja P, and Vuori I**. Effect of four-month vertical whole body vibration on performance and balance. *Medicine and science in sports and exercise* 34: 1523-1528, 2002.

221. **Torzilli PA, Grigiene R, Huang C, Friedman SM, Doty SB, Boskey AL, and Lust G**. Characterization of cartilage metabolic response to static and dynamic stress using a mechanical explant test system. *Journal of biomechanics* 30: 1-9, 1997.

222. **Trout JJ, Buckwalter JA, Moore KC, and Landas SK**. Ultrastructure of the human intervertebral disc. I. Changes in notochordal cells with age. *Tissue & cell* 14: 359-369, 1982.

223. **Turgut M, Yenisey C, Akyuz O, Ozsunar Y, Erkus M, and Bicakci T**. Correlation of serum trace elements and melatonin levels to radiological, biochemical, and histological assessment of degeneration in patients with intervertebral disc herniation. *Biological trace element research* 109: 123-134, 2006.

224. **Umehara S, Tadano S, Abumi K, Katagiri K, Kaneda K, and Ukai T**. Effects of degeneration on the elastic modulus distribution in the lumbar intervertebral disc. *Spine* 21: 811-819; discussion 820, 1996.

225. **Urban JP, Hall AC, and Gehl KA**. Regulation of matrix synthesis rates by the ionic and osmotic environment of articular chondrocytes. *Journal of cellular physiology* 154: 262-270, 1993.

226. **Urban JP, and Maroudas A**. The chemistry of the intervertebral disc in relation to its physiological funtion. *Clin Rheum Dis* 6: 51-76, 1980.

227. **Urban JP, and McMullin JF**. Swelling pressure of the lumbar intervertebral discs: influence of age, spinal level, composition, and degeneration. *Spine* 13: 179-187, 1988.

228. **Valdes AM, Hassett G, Hart DJ, and Spector TD**. Radiographic progression of lumbar spine disc degeneration is influenced by variation at inflammatory genes: a candidate SNP association study in the Chingford cohort. *Spine (Phila Pa 1976)* 30: 2445-2451, 2005.

229. **Vertel BM, and Ratcliffe A**. Aggrecan. In: *Proteoglycans: structure, biology, and molecular interactions*, edited by Iozzo RV. New York: Marcel Dekker, 2000, p. 343-377.

230. **Wang S, Xia Q, Passias P, Wood K, and Li G**. Measurement of geometric deformation of lumbar intervertebral discs under in-vivo weightbearing condition. *Journal of biomechanics* 42: 705-711, 2009.

231. **Weinbaum S, Cowin SC, and Zeng Y**. A model for the excitation of osteocytes by mechanical loading-induced bone fluid shear stresses. *J Biomech* 27: 339-360, 1994.

232. **Wing P, Tsang I, Gagnon F, Susak L, and Gagnon R**. Diurnal changes in the profile shape and range of motion of the back. *Spine* 17: 761-766, 1992.

233. **Wing PC, Tsang IK, Susak L, Gagnon F, Gagnon R, and Potts JE**. Back pain and spinal changes in microgravity. *The Orthopedic clinics of North America* 22: 255-262, 1991.

234. **Wronski TJ, and Morey ER**. Skeletal abnormalities in rats induced by simulated weightlessness. *Metabolic bone disease & related research* 4: 69-75, 1982.

235. **Wuertz K, Godburn K, MacLean JJ, Barbir A, Donnelly JS, Roughley PJ, Alini M, and Iatridis JC**. In vivo remodeling of intervertebral discs in response to short- and long-term dynamic compression. *J Orthop Res* 27: 1235-1242, 2009.

236. **Xie L, Jacobson JM, Choi ES, Busa B, Donahue LR, Miller LM, Rubin CT, and Judex S**. Low-level mechanical vibrations can influence bone resorption and bone formation in the growing skeleton. *Bone* 39: 1059-1066, 2006.

237. **Xie L, Rubin C, and Judex S**. Enhancement of the Adolescent Murine Musculoskeletal System using Low-Level Mechanical Vibrations. *J Appl Physiol* 2008.

238. **Yamazaki S, Banes AJ, Weinhold PS, Tsuzaki M, Kawakami M, and Minchew JT**. Vibratory loading decreases extracellular matrix and matrix metalloproteinase gene expression in rabbit annulus cells. *Spine J* 2: 415-420, 2002.

239. **Yamazaki S, Weinhold PS, Graff RD, Tsuzaki M, Kawakami M, Minchew JT, and Banes AJ**. Annulus cells release ATP in response to vibratory loading in vitro. *Journal of cellular biochemistry* 90: 812-818, 2003.

240. **Yao W, Jee WS, Chen J, Tam CS, Setterberg RB, and Frost HM**. Erect bipedal stance exercise partially prevents orchidectomy-induced bone loss in the lumbar vertebrae of rats. *Bone* 27: 667-675, 2000.

241. **Yasuoka H, Asazuma T, Nakanishi K, Yoshihara Y, Sugihara A, Tomiya M, Okabayashi T, and Nemoto K**. Effects of reloading after simulated microgravity on proteoglycan metabolism in the nucleus pulposus and anulus fibrosus of the lumbar intervertebral disc: an experimental study using a rat tail suspension model. *Spine* 32: E734-740, 2007.

242. **You J, Yellowley CE, Donahue HJ, Zhang Y, Chen Q, and Jacobs CR**. Substrate deformation levels associated with routine physical activity are less stimulatory to bone cells relative to loading-induced oscillatory fluid flow. *Journal of biomechanical engineering* 122: 387-393, 2000.

243. **Zar JH**. *Biostatistical Analysis*. Upper Saddle River, New Jersey: Pearson: Prentice Hall, 2010.

244. **Zhang H, He Z, Gao Y, Hinghofer-Szalkay HG, and Fan X**. Muscle composition after 14-day hindlimb unloading in rats: effects of two herbal compounds. *Aviation, space, and environmental medicine* 78: 926-931, 2007.

245. **Zhao F, Pollintine P, Hole BD, Dolan P, and Adams MA**. Discogenic origins of spinal instability. *Spine (Phila Pa 1976)* 30: 2621-2630, 2005.

246. **Zhong N, Garman RA, Squire ME, Donahue LR, Rubin CT, Hadjiargyrou M, and Judex S**. Gene expression patterns in bone after 4 days of hind-limb unloading in two inbred strains of mice. *Aviation, space, and environmental medicine* 76: 530-535, 2005.

247. **Zou J, Yang H, Miyazaki M, Morishita Y, Wei F, McGovern S, and Wang JC**. Dynamic bulging of intervertebral discs in the degenerative lumbar spine. *Spine* 34: 2545-2550, 2009.